Title

PLASMA MEMBRANE REORGANIZATION INDUCED BY CHEMICAL TRANSFORMATION in Cultura

Author

Packard, B.S.

Publication Date

1984-04-01

Lawrence Berkeley Laboratory
UNIVERSITY OF CALIFORNIA

CHEMICAL BIODYNAMICS DIVISION

PLASMA MEMBRANE REORGANIZATION INDUCED BY CHEMICAL TRANSFORMATION in Cultura

Beverly Sue Packard
(Ph.D. Thesis)

April 1984

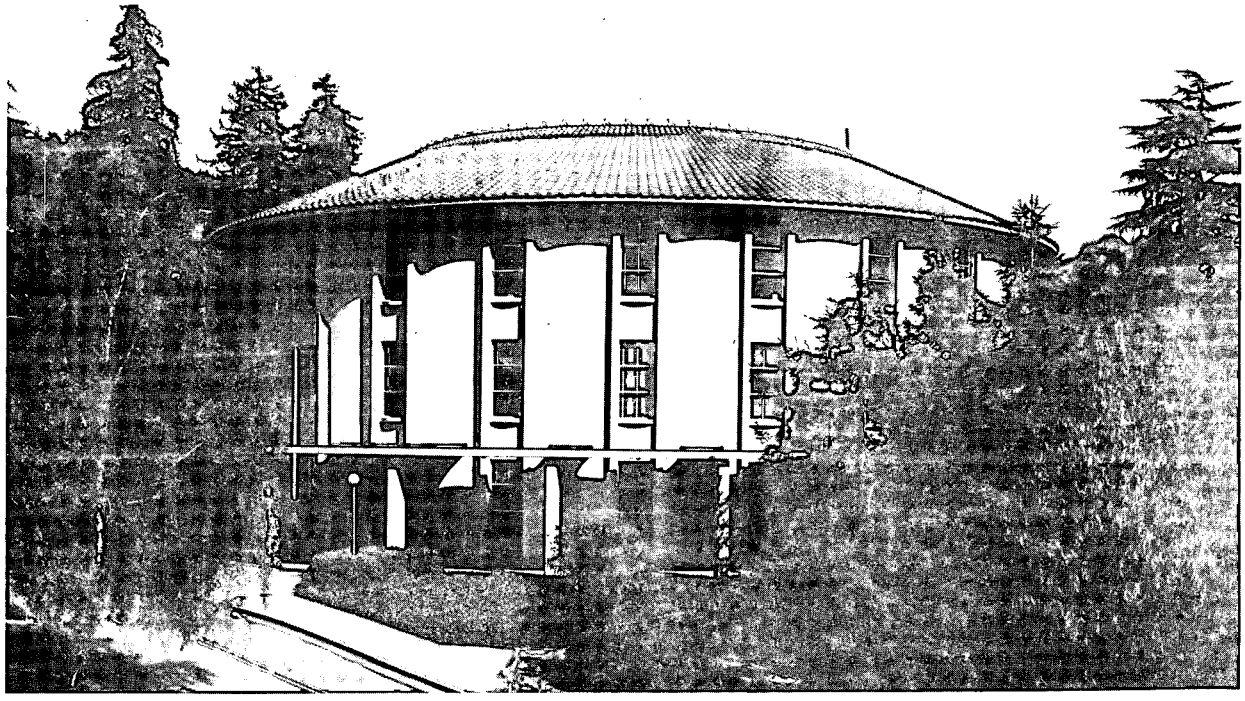

Prepared for the U.S. Department of Energy under Contract DE-AC03-76SF00098

DISCLAIMER

LBL-17712

PLASMA MEMBRANE REORGANIZATION INDUCED BY CHEMICAL TRANSFORMATION *in Cultura*

Beverly Sue Packard
Ph.D. Thesis

Lawrence Berkeley Laboratory
University of California
Berkeley, California 94720

This work was supported by the Director, Office of Energy Research, Office of Health and Environmental Research, Health Effects Research Division of the U.S. Department of Energy under Contract Number DE-AC03-76SF00098.

Plasma Membrane Reorganization

Induced by Chemical Transformation *in Cultura*

Beverly Sue Packard

Abstract

The major objective of this thesis was to gain a deeper understanding of the perturbations induced by a malignogenoid transformation on the organization of molecules constituting the surface of cells, i.e., the plasma membrane. For experimental reasons the system chosen was an epithelial cell line which, when exposed to the tumor promoting phorbol esters, exhibits properties associated with a malignant-like state *in cultura*.

Induction of an increased rigidity in the plasma membrane in parallel with the manifestation of properties associated with a transformed state was suggested by two classes of experiments. The results from one technique, fluorescence recovery after photobleaching (FRAP), indicated the induction of a second environment in the plasma membrane in which the synthetic fluorescent phospholipid collarein was immobile on the FRAP timescale in comparison to the homogeneous, mobile environment of the control cells.

Results from the other technique, the binding of epidermal growth factor (EGF) to cellular receptors, revealed a cryptic class of receptors which became accessible for binding upon chemical transformation. These two lines of evidence are consistent with a reorganization of the plasma membrane induced by tumor promoters.

Increased rigidity in the plasma membrane of a cell that has been induced to a transformed state may be associated with the autonomy to normal growth control mechanisms that transformed cells acquire. As signal transduction across a plasma membrane is generally believed to occur somewhere between the binding and internalization events, the mobility which the ligand-receptor complex is able to attain may be responsible for the quality of signal transduction. Thus, phosphorylation and higher order messenger generation may be strongly affected by the degree and type of movement accessible to the molecular components of sequential or cascading events.

Thus, by both a biophysical and a biochemical technique, this work indicates that a rigidity is induced in the plasma membrane of an epithelial cell that has been transformed to a malignogenoid state. This putative rigidity may effect or be associated with an autonomous state by preventing normal molecular movement in the plasma membrane and, thus, perturbing transduction of signals essential for normal control.

Acknowledgements

The one characteristic associated with Ph.D. theses that seems to transcend all disciplines is that the acknowledgements are the most heavily trafficked sections. In addition to wanting to have something for the masses there really are individuals I would like to acknowledge; therefore, I have included one such section in this book. I have tried to minimize its viscosity.

The primary list of people I acknowledge is:

Mel Klein for exposing me to areas of science that were not in my realms of thinking by January, 1982 and, thus, for inducing lateral connections. Additionally, he has always made himself available for discussions of ideas, experiments, and (re)^{n}writings.

Mina Bissell for allowing me to work on biologic problems in a wonderful place, to learn about grantwriting, and to get to know what a very fat person is like in the second person.

Mike Saxton for building the FRAP instrument (Chapter V), for teaching me about the diffusion equation (especially in archipelagos), and for a course in mathematical function appreciation.

Kerry Karukstis for teaching me how to measure fluorescence lifetimes which resulted in my greatest day in science -- September 1, 1982.

Knute Fisher for letting me get my hands into freeze fracture work and sticking with the project until some "good" samples finally worked (Figures II-7 through II-10).

David Wolf for collaborating on the liposome lifetime work (Chapter IV-2) and for insights into fluorescence and the "ways of science".

DAP, a.k.a. David Ari Pearlman, for DAPGRAPH and TABLE. Additional thanks for strongly urging me many times to get everything I want from a store and a little bit more.

Gordon Parry for eagerly listening to some fairly half-baked explanations and suggesting some classical ways to support them a bit more concretely.

Mr. Lust, a.k.a. Bill Love, for help and fun in light microscopy as well as for being my contest partner.

Shirley Ebbe for advertising in Experimental Hematology in 1980 for training grant trainees and for grant support (N.I.H. T32 AM07349Z) for my entire time at Berkeley.

Gloria Goldberg for allowing me to help her help me help her pull this thesis through the LCB word processor.

The secondary list of acknowledgees includes many of the inmates of LBL buildings 3, 83, 1, 10, 90, 76, 35.5, and 69 for a very broad range of activities (This includes you, Alan, for the cardiolipin, in cultura, and other discussions.). As I don't want to pursue this much further,

I'll just leave it like this: "You know who you are. Thanks."

This work was supported by the U.S. Department of Energy's Office of Energy Research, Office of Health and Environmental Research, Division of Health Effects Research (Contract No. DE-AC03-76SF00098).

Abbreviations

TPA = 12-O-tetradecanoylphorbol 13-acetate

PDD = phorbol 12,13-didecanoate

DMBA = dimethylbenz[α]anthracene

MDCK = Madin-Darby canine kidney

MEM = minimal essential medium

ρ = density of

Δ = change in

cXMP = cyclic nucleotide. X=A: cyclic adenosine monophosphate (cAMP); X=G: cyclic guanosine monophosphate (cGMP).

PC = phosphatidyl choline

PGE = prostaglandin E

Na^+,K^+-ATPase = sodium, potassium adenosine triphosphatase

NBD = 12-(N-methyl-N-(7-nitrobenz-2-oxa-1,3-diazol-4-yl))

C_NDiI = 1,1'-dihexadecyl-3,3,3'3'-tetramethylindo-3-carbocyanine

PE = phosphatidyl ethanolamine

LR = lissamine rhodamine-B sulfonyl chloride

CL = cardiolipin

PE = phorbol ester

EGF = epidermal growth factor

τ = fluoresence lifetime

α = amplitude of fluorescence lifetime component

1-comp = one component

2-comp = two components

DSPC = distearylphosphatidyl choline

DOPC = dioleylphosphatidyl choline

NFY = normalized fluorescence yield

SA = stearylamine

PA = phosphatidic acid

Table of Contents

Chapter I

Introduction

Biologic membranes are self-assembling systems in which phosholipids aggregate into bilayers and serve as a two-dimensional solvent for cholesterol, proteins, glycoproteins, and glycolipids. The molecules of these noncovalent assemblies are in constant motion, the degree and type of movement depending on some combination of the chemistry of the individual molecules, the molecules' physiologic roles, the cell's physiologic state, and local environmental influences.

Structurally, all biologic cells possess a surrounding membrane, the plasma membrane. Its elements are associated with cellular functions such as protection, transport, structure, recognition, and signal transduction. The first is due largely to the amphiphilic nature of membranes in general while the latter ones are effected by the protein and glycoprotein receptor molecules embedded in the membrane.

A property that all biologic cells acquire when transformed to a malignant state is autonomy to regulation by normal control mechanisms; a considerable amount of evidence suggests that the plasma membrane is intimately involved with the primary events of malignant transformation

(1). Control often involves the binding of polypeptide growth factors to the membrane receptor molecules of target cells (2). Perturbations in the cellular affinity may be brought about by changes in the number, conformation, and degree of aggregation of receptors as well as anabolic and/or catabolic characteristics of receptors, ligands, and receptor-ligand complexes. Additionally, the macromolecules on which cells sit, nominally the extracellular matrix, influence the cellular state (3).

This thesis was aimed at further understanding the influence of transformation from a normal to a malignant-like state on the organization of plasma membrane molecules. Several approaches were employed: measurement of the lateral diffusion of a synthetic phospholipid in the plasma membrane, binding of a growth factor to its cellular receptors, phase and Nomarski microscopy, freeze fracture electron microscopy, and fluorescence lifetime determinations of fluorophores in various physical states.

References

1. Poste G. and Nicolson, G.L. Cell Surface Reviews vol. 1-N.
2. Sato, G.H. and Ross, R. (1979) Hormones and Cell Culture, Cold Spring Harbor conferences on cell proliferation, vol. 6.
3. Bissell, M.J., Hall, H.G., and Parry, G. (1982) J. Theor. Biol. 99: 31-68.

Chapter II

Model System

The major biologic question at which this thesis was targeted concerns the plasma membrane changes associated with transformation to a malignant phenotype; therefore, it was necessary to find a system which exhibits properties of the transformed state (Figure II-1). Several types of models have been and continue to be used; they include spontaneously occurring tumors, chemically or virally induced tumors *in vivo*, and chemical or viral treatment of organs, tissues or cells *in cultura* (1,2).

The degree of control one has over an experiment increases as one progresses from *in vivo* to *in vitro* conditions. Therefore, cells that are able to adapt to life *in vitro* were considered to be the starting system of choice. The cells initially tried in this study were secondary avian tendon cells having the advantage of the reasonably well characterized and readily available transformation model of Rous sarcoma virus infection and transformation (3). However, as described in chapter III, the inability of these cells to maintain a homogenous distribution of fluorescence in their plasma membranes for the time necessary to make a physical measurement made this an unacceptable system.

In contrast, several lines of epithelial cells in culture showed a homogeneous distribution of the synthetic fluorescent phospholipid collarein. Viral transformation of an epithelial cell line is not a trivial biologic operation; much work has gone into characterizing the morphologic, biochemical, and biophysical effects of a chemically heterogeneous class of molecules known as tumor promoters on cells in culture (as well as the original observations of tumor promotion in vivo) (4,5) (Fig. II-2). Alterations in the following plasma membrane-associated phenomena have been correlated with the transformed state induced by the tumor promoting phorbol esters: cell shape (6), enzymatic activity, i.e., protein kinase C (7,8), and proteins involved in prostaglandin synthesis (9), hexose transport (3), growth factor receptor affinity (10-13), phospholipid and protein synthesis (14,15), membrane rigidity (16), cellular permeability (17), electrical resistance (17), and metabolic cooperativity (18). Therefore, chemical transformation of an epithelial cell line in culture was considered.

As shown in Figure II-3, which depicts the two-stage model of carcinogenesis, exposure of organisms that have been preconditioned with initiators, e.g., 7,12-dimethylbenz[α]anthracene, to tumor promoters can result in the appearance of tumors. Incubation of cells in culture with these agents can induce characteristics considered to be pathognomonic for transformation (Figure II-1).

The phorbol esters (Figure II-4) represent a class of tumor promoters, the best known and most studied being 12-tetradecanoylphorbol 13-acetate (TPA). In addition to the biologically active TPA and phorbol 12,13-didecanoate (PDD), there exist biologically inactive congenors, e.g., 4α-phorbol 12,13-didecanoate (4α-PDD).

Thus, the model finally decided upon was the chemical transformation by phorbol esters of a line of epithelial cells derived from the kidney of a female cocker spaniel in 1958 in Berkeley, the Madin-Darby canine kidney (MDCK) cell line (19). Conditions under which these cells have been shown to exhibit biochemical, physiologic, and morphologic characteristics of transformation, i.e., 50 ng/ml for two hours at 37^{o}C, were used. An additional advantage was that the difference in time between a control cell and a cell exhibiting transformoid properties was just two hours.

In figures II-5 and II-6 the morphologic characteristics of treated cells (b) are compared with those of controls (a) under phase and Nomarski optics, respectively. The most striking changes involve the overall cellular shape. In II-5 the general homogeneity of the control cells appears in striking contrast to the swirling cellular architecture often resulting in focal arrays of the treated cells. In Figure II-6 the sharply delineated lateral aspects of the cell surfaces under polarized light microscopy in the control cells contrast with their virtual absence upon treatment with TPA.

Despite the sharply delineated morphologic alterations visible at the light microscopic level, there were no apparent changes observed at the electron microscopic level using the technique of freeze fracture. Cellular regions that were suspected of being altered by the phorbol esters and, therefore, were examined in particular were: the apical surface (specifically the microvilli) (Figure II-7), the junctional arrangements in the lateral aspects of the plasma membrane (Figure II-8), the nuclear pores (Figure II-9), and the general relationships of cellular organelles to each other (Figure II-10). However, the microvilli, both quantitatively and qualitatively, in the treated cells were indistinguishable from those of the controls. Similarly, characteristics of the lateral surfaces, nuclear region, and the organelle-organelle distribution, in general, did not appear to have been perturbed by TPA.

Thus, biologically active phorbol esters induce a rounding up of MDCK cells resulting in enhanced refractility and, under appropriate conditions, eventual loss of contact with neighboring cells. The perturbations which effect these changes are in evidence at the light microscopic level but undetectable with freeze fracture electron microscopy. The questions to be addressed were whether the changes so obvious at the light level affect organization of plasma membranes at the molecular level and, if so, what is the relationship between molecular motions and this type of transformation.

Figures

Figure II-1. Wiring diagram of perturbations associated with cellular transformation. Δ=change in; ρ=density.

Figure II-2. Pleiotypic effects of phorbol esters.

Figure II-3. Two-stage model of carcinogenesis. Dimethylbenz[α]anthracene (DMBA) is an initiator, i.e., exposure of organisms to this agent above a treshold concentration will result in tumors but below this level no tumors will be induced. If subthreshold initiator exposures are followed in a defined temporal sequence with a second chemical, a promoter, then tumor formation may be induced. Tumors will not be observed if promoter exposure is not preceded by initiator exposure.

Figure II-4. Structures of phorbol esters. a. TPA: R^1=tetradecanoyl, R^2=acetate; PDD: R^1=R^2=decanoyl. b. 4_α-PDD: R^1=R^2=decanoyl.

Figure II-5. MDCK cells under phase contrast optics. a. Control, i.e., treated with 0.005% MeOH for 2 hours at 37°C. b. Chemically transformed, i.e., treated with 50 ng/ml TPA in 0.005% MeOH for 2 hours at 37°C (X245).

Figure II-6. MDCK cells under Nomarski optics. Conditions same as in II-5 (X769).

Figure II-7. Freeze fracture electron micrograph of MDCK cell. Conditions for fixation and processing for Figures II-7 to II-10 were: subsequent to removal of media containing phorbol esters or methanol (control), the cells were washed twice with MEM, fixed in glutaraldehyde (buffer = minimal essential medium (MEM)) for one hour at 37^{o} in 2%, followed by (at room temperature) three washes with MEM, 20% glycerol in MEM, and freezing via freon 123 into liquid nitrogen). All fracturing was done as reported in reference 20. Apical surface E face depicting microvilli (X13,900).

Figure II-8. MDCK cell tight and gap junctions on lateral aspect of plasma membrane (X50,000).

Figure II-9. Nuclear envelope (X25,600).

Figure II-10. Cytoplasm of MDCK cell (X51,700).

Figure II-1

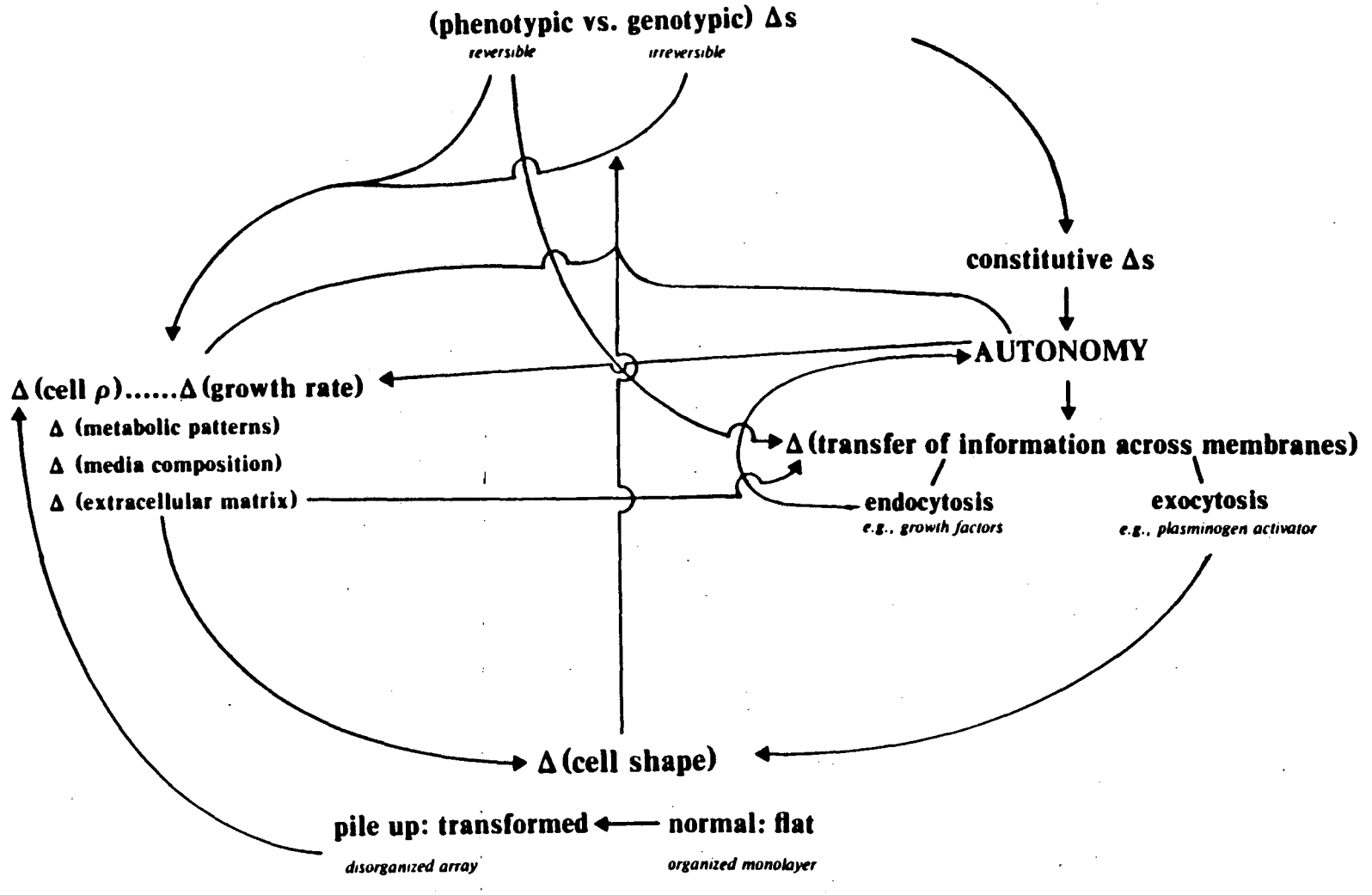
(phenotypic vs. genotypic) Δs
reversible
irreversible
constitutive Δs
AUTONOMY
Δ (cell ρ).....Δ (growth rate)
Δ (metabolic patterns)
Δ (media composition)
Δ (extracellular matrix)
Δ (transfer of information across membranes)
endocytosis
e.g., growth factors
exocytosis
e.g., plasminogen activator
Δ (cell shape)
pile up: transformed
disorganized array
normal: flat
organized monolayer

Figure II-2

Pleiotypic effects of phorbol esters

1. biologic

a. ↑ cell proliferation

b. inhibition or stimulation of differentiation

2. morphologic

↑ extension of cell processes (actin closely apposed to plasma membrane; intermediate filaments intact)

↓

cells elongate

↓

↓ flattening; rounding up

↓

↑ refractility

(↓ intercellular boundaries)

↓

↓ contact with neighboring cells

↓

loss of orientation

↓

↓ contact inhibition

3. biochemical

stimulation of macromolecular synthesis and proliferation

a. protein kinase C activity

b. Δ cXMP (↑cGMP, ↓cAMP)

c. ↑ PC (+ other phospholipids)

d. ↑ PGE, $PGE_{2\alpha}$ production ← deacylation of phospholipids

inhibited by indomethacin

e. ↑ microsomal enzymes, e.g., Na^+,K^+-ATPase, 5'-nucleotidase

f. induction of plasminogen activator

g. loss of surface fibronectin

h. ↑ hexose transport

i. metabolic cooperativity

j. Δ (growth factor binding)

4. biophysical

a. Δ (membrane rigidity)—fluorescence depolarization

b. ↑ cellular permeability

c. ↓ cellular electrical resistance

Figure II-3

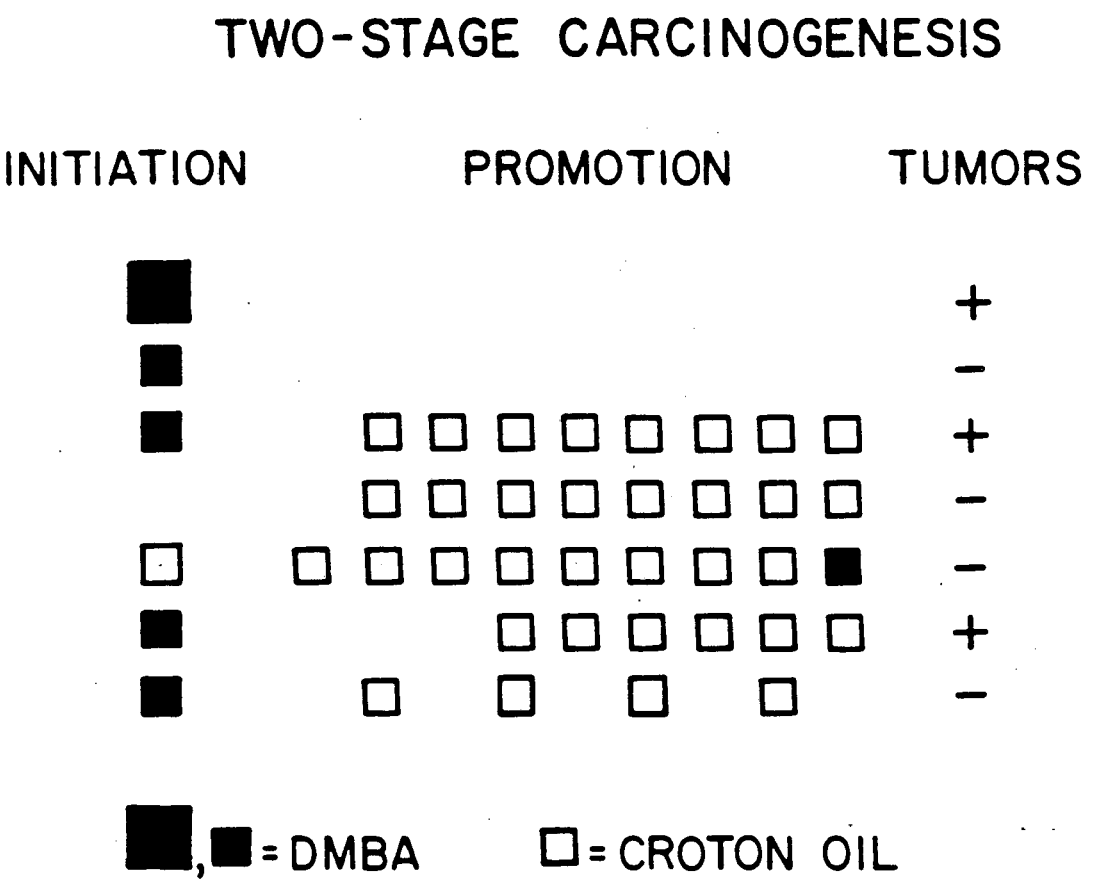

XBL 806-4243

Figure II-4

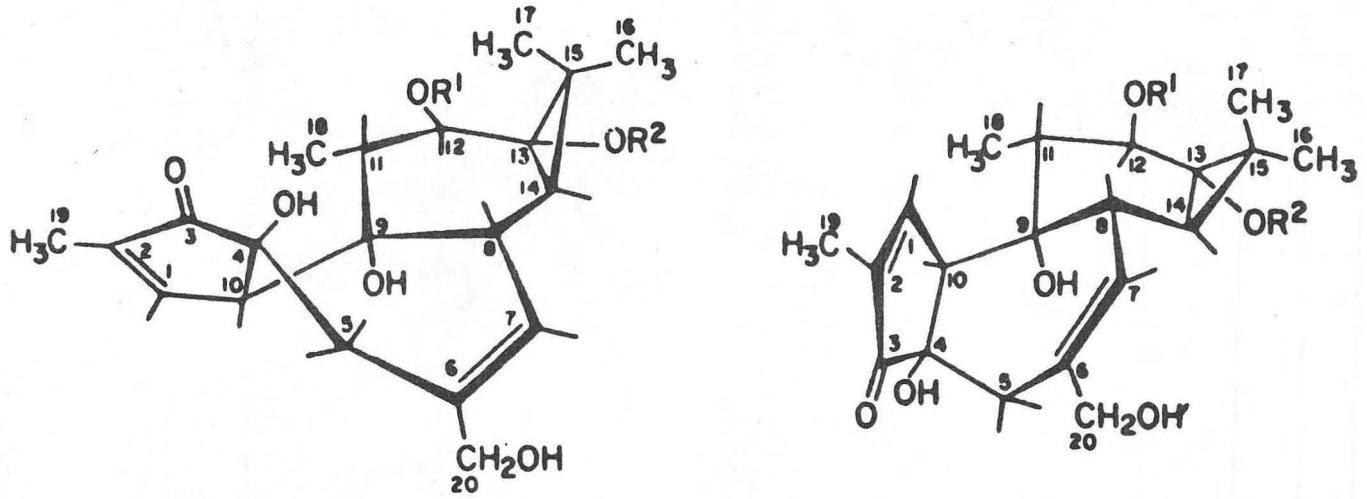

XBL 841-449

Figure II-5

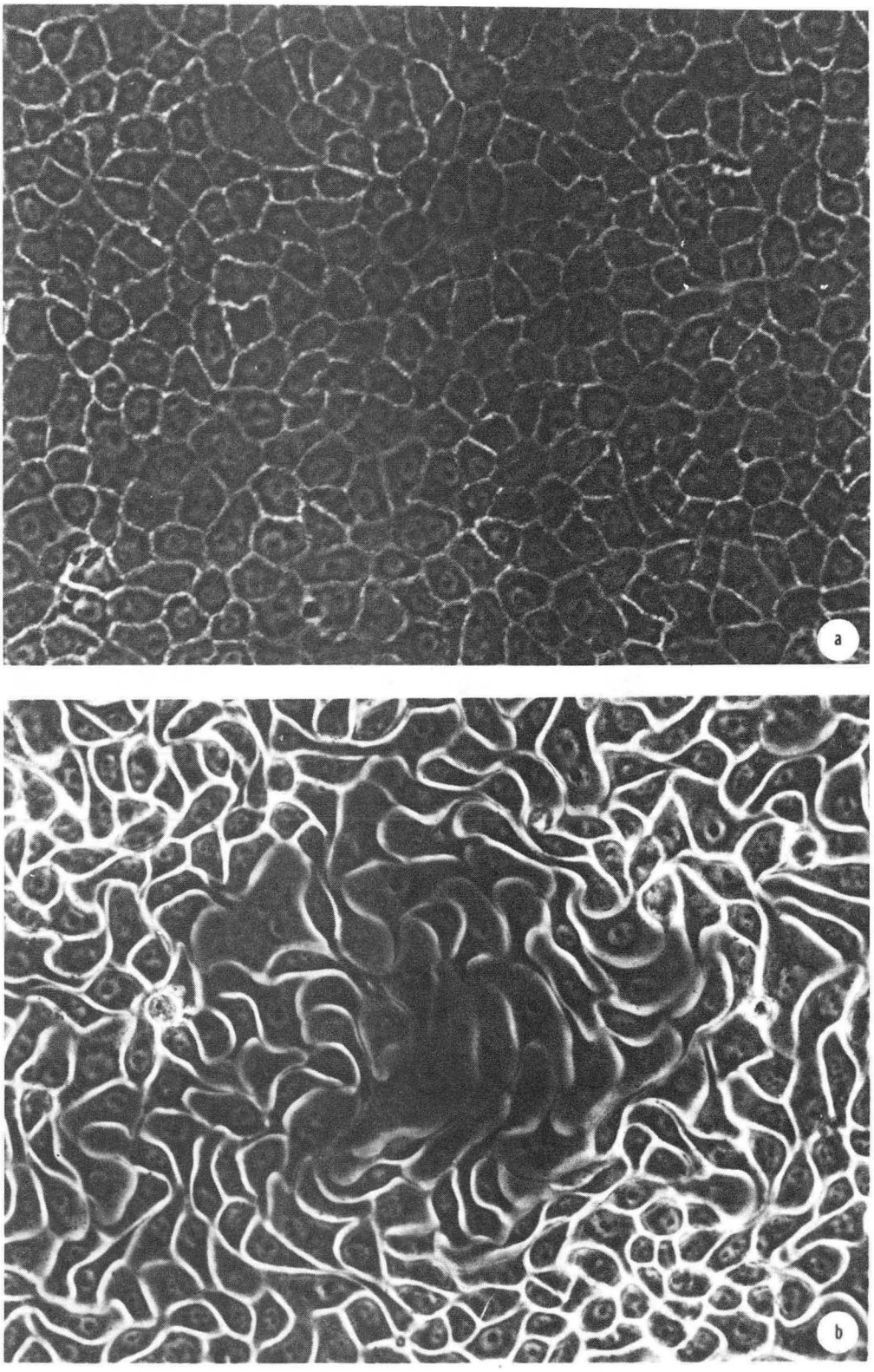

XBB 844-3171

Figure II-6

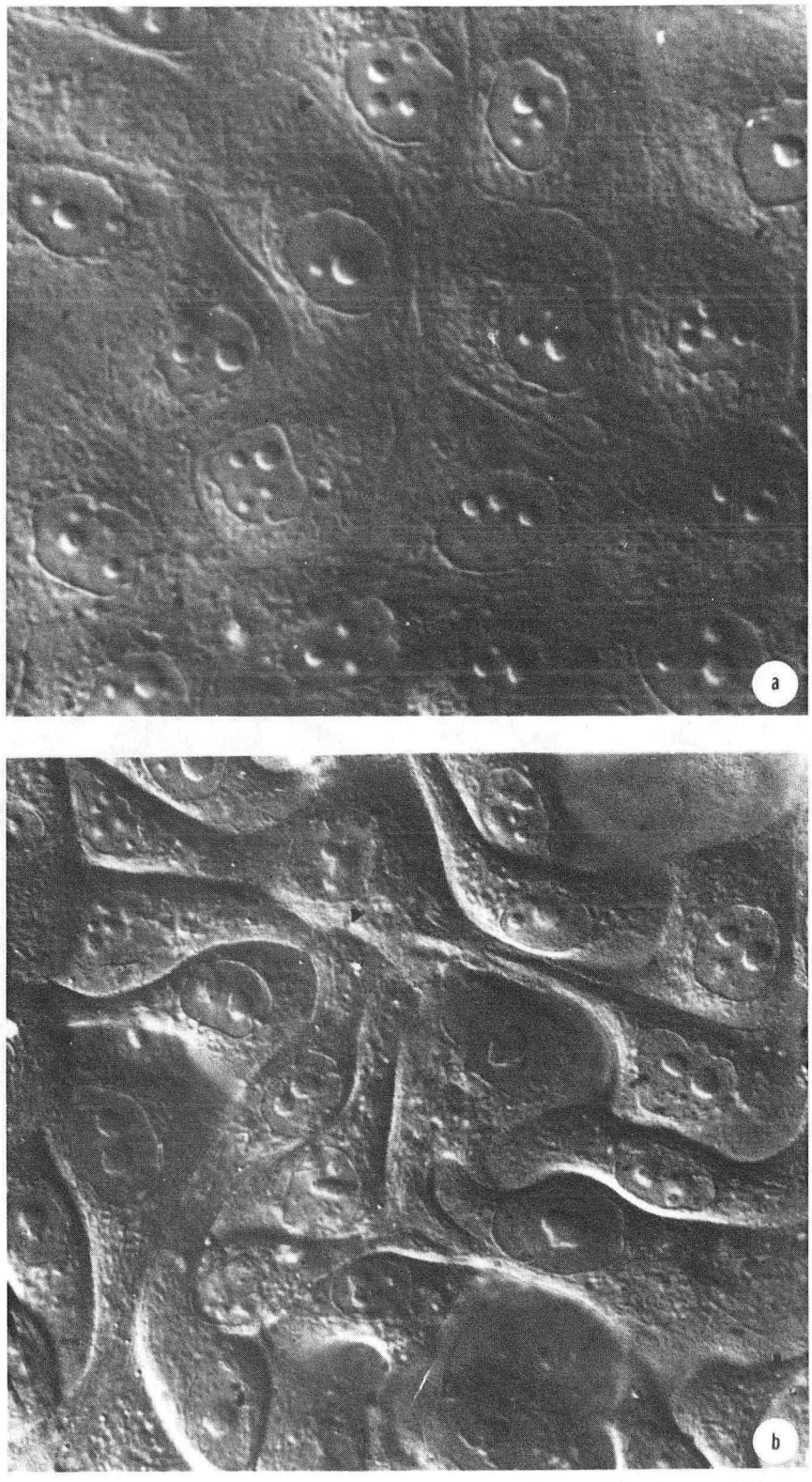

XBB 844-3172

Figure II-7

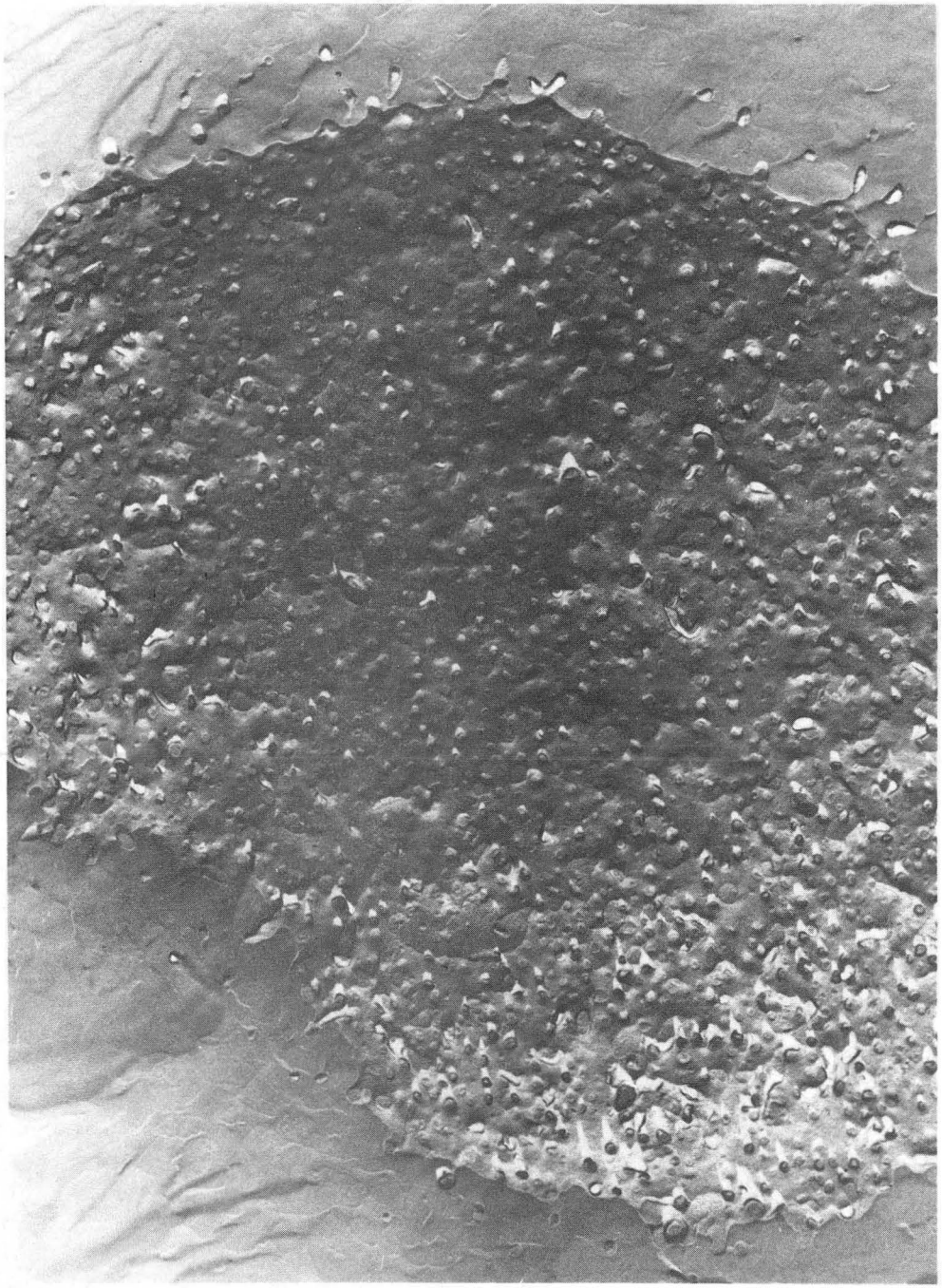

XBB 844-3173

Figure II-8

XBB 844-3174

Figure II-9

XBB 844-3175

Figure II-10

XBB 844-3176

References

1. Becker, F., ed. (1975-82) Cancer: a Comprehensive Treatise vol. 1-6. Plenum Press, New York
2. Carcinogenesis-a Comprehensive Survey. vol. 1-6 (1976-82) Raven Press, New York.
3. Bissell, M.J., Hatie, C., and Calvin, M. (1979) Proc. Nat. Acad. Sci. 76: 348-52.
4. Blumberg, P.M. (1980) Crit. Rev. Toxicol. 8: 153-97.
5. Diamond, L., O'Brien, T.G., and Baird, W.M. (1980) Adv. Ca. Res. 32: 1-74.
6. Driedger, P.E. and Blumberg, P.M. (1977) Cancer Res. 37: 3257-65.
7. Castagma, M., Takai, Y., Kaibuchi, K., Sano, K., Kikkawa, U., and Nishizuka, Y. (1982) J. Biol. Chem. 257: 7847-51.
8. Niedel, J.E., Kuhn, L.J. and Vandenbark, G.R. (1983) Proc. Nat. Acad. Sci. 80: 36-40.
9. Ohuchi, K. and Levine, L. (1978) J. Biol. Chem. 253: 451-60.
10. Shoyab, M., De Larco, J.E., and Todaro, G.J. (1979) Nature 279: 387-91
11. Lee, and Weinstein, B. (1978) Science 202: 313-5.
12. Brown, K.D., and Dicker, P., and Rozengurt, E. (1979) Biochem. Biophys. Res. Comm. 86: 1037-43.
13. Yaketani, Y. and Oka, T. (1983) Proc. Nat. Acad. Sci.

80: 2647-50.

14. Wertz, P.W. and Muller, G.C. (1978) Cancer Res. 38: 2900- 2904.
15. Cabral, F. Gottesmann, M.M., and Yuspa, S.H. (1981) Cancer Res. 41: 2025-8.
16. Fisher, P.B., Cogan, U., Horowitz, A.D., Schacter, D., and Weinstein, B. (1981) Biochem. Biophys. Res. Comm. 100: 370-6.
17. Ojakian, G.K. (1981) Cell 23: 95-103.
18. Yancey, S.B., Edens,J.E., Trosko, J.E., Chang, C.-C., and Revel, J.-P. (1982) Exp. Cell Res. 139: 329-40.
19. Madin, S.H. and Darby, N.B. As catalogued in: (1975) American Type Culture Collection of Strains 2: 47.
20. Fisher, K. and Branton, D. (1974) Meth. Enzym. 32: 35-44.

Chapter III

Fluorescent Probes

One of the major objectives of this work was to measure the lateral diffusion of molecules in the lipophilic/hydrophobic domains of the plasma membrane (Chapter IV); therefore, it was essential to use a probe molecule that would report exclusively from this membrane. The method of choice involved the use of a fluorescent molecule (Chapter IV).

Many reports have appeared in the literature in which the signal from a fluorophore has been reported to be coming exclusively from the plasma membrane (1,2). Structures of probes tried in this study are shown in Figure III-1.

As all of these molecules are amphiphilic with the ratio of hydrophobic to hydrophilic domains high, their solubilities in aqueous media are quite limited. Therefore, delivery to cells requires a cosolvent or carrier molecule; ethanol (final concentration = 0.4%) or lipid-free albumin (fluorophore:albumin::2:1) was used.

All four fluorophores tried (Figure III-1) showed similar patterns of staining: an initial fairly homogeneous distribution over the entire cell surface followed by the appearance of dots (ca. 0.5 μm diameter) exclusive of the nuclear region resulting in a punctate pattern (Figure III-2). The transition from homogeneity to heterogeneity can

best be described by a gradient with time the independent variable (This statement is approached experimentally in Chapter IV (Figure IV-5).). Thus, as visualized under the fluorescence microscope the dyes appeared to be associating with the plasma membrane initially, this being followed by internalization into intracellular vesicles. The method of delivery did not significantly affect this transition; neither a drop in temperature to $4^{o}C$ nor addition of fluorophores to cells in the presence of the metabolic inhibitor sodium azide (NaN_3) slowed down internalization sufficiently to make these conditions reasonable alternatives.

However, the magnitude of the gradient appeared to vary with the chemical structure of the probe molecule. 12-(N-methyl-N-7-(nitrobenz-2-oxa-1,3-diazol-4-yl)) phosphatidyl choline (NBD-PC) showed the highest surface to intracellular staining under the fluorescence microscope. As this molecule is a phospholipid with a zwitterionic headgroup, it was reasoned that perhaps by using a pseudodimer of this type of structure an attenuation of internalization could be achieved. Cardiolipin (CL), a phospholipid with four hydophobic long chains and two phosphates in the headgroup region, was chosen as the phospholipid component. Since a high degree of charge in the headgroup region seemed to be essential for retention in the plasma membrane and a molecule with a fluorescent signal was the objective, lissamine rhodamine-B sulfonyl chloride (LR) (structure

shown in Figure III-3) was chosen as the fluorophore. The latter is extremely sensitive to water (sulfonyl chloride is readily hydrolysed) and cardiolipin possesses a proton on the 2-carbon of the glycerol backbone that is ionizable; therefore, pyridine, a basic solvent that can be purified to an anhydous state, was used as the solvent.

LR (Molecular Probes, Junction City, OR.) and cardiolipin (PL Biochemicals, Inc., Milwaukee, WI. or Sigma Chemical Co., St. Louis, MO.) in a 2:1 ratio were stirred in pyridine for 24 hours at room temperature (Figure III-3). Dryness of the pyridine was absolutely essential; therefore, the solvent was refluxed for at least 24 hours over Na and benzophenone. All other manipulations involving starting materials were carried out in a dry box under inert conditions. After removal of the solvent, the product was spotted on silica gel plates, which were developed in chloroform:methanol:water::65:25:4. The single spot with an R_f of 0.70 was scraped and characterized.

The product was named collarein. This was derived as follows: the C and the first L from cardiolipin, the second L and the R from lissamine rhodamine, the "ein" from the prototypic fluorophore fluorescein, and the "O" and the "A" from the apparent collars the dye makes around the MDCK (and epithelial) cells (Figure III-4).

Characterization of collarein

Solubility Properties

The solubility properties of collarein were significantly different from those of the starting materials. Both CL and LR were soluble in dimethylsulfoxide and chloroform. In contrast, when the product was placed in either of these solvents in order to take an nmr spectrum, a heterogeneous solution was attained; the only organic solvent in which collarein showed significant solubility was methanol. Thus, all nmr data are from methanol solutions.

Optical spectra

Visible spectra were recorded using methanol as the solvent on a Hewlett-Packard spectrophotometer at concentrations increasing logarithmically over four orders of magnitude. The major peak in the visible spectrum (Figure III-5) occurred at 555 nm; a shoulder was present at 514 nm. The extinction coefficient at 555 nm was calculated to be *ca*. 1.2×10^5 (mole-cm/l) by the use of the Beer-Lambert law.

Fluorescence spectra of collarein in methanol (Figure III-6) were recorded on a Perkin-Elmer fluorescence spectrophotometer model MPF-2A, exciting at either 555 nm., the maximum absorption wavelength collarein, or 488 nm., the wavelength of the Ar ion laser being used at the time. Peaks in the emission spectra from both were at 574 nm.

Optimal conditions for homogeneous staining of MDCK cells (and three other epithelial cell lines) were as

follows: cells, which had been grown in medium containing 10% serum, were washed twice with serum-free minimal essential medium (MEM) at ambient temperature, incubated for 17 minutes with a solution of MEM containing collarein at an absorbance of 1.83 O.D. units; this was followed by six washes with MEM. Figure III-4 shows MDCK cells stained with collarein (control (a); TPA-treated (b)) under the fluorescence microscope. By optical sectioning using the argon ion laser as the exciting light, collarein appeared to be homogeneously distributed over both the apical and basolateral surfaces.

Glass coverslips on which the confluent cells had been grown and stained were removed and placed in quartz cuvettes. A fluorescence spectrum was obtained using an home-built instrument which has as its components a 500 W xenon arc lamp, grating monochromators for excitation and emission, and a single-photon counting detection system. The peak was centered at ca. 575 nm. An excitation spectrum showed 530 nm to be the most efficient exciting wavelength, i.e., the best signal:noise.

Mass Spectroscopy

Several attempts were made to attain a mass spectrum of this compound at both the Space Sciences Lab and the U.C. Berkeley Chemistry Department; the techniques of gas chromatography-mass spectroscopy and field ionization were used. However, in each case the compound decomposed before

any data were obtained.

NMR Spectra

Proton nmr spectra were taken on the U.C. Berkeley Chemistry Department 250 MHz spectrometer. The solvent for all spectra, d_4-methanol (99.96%) (Aldrich, Milwaukee, WI, or Eastman Chemical Co., Rochester, N.Y.,) has absorption peaks at 3.35 (methyl) and 4.95 (hydroxyl) downfield from the singlet of tetramethylsilane (TMS) (Aldrich) which was included in each tube as the standard (1% by volume).

In the spectrum of LR (Figure III-7) the ethyl groups are represented by a triplet at 1.35 ppm (methyls) and a quartet at 3.65 ppm (methylenes). The peaks from ca. 7 to 8.5 are due to the aromatic protons with the singlet at 8.7 coming from the proton between the sulfonate and sulfonyl chloride, the doublet at ca. 8.1 from the proton alpha to the sulfonyl chloride as drawn in Figure III-3 and beta to the three fused rings, and the multiplets between ca. 6.9 and 7.4 from the remaining aromatic protons. The ratios of the integrated areas are 20:9::aliphiatic:aromatic.

The ^{1}H-nmr spectrum of CL (Figure III-8) is represented by the absorptions from the aliphatic (including allylic) protons from 1 to 4.5 ppm and from the vinyl protons at ca. 5.5 ppm.

The peak positions in collarein's spectrum (Figure III-9) from 0 to ca. 5.5 ppm are a composite of peaks from the spectra of its starting materials. In the aromatic region

the doublet at ca. 8.1 ppm in the spectrum of LR has moved upfield; this is due to the replacement of a sulfonyl chloride by a sulfonate ester. Additional absorptions relative to the spectrum of LR in the aromatic region are observed due to the superposition of the pyridinium group in place of one of the phosphatidic acids of cardiolipin. The chemical shifts and integrated peak areas of (aliphatic + vinyl):aromatic::6.60:1 (vs. the theoretical prediction of 6.64) are consistent with the structure shown in Figure III-10.

Figures

Figure III-1. Stuctures of fluorescent probes which internalized in MDCK cells within 15 minutes: a. NBD-cholesterol. b. DiI-C_{16}. c. NBD-phosphatidyl choline (tailgroup labeled). d. rhodamine headgroup-labeled phosphatidyl ethanolamine.

Figure III-2. MDCK cells after incubation with rhodamine-B. An initial fairly homogeneous distribution is followed by the appearance of "dots" exclusive of the nuclear region. (X640).

Figure III-3. Synthesis of collarein. Lissamine rhodamine-B sulfonyl chloride plus cardiolipin in dry pyridine.

Figure III-4. MDCK cells after a 17 minute incubation with collarein. Note apparent collars around cell in addition to apical staining. (a) Control (0.005% methanol) cells. (b) TPA-treated cells. (X640).

Figure III-5. Visible absorption spectrum of collarein in methanol. The major peak is at 555 nm and a shoulder is present at 514 nm.

Figure III-6. Emission spectra of collarein. a. $\lambda_{excitation}$=554 nm. b. $\lambda_{excitation}$=488 nm.

Figure III-7. Proton nmr spectrum of lissamine rhodamine-B

sulfonyl chloride. Peaks at 3.35 and 4.95 ppm are due to absorptions from the methyl and hydroxyl protons, respectively, of impurities in d_4-methanol, the solvent. These peaks are present in the spectra of Figures III-7,8, and 9. The triplet centered at 1.35, the quartet at 3.65, and the peaks from ca. 7 to 8.5 ppm are from the methyl, methylene, and aromatic protons, respectively.

Figure III-8. Proton nmr spectrum of cardiolipin. (solvent = d_4-methanol).

Figure III-9. Proton nmr spectum of collarein. (solvent = d_4-methanol).

Figure III-10. Structure of collarein.

Figure III-1

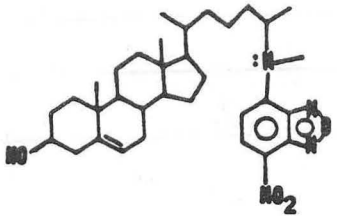

a

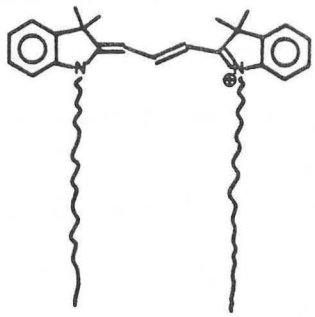

b

c

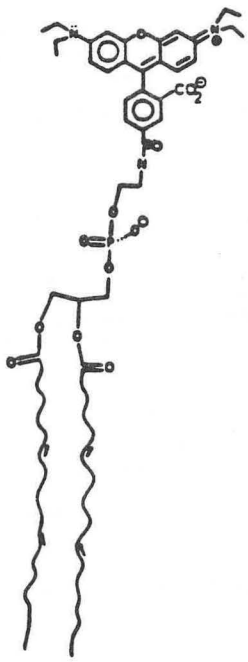

d

Figure III-2

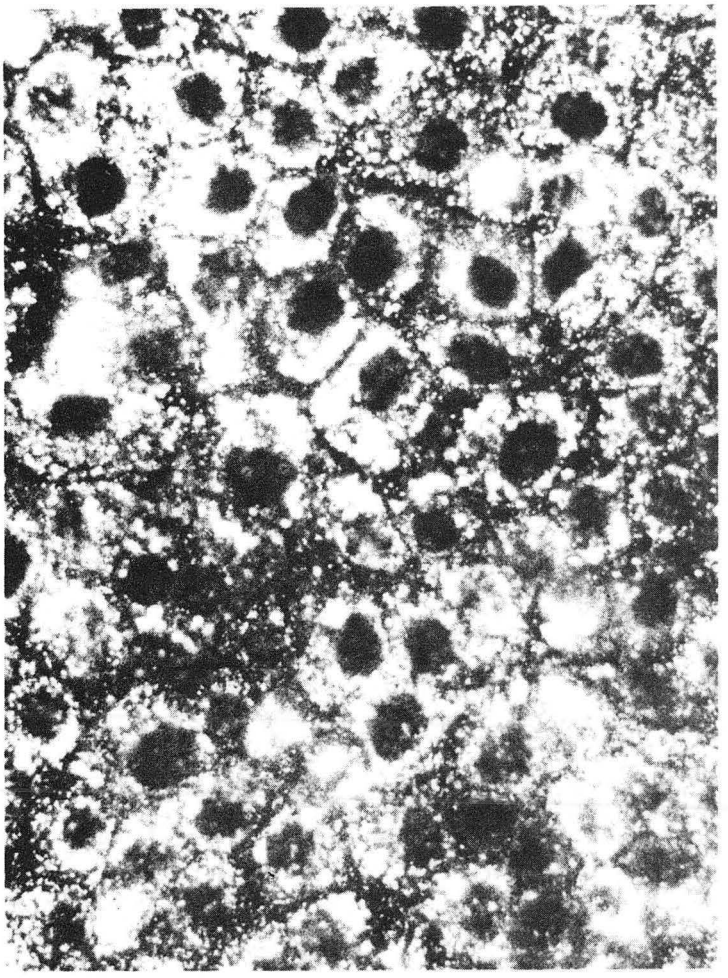

XBB 844-3177

Figure III-3

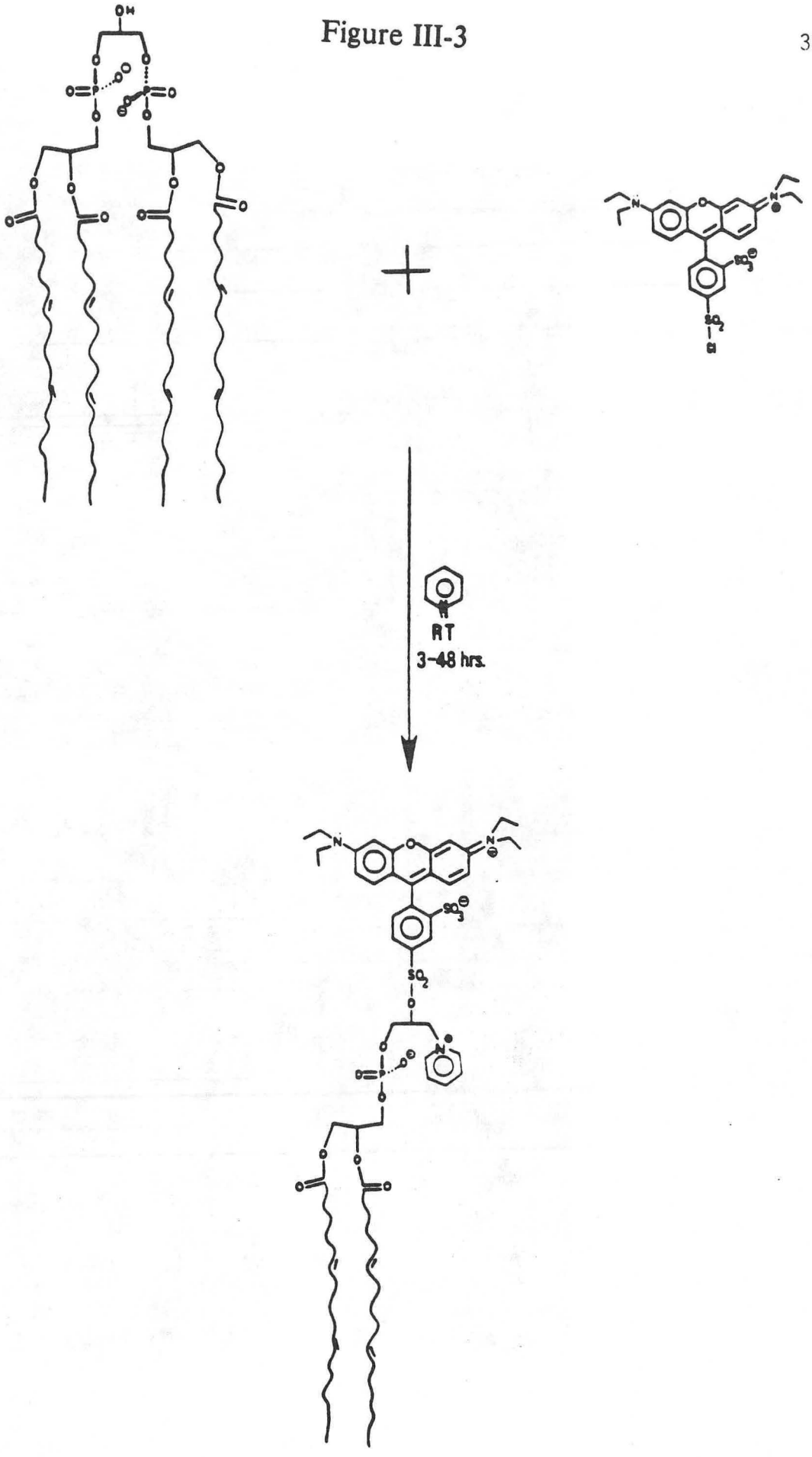

Figure III-4

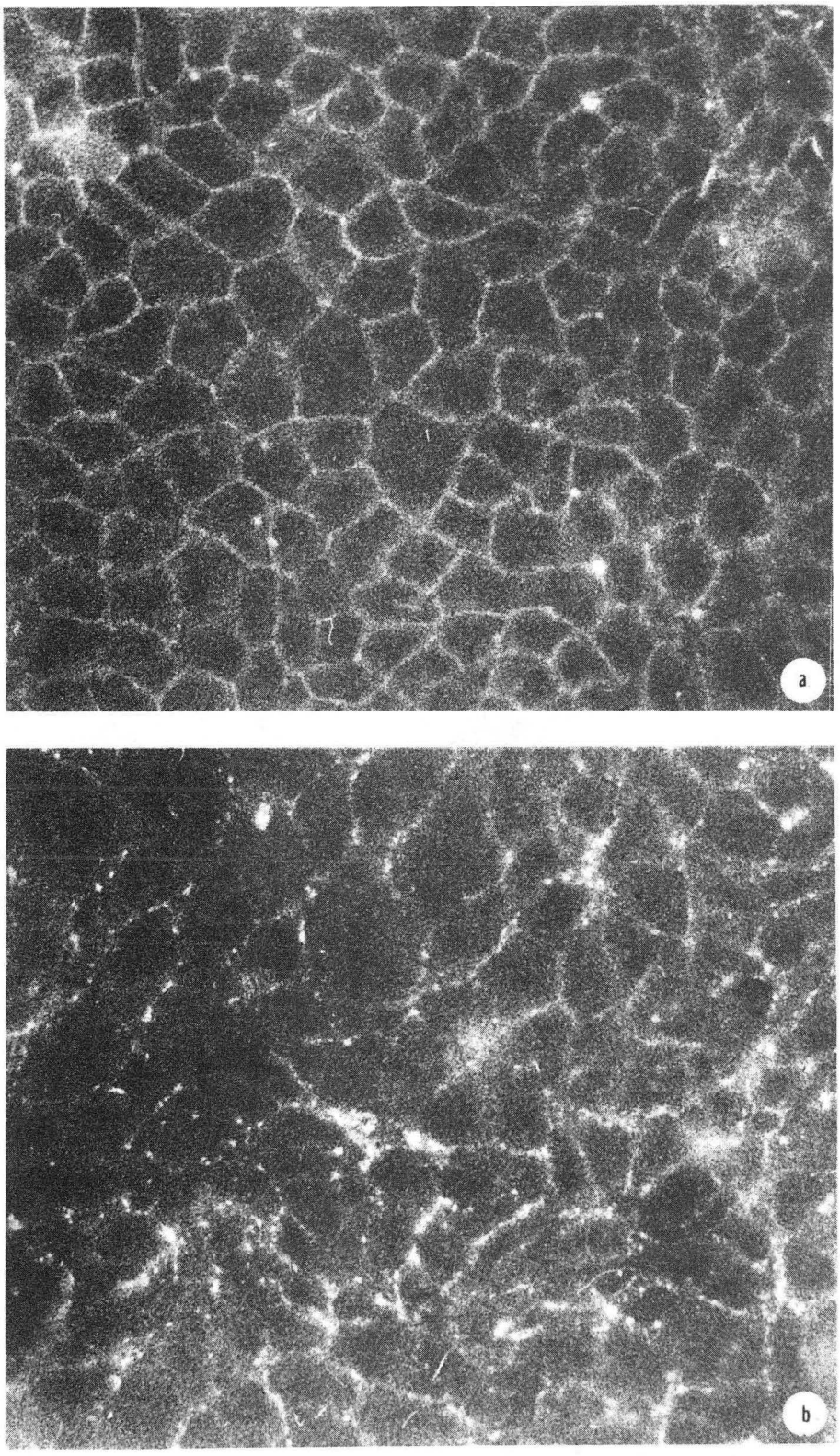

XBB 844-3178

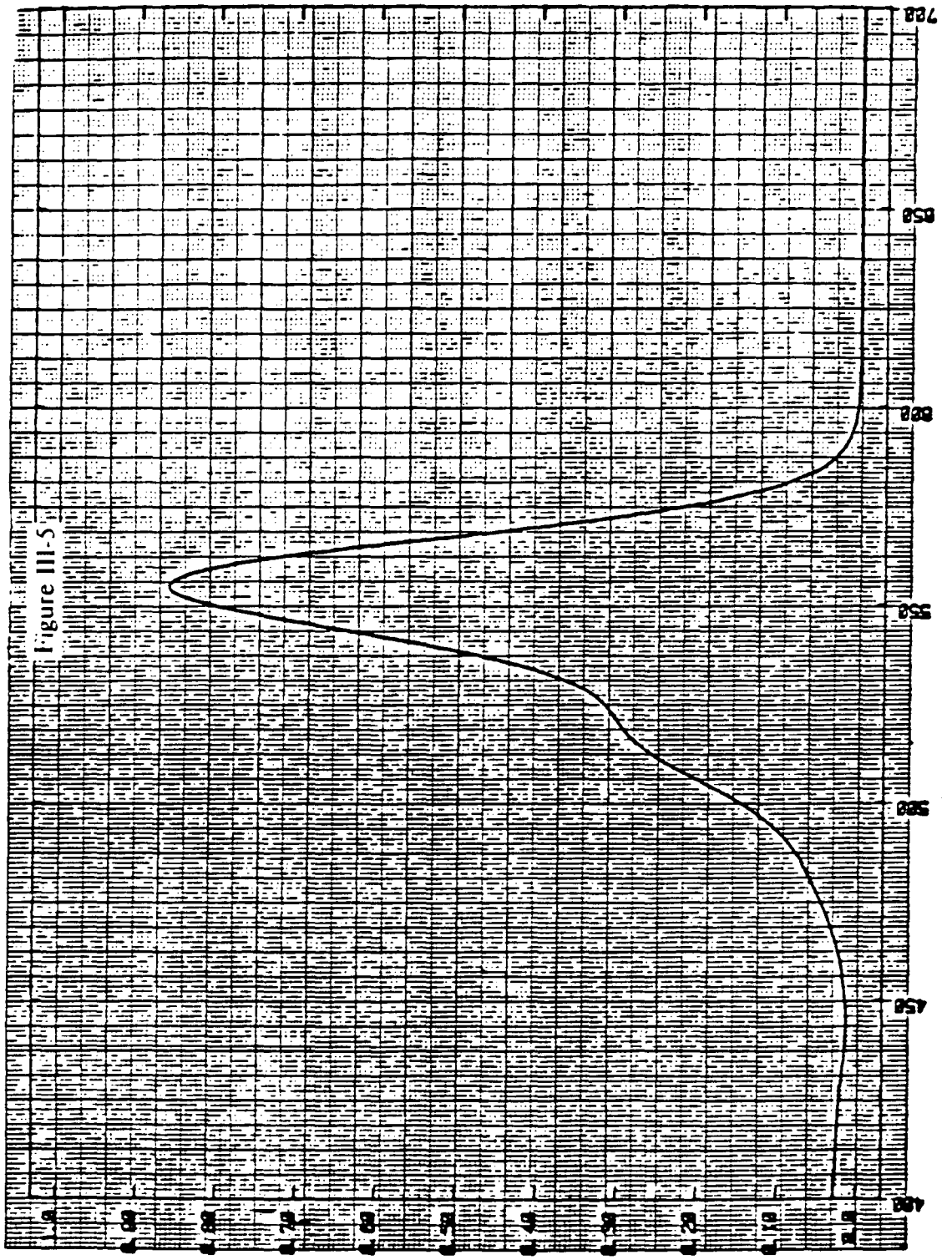

Figure III-5

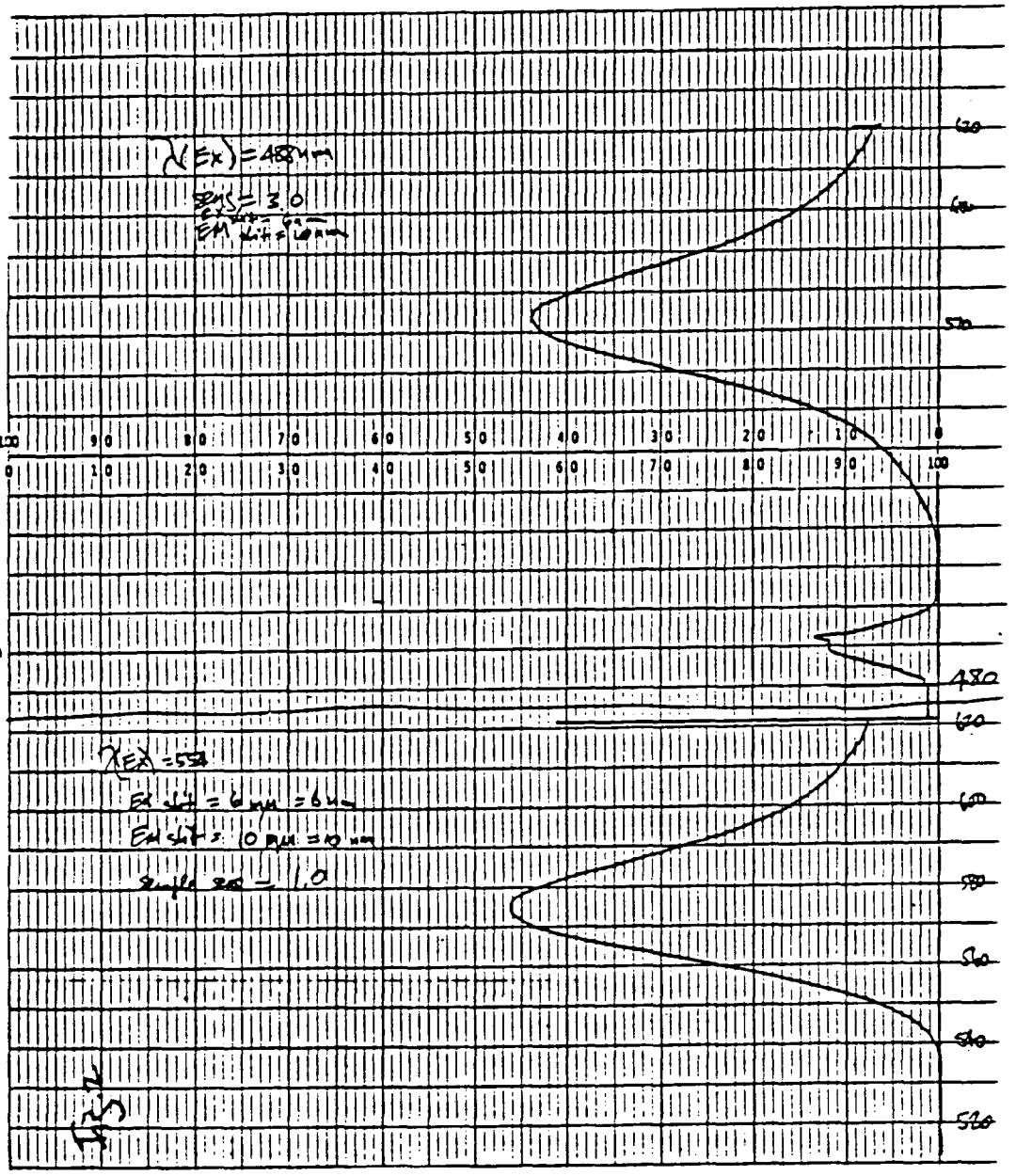
λ(Ex) = 488 nm
Ex slit = 6 nm = 6 nm
Em slit = 10 nm = 10 nm
Sample rate = 1.0
λ(Ex) = 554
Ex slit = 6 nm = 6 nm
Em slit = 10 nm = 10 nm
Sample rate = 1.0

Figure III-6

Figure III-7

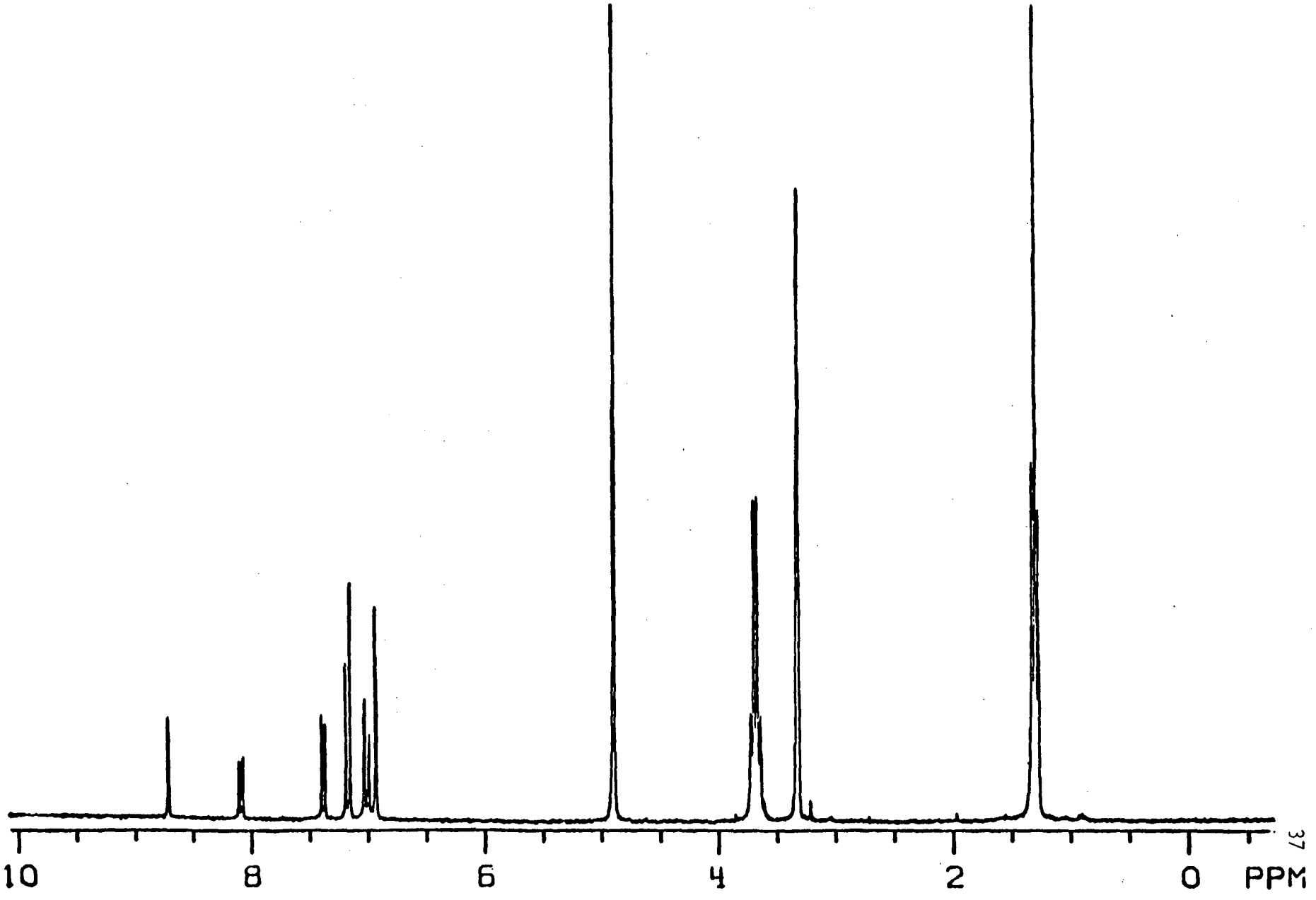

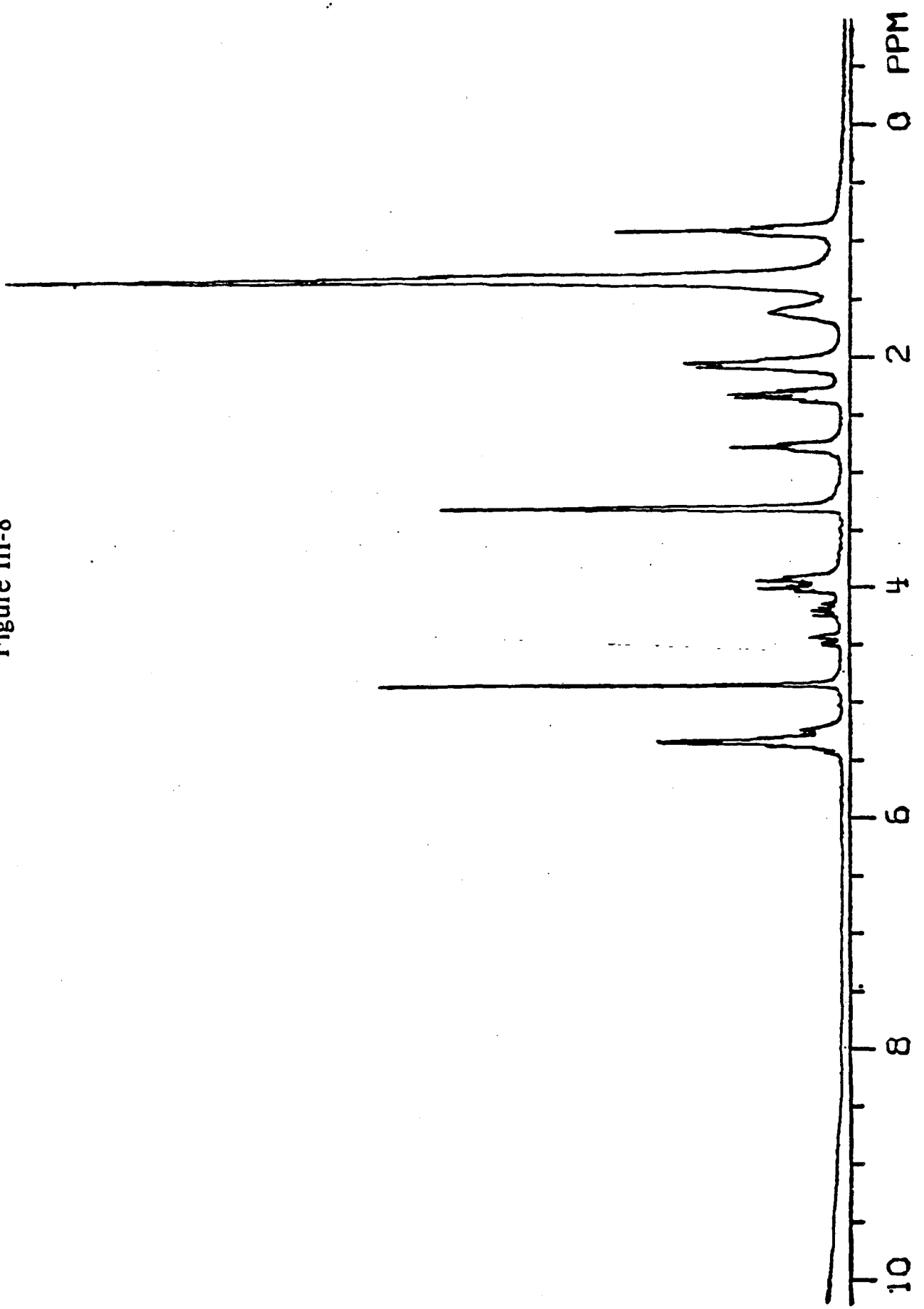

Figure III-8

Figure III-9

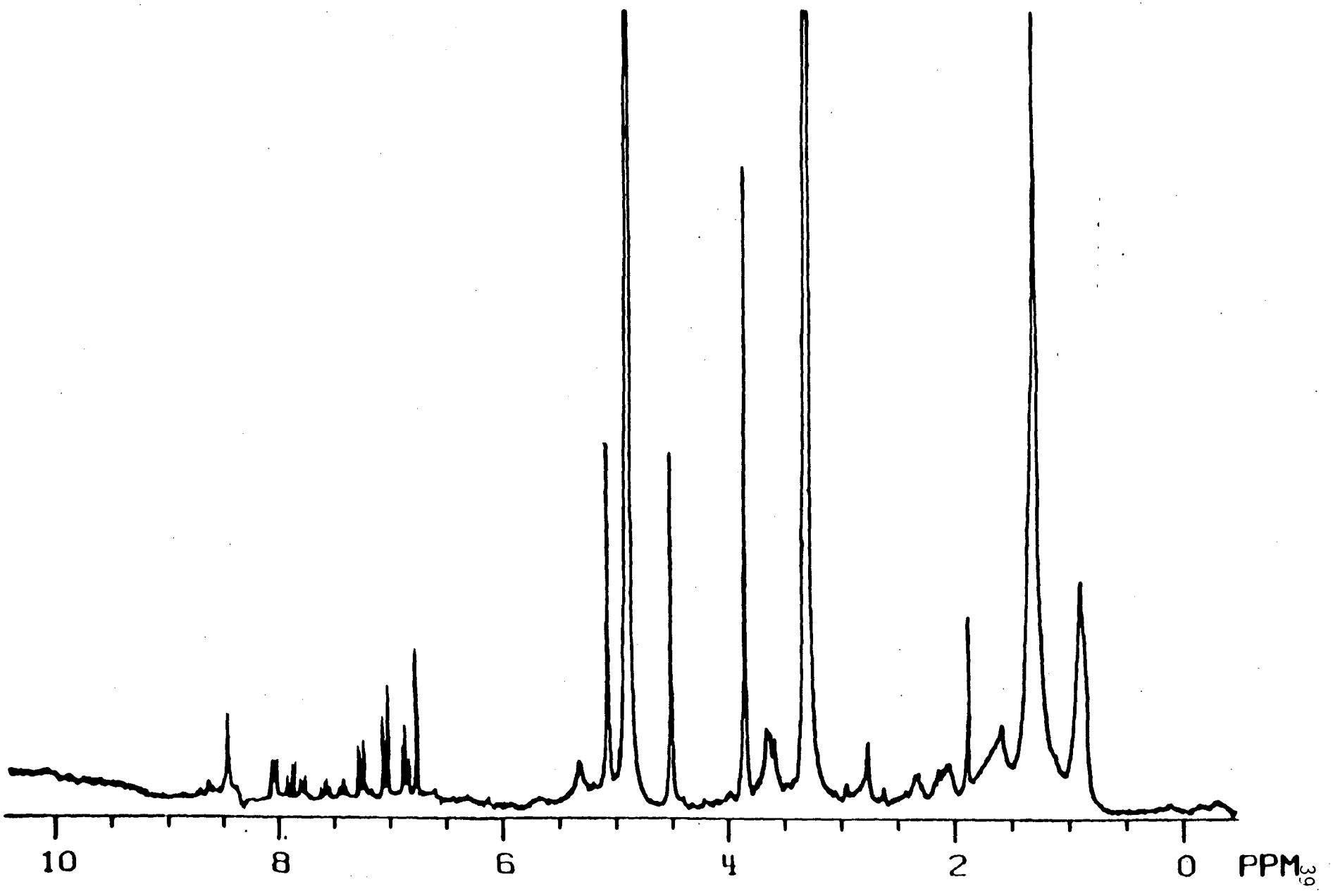

Figure III-10

Collarein

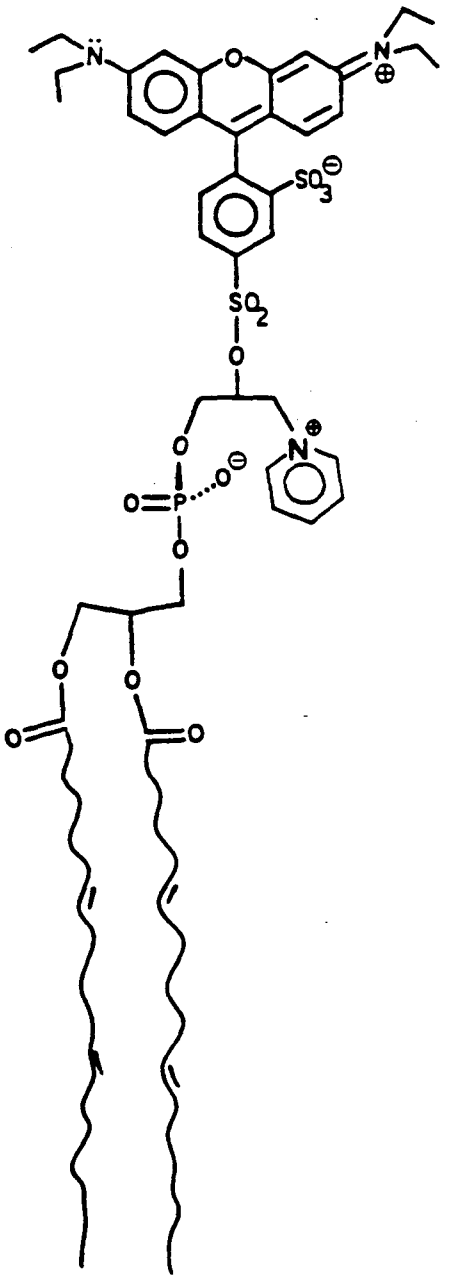

References

1. Taylor, D.L. and Wang, Y.-L. (1980) Nature 284: 405-10.

2. Dragsten, P.R., Blumenthal, R., and Handler, J.S. (1981) Nature 294: 718-22.

Chapter IV

Fluorescence Lifetimes

Fluorescence lifetimes are functions of environment; some factors which may influence the magnitude of this parameter are listed in Figure IV-1. In order to define more clearly the apparent spatial homogeneity and consequent putative environmental exclusivity of collarein (Chapter III), the fluorescence lifetime of this synthetic fluorescent phospholipid was measured in Madin-Darby canine kidney (MDCK) cells. These results were compared with the lifetime data of fluorophores that showed heterogeneous spatial distributions in the same cells.

To gain more insight into the environmental sensitivity of this type of measurement in systems of biologic interest fluorescence lifetime measurements were performed on fluorophore-containing liposomes possessing various physical and chemical characteristics. Additionally, absorption, emission, lifetime, and fluorescence yield values of a fluorescent molecule in five solvents over a range of concentrations are presented in the appendix to this chapter.

Cells

The use of molecular probes for studying cellular phenomena requires knowledge of probe locations (1). For

fluorescent molecules locations are usually determined by inspection under a fluorescence microscope, steady state fluorescence spectroscopy, and/or subcellular fractionation (2,3). The first method of detection, within its resolution limit, presents the spatial distribution, but environmental information of a very limited nature, the second is often of insufficient environmental sensitivity to distinguish among cellular compartments, and the third requires destructive manipulations. Measurement of fluorescence lifetimes (4,5) is a noninvasive type of kinetic spectroscopy for determining fluorescence compartmentalization and may provide a complementary or additional class of information in cases where any or all of the currently used methods are deficient.

In this work the principle of variation in lifetimes with environment to measure quantitatively the fraction of fluorescence in different cellular compartments in parallel with visualization under the fluorescence microscope was used. After brief periods of incubation with different dyes, cells of the Madin-Darby canine kidney (MDCK) line exhibited particular patterns when examined under the fluorescence microscope. Based on the known sensitivities of fluorescent molecules to their environments (5), we predicted that partitioning of such molecules among physically and/or chemically distinct cellular compartments would give rise to a distribution of fluorescence lifetimes.

Subsequent to incubation with rhodamine-B (Figure IV-

2a) or the indocarbocyanine diI-C_3-16 (diI) (Figure IV-2b), MDCK cells exhibit spatial heterogeneity under the fluorescence microscope and multiple component lifetimes. In contrast, collarein (Figure IV-2c), a rhodamine-B derivative that was designed and synthesized for the property of localization in the plasma membrane, appears to be homogeneously and exclusively distributed over the cell surface; this dye exhibits a single-component lifetime.

In addition the long-term time-dependent behaviors of these fluorescence distributions were studied.

Materials and Methods

Cells

Monolayer cultures of Madin-Darby Canine Kidney (MDCK) cells, were grown to confluence on glass coverslips (ca. 10 X 22 mm) in Minimal Essential Medium (MEM) (GIBCO, Grand Island, N.Y.) containing 10% fetal calf serum (GIBCO) and 20 mM Hepes buffer (Sigma) at pH 7.4, 310 mosm, and 37°C. After two washes with serum free medium, cells were exposed to serum free media containing fluorescent dyes for periods of time specific for each dye and dye concentration. After six washes with phosphate buffered saline (PBS), coverslips were either examined and photographed under a Zeiss fluorescence microscope or transferred to cuvettes which were then placed in the fluorescence lifetime apparatus.

For radioactive tracer studies, cultures were exposed to 0.05% trypsin (Difco, Detroit, MI) for 15 or 25 minutes after isotope exposure and subsequent washings. (The number of adherent cells remained constant pre- and post-trypsin treatment due to the fact that MDCK cells contain tight junctions and the trypsin solution was free of any chelating agent.) Following six more washes, cells were exposed to 2.0% sodium dodecyl sulfate for two minutes, removed with a rubber policeman, and counted for ^{14}C incorporation.

Dyes. Rhodamine-B (Sigma Chemical Co., St. Louis, MO or laser grade from Eastman Kodak Chemicals, Rochester, NY) was diluted to a final concentration of 8 μg/ml. DiI,

synthesized by the method of Sims et al (6), was either diluted via ethanol (final concentration 0.4%) or complexed to lipid-free albumin (Sigma and/or ^{14}C-labeled from Miles Laboratories, Elkhart, IN.) at a ratio of two dye molecules to one protein (7); the concentration of diI in both incubation media was 2 μg/ml.

Lifetime measurements. Fluorescence lifetimes were measured by a single-photon timing system using a previously described apparatus (8,9) which contains a Spectra Physics synchronously-pumped mode-locked dye laser (SP 171 argon ion laser, SP 362 mode locker, and modified SP 375 dye laser) operating with rhodamine 6G with a 12 nsec pulse separation and a pulse full-width at half maximum of ca. 8 psec. The limit of resolution of the instrument is ca. 25 psec. Excitation of samples was at 580 nm and emission was detected at 650 nm with a cooled RCA C31034A photomultiplier. Cells were counted long enough to acquire a predetermined number of photons in the peak channel of a 1024-channel Northern NS636 multichannel analyzer. The response function (curves labeled E in figures 3,5,6, and 7) of the apparatus was determined by measuring the scattering of the pulsed laser light at the excitation wavelength (580 nm) from a sample containing unlabeled cells or a colloidal suspension of Ludox particles. Background scattering by the Ludox particles at the emission wavelength rarely exceeded the dark count rate. The scattering function was

deconvolved from the raw data leading to the true decay. The true decay was obtained by iterative reconvolution with an assumed decay law approximated by a sum of exponentials:

$$r = \sum_{i}^{n} \alpha_i e^{-t/\tau_i}$$

where α_i is the fraction, normalized to one, of fluorescence with lifetime τ_i. Minimizations of the deviations between experimental and reconvoluted curves were achieved by using the minimal number of terms for convergence (10). Deviations from attempted fits are indicated by the pattern and magnitude of ΔI.

Results

Incubation of MDCK cells with rhodamine-B. Cells, incubated with rhodamine-B for three minutes at room temperature, exhibited evidence of more than one fluorescent component both under the fluorescence microscope (Figure IV-3a) and by measurement of the fluorescence decay in the fluorescence lifetime apparatus (Figure IV-4). Under the microscope, fluorescence appeared to be distributed mainly in two locations: the apical plasma membrane and vesicular accumulations exclusive of the nuclear region. A single exponential component fit to the measured fluorescence decay curve gave large deviations (Figure IV-4a) (ΔI units of 1000). A two-exponential component fit (Figure IV-4b) resulted in a significant improvement as indicated by the pattern and decrease in ΔI units from 1000 to 400. Inclusion of a third component did not statistically improve the fit. Thus, the molecule has at least two environments which lead to two resolvable lifetimes.

A time-dependent study showed (Figure IV-5) that the normalized fraction of the long lifetime component decreased linearly over a 120 minute time course while the short lifetime component showed complementary behavior. (The sum of amplitudes of the two components, α_1 and α_2, is normalized to unity at each time point.) Additionally, the total fluorescence yield decreased for the first sixty minutes after which it leveled off. The latter may be due to a catabolic mechanism which approaches saturation at 60

minutes.

MDCK cells plus diI. As diI is water insoluble, it requires a carrier; two were tried: ethanol and lipid free albumin. Time of incubation for both was 5 minutes at room temperature. Delivery via either carrier resulted in a similar fluorescence distribution under the fluorescence microscope (Figure IV-3b).

A single exponential decay component fit for data obtained from cells incubated with diI delivered via ethanol showed large deviations (Figure IV-6a). The exponential series mode was employed to fit these data as the computer was unable to attain a reasonable fit in the normal nonlinear least squares mode due to its limit of resolving four exponential components. Figure IV-6b shows the most reasonable (by the criterion of the minimal value of ΔI) fit attained -- five components.

A single component showed large deviations for data from diI delivered via albumin (Figure IV-7a). (The lifetime of diI as part of the albumin complex is ca. 45 psec.) However, the computer was able to effectively minimize deviations with two components (Figure IV-7b).

For diI delivered via either system the number and relative fractions of molecules with each lifetime remained fairly constant for 120 minutes, with spectra taken every 30 minutes. (The lifetimes of diI in acellular PBS, solubilized via either carrier, was predominantly 45 psec.)

However, total fluorescence yields were dramatically different between the two systems. For ethanol delivery the fluoresence yield remained constant, increasing just slightly over the 120 minute time course. In contrast, diI delivered via albumin, showed a three-fold increase in fluorescence yield, leveling off between 75 and 120 minutes.

The diI-albumin experiment was performed four times. Qualitatively, data were the same, i.e., two lifetime components and the fluorescence yield increasing with time, finally leveling off; quantitatively, lifetimes varied within limits: for the long lifetime component, 1.18 to 2.50 nsec. and for the short lifetime component 0.360 to 0.790 nsec., with fluorescence yield leveling off at 75 to 120 minutes.

To probe the fluorescence yield increase further, diI was delivered via ^{14}C-spiked albumin. Following a five minute incubation with this radioactive complex, cells were exposed to 0.05% trypsin for 15 or 25 minutes. After six washes with PBS, 50-60% of the radioactivity remained with the cells, and fluorescence data were fit by two exponentials. However, the fraction of molecules with the long lifetime was significantly decreased (less than 10% as opposed to 20-46% without trypsinization) and the lifetime of this component was significantly increased relative to nontrypsin-treated cells. (In some cases, decay was not completed by the next laser pulse.).

Additionally, when medium containing the diI-albumin

complex was pipetted onto the cellular monolayer and removed immediately, a small but finite amount of radioactivity, that was trypsin insensitive, remained associated with the cells. Examination under the fluorescence microscope indicated that all fluorescence appeared in vesicular structures, exclusive of the nuclear region.

MDCK cells plus collarein. Exposure of cells to collarein resulted in a homogeneous distribution of fluorescence over the cell surface, both the apical and basolateral aspects (Figure IV-3c). The fluorescence decay curve of collarein is fit with a single exponential (Figure IV-8a). When a two-component fit was attempted, a second component with a lifetime (1 psec.) below the limit of resolution of the instrument and a negative amplitude appeared (Figure IV-8b). Single exponential fits showed deviations due to just statistical noise to data acquired for each spectrum at thirty minute intervals over a four and one-half hour period. The total fluorescence continuously decreased over time.

Discussion

Because fluorescence lifetimes are functions of environments, the number of spectroscopically distinguishable environments a fluorophore occupies can be reflected in the multiplicity of its lifetime components. The functional dependence of fluorescence lifetimes on environment was used to study the kinetics and multicomponent behavior of three fluorescent molecules.

When cells that have been incubated with rhodamine-B for three minutes are examined under a fluorescence microscope, the fluorescence appears to be on the apical surface and in intracellular vesicles. (The initial entry of dye into the cells is probably by diffusion as evidenced by the rapid time course.) The fluorescence lifetime decay curve is best fit by two exponentials, with time constants of about 1.9 and 0.3 nsec. (Figure IV-4b). As time progresses, the plasma membrane component is endocytized (probably by an adsorptive mechanism) (11)), and the concentration of fluorescence in the vesicular compartment increases (Figure IV-3a); the decay curves are fit in temporal sequence by an increasing fraction of short lifetime component (Figure IV-5). It is reasonable to ascribe the decrease in lifetime when going from the cellular surface to the intracellular vesicles to the increasing proximity of dye molecules to each other, making quenching more facile. (This mechanism was suggested by the decrease in lifetime that we observed when these

measurements were performed on a series of acellular, graded solutions of rhodamine-B in PBS as the concentration was increased from 8 to 800 μg/ml.) The decrease in overall fluorescence is probably due principally to cellular catabolism as the fluorescence yield is also diminished in dye containing cells that have been kept in the dark; quenching is probably an additional influencing factor.

When diI was delivered by either ethanol dilution or as part of an albumin complex, the spatial distribution of fluorescence was not significantly different (Figure IV-3b). However, ethanol may induce sufficient cellular alteration that the dye molecules take up a near continuum of environments and, hence, exhibit a corresponding distribution of lifetimes. Nonexponential behavior and a negative amplitude of one component (α_4) indicative of energy transfer are suggested in the data analysis; a negative amplitude due to a rise time has been reported for low temperature fluorescence kinetic behavior of chlorophyll pigments in spinach chloroplasts (11). Nonrandom behavior in the deviations' plot over the time interval corresponding to the exciting pulse may be a reflection of this rise time and/or some Raman scattering. This type of reasoning would help to account for the large number of components (five) required for a reasonable fit (Figure IV-6). However, as the computer program is inefficient at resolving more than four lifetimes, the significance of these data and fit is questionable.

In constrast, data from cells to which diI was delivered as part of an albumin complex were fit by a sum of two exponentials (Figure (IV-7b); curves were almost superimposable (slight shortening of the decay time) over a 120 minute time course. This two-component behavior in conjunction with the increasing fluorescence yield is consistent with there being a total of three cellular compartments in which the dye can reside (Figure IV-9). Initially, it can bind to both the plasma membrane and intracellular vesicles. With time the surface component may be endocytized into vesicles. (As with rhodamine-B, the fraction of vesicular dye at time t=0 probably has entered the cell by a diffusive process with later internalization due to adsorptive endocytosis.) Fluorophores can then redistribute into intracellular membranes from which a small fraction may recycle back to the plasma membrane, perhaps as part of the normal cellular membrane recycling (12). The environments within the two membrane compartments may be expected to be fairly similar and, thus, when populated at similar concentrations, it is reasonable to expect lifetimes to be fairly close. In nontrypsin-treated cells lifetimes within a 1.18 to 2.50 nsec range are observed. The increase in the long lifetime component observed in cells treated with trypsin, an enzyme thought to act only on surface proteins, can be explained by a decrease in fluorophore concentration in the plasma membrane compartment, resulting in a decrease in fluorophore-

fluorophore proximity and, thus, less efficient quenching. As with rhodamine-B, the increased mutual proximity of dye molecules in the vesicles would be expected to result in decreased lifetimes. If the fluorescence yields in the various compartments differ and fluorophores are traversing from one to another, then only when steady state levels are approached would the fluorescence yield be expected to level off (13).

In contrast to rhodamine-B and diI, collarein, a fluorescent dye that was designed and synthesized for the property of exclusive localization in the plasma membrane, exhibits homogeneous fluorescence over the cell surface under the fluorescence microscope (Figure IV-3c); spectra taken every half hour up to four and one-half hours after removal of the dye containing medium were fit by single exponentials with deviations due only to statistical noise (Figure IV-8). These data are consistent with this synthetic, fluorescent phospholipid having a single environment when in a fluorescent state. (The appearance of the 1 psec lifetime is physically meaningless in an instrument with a limit of resolution of ca. 25 psec.) The observed decrease in fluoresence yield is probably due to catabolism or conversion to an otherwise nonfluorescent state.

Liposome studies

To gain a deeper understanding of the influence of the physical environment on fluorescence lifetimes, measurements of the 1,1'-dialkyl-3,3,3',3'-tetramethylindocarbocyanine (D_NDiI-C_3 (N = 12, 18, and 22) probes (Figure IV-2b) in a series of phospholipid bilayer environments were made. The effects of the bilayer physical state and DiI chain length, DiI concentration, charge and hydrogen bonding in the head group region, and cholesterol concentration were examined. Decays for fluorophores in all systems in this study were best fit by a sum of two exponentials. Both the magnitude of the average lifetime and the percent due to a short (300±190 psec.) lifetime component corresponded with the degree of order of phospholipids in the bilayer.

Materials and Methods

All phospholipids were purchased from Sigma (St. Louis, MO.) and stored at -20°C; previous batches from these lots had been verified to be of 99+% purity by thin-layer chromatography and quantitation with an Iatroscan TH-10 analyzer and differential scanning calorimetry (15). The C_NDiI's were prepared by Molecular Probes (Junction City, OR.) as perchlorates. Their structure is shown in Figure IV-2b. Purity of the dyes was confirmed by thin-layer chromatography.

For sample preparation, the dyes were dissolved in $CHCl_3$:MeOH::2:1, and their concentrations were determined

spectrophotometrically (14). For the preparation of liposomes appropriate concentrations of lipids were premixed in $CHCl_3$:MeOH::2:1. A solution of dye and lipids was shaken on a Vortex, dried at room temperature under vacuum for at least eight hours and stored under nitrogen.

Liposome preparations. All liposomes were made by the following procedure: Phosphate buffered saline (PBS) at 80-82°C was added to test tubes containing phospholipid and dye molecules (also equilibrated to 80-82°C) dried on the tube walls. The tubes were rigorously agitated using a Vortex immediately for a total of 60 sec, returning them to the 80-82° water bath every 20 sec for 2-5 sec. After equilibration to room temperature, contents were transferred to quartz cuvettes and measurements were performed.

Liposomes in the gel, fluid, and 1:1::gel:fluid states were obtained by using distearoylphosphatidyl choline (DSPC), dioleylphosphatidyl choline (DOPC), and a 1:1::DSPC:DOPC mixture. (Phase transitions occur for DSPC and DOPC at 55 and -12°C, resp.) In order to determine partition coefficients diIs of chain lengths 12, 18, and 22 at a concentration of $1:10^4$::diI:phospholipid were present in each tube so that for this set of experiments a total of nine measurements was made.

To examine the effect of DiI concentration on fluorescence lifetimes a series of egg phosphatidyl choline (PC) liposomes was made with the concentration of DiI (N=18) increasing from 9.9×10^{-4} to 9.1 mole %.

The effects of headgroups and surface charge were examined by comparing the measured parameters of diI in the following phospholipidic environments: phosphatidylcholine (DOPC,DSPC), phosphatidylcholine:phosphatidylethanolamine (DPPC:DPPE)::1:1, stearylamine (SA), and phosphatidic acid (PA). The dye:phospholipid ratio was $1:10^4$ as above.

The effect of cholesterol was examined by measuring a series of DPPC liposomes which contained cholesterol concentrations ranging from 0 to 50 mole% in increments of 5%.

Lifetime measurements. Fluorescence lifetimes were measured by the instrument described above for the cell work except that for the diI-liposomes measurements the dye laser was removed. Thus, the 514.5 line of the argon ion laser was used as the source of excitation; fluorescence of diI was detected at 565 nm. Samples were counted long enough to acquire 1×10^4 photons in the peak channel of the multichannel analyzer. The response function (curves labeled E in figure 2) of the apparatus was determined by measuring the scattering of the pulsed laser light at the excitation wavelength (514.5 nm.) from an unlabeled liposome sample or a colloidal suspension of Ludox particles.

Data Analysis

The average lifetime was defined as:

$$\langle \tau \rangle = \frac{\sum_{i=1}^{n} \int t \alpha_i e^{-t/\tau_i}}{\sum_{i=1}^{n} \int \alpha_i e^{-t/\tau_i}}$$

which, upon integration, is:

$$\langle\tau\rangle = \frac{\sum_{i=1}^{n} \alpha_i \tau_i^2}{\sum_{i=1}^{n} \alpha_i \tau_i}$$

Partition coefficients. The following assumptions were made in the derivation of the partition coefficient in the gel phase, (α_g):

(1) The signal is composed of α_g, the fraction of the signal from the biexponential decay of diI in the gel state, and α_f ($1-\alpha_g$), the fraction from the biexponential decay of diI in the fluid state. Therefore, it is necessary to include four exponential terms in the expression for the average lifetime ($\langle\tau\rangle$), i.e., two from the gel and two from the fluid.

(2) The 1:1::DSPC:DOPC mixture exhibits the behavior of a system containing equal parts of gel and fluid phase. Therefore, if all of the dye partitions into one phase, then the diI:phospholipid will be twice that as in the monophospholipid systems.

Using these assumptions, the average lifetime is represented by:

$$\langle\tau\rangle = \frac{\alpha_g \sum_{i=1}^{n} \alpha_{ig} \tau_{ig}^2 + (1-\alpha_g) \sum_{i=1}^{n} \alpha_{if} \tau_{if}^2}{\alpha_g \sum_{i=1}^{n} \alpha_{ig} \tau_{ig} + (1-\alpha_g) \sum_{i=1}^{n} \alpha_{if} \tau_{if}} \qquad \text{where } n=2$$

By rearranging and collecting terms, one can make the following substitutions:

$$TF_i = \tau_{if}\langle\tau\rangle - \tau_{if}^2$$

$$TG_i = \tau_{ig}\langle\tau\rangle - \tau_{ig}^2$$

Thus, the fraction of diI in the gel phase, α_g, is:

$$\alpha_g = \frac{\sum_{i=1}^{n} \alpha_{if} TF_i}{\sum_{i=1}^{n} (-\alpha_{ig}) TG_i + \sum_{i=1}^{n} \alpha_{if} TF_i} \qquad \text{where n=2}$$

and α_f, the fraction in the fluid phase, is equivalent to 1-α_g.

Results

In all cases DiI's in bilayer environments did not exhibit monoexponential decays; empirically, convergence was approached when curves were fit by a sum of two exponential terms. Data from the four experiments are given in Tables IV-1 and IV-2.

Physical states. Using the data of Table IV-2 with the equations derived in the materials and methods section, one obtains the following partition coefficients:

$$C_{12}: \alpha_g = 0.01$$

$$C_{18}: \alpha_g = 0.93$$

$$C_{22}: \alpha_g = 0.22$$

Concentration Series. The average lifetime is plotted as a function of the logarithm to the base ten of the percent diI:phospholipid in Figure IV-10. These data indicate that up to $1:10^3$::DiI:phospholipid the average lifetime yield is approximately linear; above this concentration the lifetime begins a rapid descent.

Headgroup Series. Plots of the average lifetimes as functions of additions of positive, i.e., stearylamine, and negative, i.e., phosphatidic acid, resp., charge are shown in Figure IV-11.

Cholesterol Series. The average lifetime is plotted as a function of cholesterol concentration in DPPC in Figure IV-12. As the concentration of cholesterol is increased the average lifetime rises slightly between 0 and 10%; this is followed by a sharp rise (from ca. 1.2 to 1.5 nsec.) between

10 and 20%. The value remains at ca. 1.5 nsec. from 20 to 30%. Above 30% the average lifetime drops and at 45%. begins to level off at ca. 1.1 nsec. Figure IV-13 shows that above 20% cholesterol the relative ratio of short to long lifetimes also is affected. Up to 20% cholesterol the short component (τ_1 ca 330 psec.) contributes ca. 20% to the total lifetime. Above this concentration the contribution of the shorter lifetime (α_2) begins to increase as its magnitude (τ_2) decreases.

Discussion

In the present study the $C_N$diI's exhibited nonmonoexponential decays in all bilayer systems studied. This is in agreement with much data obtained by others for fluorescent dyes in noncellular systems (16,17). The nonmonoexponentiality may derive from ground state microheterogeneity or excited state reactions (4) as well as physical contacts between probe molecules.

Partitioning behavior of an amphipilic probe into phopholipid bilayer environments is a function of the interactions of both the acyl chains and the headgoups (18-21). Thus, the selectivity of probes which differ only by chain lengths is due to interactions in the hydrophobic core of the bilayer predominantly. If lengths of the acyl chains of the phosphlipids are identical and, thus, the gel and fluid phases are a consequence of the degree of unsaturation only, one would predict that a probe of chain length equivalent to that of the phospholipid tails would select the more ordered gel phase where its presence would cause virtually no perturbation in the packing of the hydrophobic tails and therefore an entropy change of decreased magnitude compared with the fluid phase. This appears to be the case for C_{18}-DiI which shows a 9:1 preference for the gel phase.

In contrast, DiI with a chain length of sufficient dissimilarity to that of the phospholipids would be expected to perturb the tight packing of the gel state and, therefore, to partition into the more disordered fluid with

greater facility. Thus, due to the ability of a shorter chain to cause the terminal regions of the phospholipid chains to kink and a longer probe chain to bend in order to fit the bilayer thickness, one would predict that DiI with a twelve or twenty carbon chain, resp., would prefer the fluid phase. Therefore, it is not surprising to calculate for C_{12}-DiI virtually no affinity for the gel phase (α_g=0.00)and for C_{22}-DiI ca. a 4:1 preference for the fluid while C_{18}-DiI selects the gel 9:1 over the fluid. Additionally, the average lifetime is the longest for those probes that prefer the gel state and find one into which to partition, e.g., DiI-C_{18} in DSPC or the 1:1 mixture.

The almost linear dependence of the average lifetime on the log(DiI/PC) (Figure IV-10) in the $1/10^4$ concentration range suggest that variations observed in these values in various bilayer environments are induced by the physical state of the surrounding lipids as opposed to probe-probe associations per se.

As in all liposome systems studied, upon initial addition of a second phospholipid to a bilayer with a single headgroup both the average lifetime and the fluorescence yield drop. As the concentration of the second lipid is increased the effect of charge can be observed to be consistent with the basic electrostatic maxim that complexes composed of oppositely charged species tend to be more stable than those composed of similarly charged components. DiI possesses a positively charged headgroup and would be

expected to be electrostatically attracted to the negatively charged phosphatidic acid in contrast to the expected repulsion from the positively charged stearylamine. Therefore, an increase in lifetime with increasing negative charge as phosphatidic acid is doped into bilayer environment(s) and the inverse relationship with increasing positive charge in the form of stearylamine (Figure IV-11) are consistent with this concept. Thus, the headgroup series also supports the association of order with increased fluorescence lifetime and yield.

Phosphatidylethanolamine (PE) by virtue of its ability to hydrogen bond may cause an increase in order in the headgroup region; this may explain the protracted lifetime and consequent increased average lifetime observed in the presence of PE (Table IV-1). Consistent with this is the lack of a pretransition observed for phosphatidylethanolamines which has been ascribed to the relatively small headgroup size (22).

Data from the cholesterol series are in accord with its observed effects on phase transitions in lipid bilayers (23-25). The peak in average lifetime which is centered between 20 and 30 mole% cholesterol (Figure IV-12) suggests that in this range the diI molecules are probing an environment of relatively increased order. Presti et al have suggested that below 20 mole% pure phospholipid domains coexist with 2:1::phospholipid:cholesterol complexes, between 20 and 33 mole% boundary lipids are disappearing leaving the 2:1

complexes in media of increasing cholesterol concentration, and between 33 and 50 mole% cholesterol-rich domains coexist with the remaining phospholipids in 1:1 hydrogen-bonded complexes with cholesterol (26). The putative association of the first and tighter associating phospholipid with cholesterol is via a hydrogen bond between the carbonyl in the 2-position of the glycerol backbone of the phospholpid and the β-hydroxyl of the cholesterol. Since diI does not possess a hydroxyl but does have the amphiphilic character of a phospholipid, in the 0 to 20 mole% range the dye is probably probing both the remaining pure phospholipid domains and acting as the second and looser associating lipid with cholesterol; the average lifetimes observed in this range are in accord with this suggestion. In the 20 to 33% range the probe's mobility is restrained due to the almost homogeneous, rigid environment; thus, the order has increased as has the average lifetime. Above 33 mole% there is no longer a pure phospholipid phase; the membranes have become so rich in cholesterol that each cholesterol molecule can find but one phospholipid with which to associate. This results in the phospholipid-cholesterol associations become predominantly 1:1 complexes. Since the diI molecules associate with cholesterol as a second amphiphilic molecule and thus require a finite degree of mobility, the addition of cholesterol above ca. 30 mole% appears to limit the ability of diI molecules to find cholesterol-phospholipid complexes in order to associate with them. This may result

in the dye molcules self-aggregating with a consequent increase in the percent of short lifetime component (Figure IV-13) and, therefore, a diminished average lifetime (Figure IV-12).

Thus, the increases in average lifetime induced by either the addition of phoshatidylethanol, a phospholipid with a small headgroup and potential to hydrogen bond, or cholesterol (in the 20 and 30 mole%), a steroid containing a β-hydroxyl, may be due to the abilities of either to act as a filler with the resultant abolishment of pretransitions (26).

The general features of this study point toward a correlation between the degree of order in the bilayer and the average lifetime. Thus, as the degree of order in a phospholipid bilayer environment increases, the fluorescence lifetime of an amphiphilic fluorescent molecule increases.

Figures

Figure IV-1: Some factors which may influence fluorescence lifetimes.

Figure IV-2: Structures of three fluorescent dyes. (a) rhodamine-B, (b) the carbocyanine diI with two C_{16} chains and a three carbon bridge, (c) collarein.

Figure IV-3: Fluorescence micrographs of MDCK cells stained with (a) rhodamine-B, 60 minutes after incubation, (b) diI, and (c) collarein.

Figure IV-4: Fluorescence decay curve of MDCK cells subsequent to incubation with rhodamine-B. Curves labeled E are the excitation profiles induced by the laser pulse and the response of the system. Curves labeled F are the experimental fluorescence decay (noisy) and the calculated fit (smooth) essentially superimposed. Deviations' plots are below. Fits for: (a) single exponential and (b) sum of two exponentials. The ordinates in all cases are in photon counts.

Figure IV-5: The amplitudes of long lifetime (□-□-□-[ ]), short lifetime (0-0-0-0) and total (normalized to t=0 value) fluorescence yield (X-X-X-X) as functions of time after incubation

with rhodamine-B). (Amplitudes are normalized such that = 1 at each time point.) (The long lifetime component at t = 0 is always present in greater abundance than the short; however, exact slopes vary depending on cell culture passage number.)

Figure IV-6: Fluorescence decay curve for MDCK cells plus diI introduced via ethanol. (a) single exponential and (b) sum of five exponentials.

Figure IV-7: Fluorescence decay curve for MDCK cells plus diI introduced via albumin complexation. (a) single exponential and (b) sum of two exponentials.

Figure IV-8: Fluorescence decay curve for MDCK cells after exposure to collarein. (a) single exponential and (b) two exponentials. (The lifetime of collarein in PBS is ca. 1.5 nsec.)

Figure IV-9: Three compartment model to describe the distribution of diI delivered via albumin complexation. a. The plasma membrane (τ>1.18 nsec.). b. Intracellular vesicles (0.36 < τ < 0.79 nsec.). c. Intracellular membranes (>1.18 nsec.)

Figure IV-10: The average fluorescence lifetime ($<\tau>$) and the logarithm to the base 10 of the normalized fluorescence yield (log(NFY)) are plotted as a function of the logarithm to the base 10 of the

Tables

Table IV-1: Lifetime data from liposomes studies. Columns represent composition of liposomes, lifetimes (t) using one component fits (1-comp), fractions (a_i) and lifetimes (t_i) using two component fits (2-comp), and average lifetimes (<t>), respectively. Additionally, in some cases normalized fluorescence yield (NFY) data are given. Data from five experiments presented are: gel vs. fluid, concentration series, headgroups, cholesterol series, and H-bonding.

Table IV-2: Data from gel vs. fluid study in matrix format. α_n=fraction of fluorescence with lifetime τ_n. Centrally located number, e.g., 0.89 for DSPC/C_{12}DiI, is the average lifetime (<τ>).

Figure IV-1

Factors affecting τ

1. pH
2. metal ion concentration
3. viscosity
4. polarity
5. hydrophilicity
   hydrophobicity
6. dielectric constant
7. shift in absorption spectrum
   shift in emission spectrum
8. proximity to acceptor
9. self-quenching

XBL 832-8186

Figure IV-2

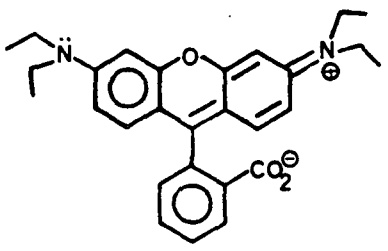

a

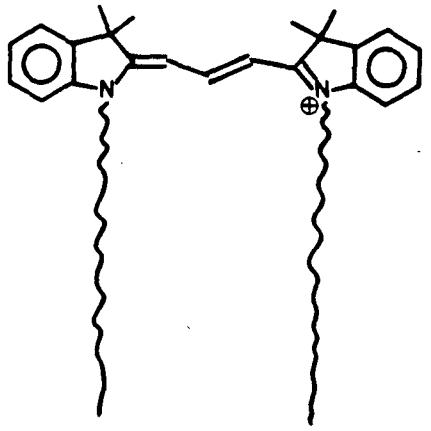

b

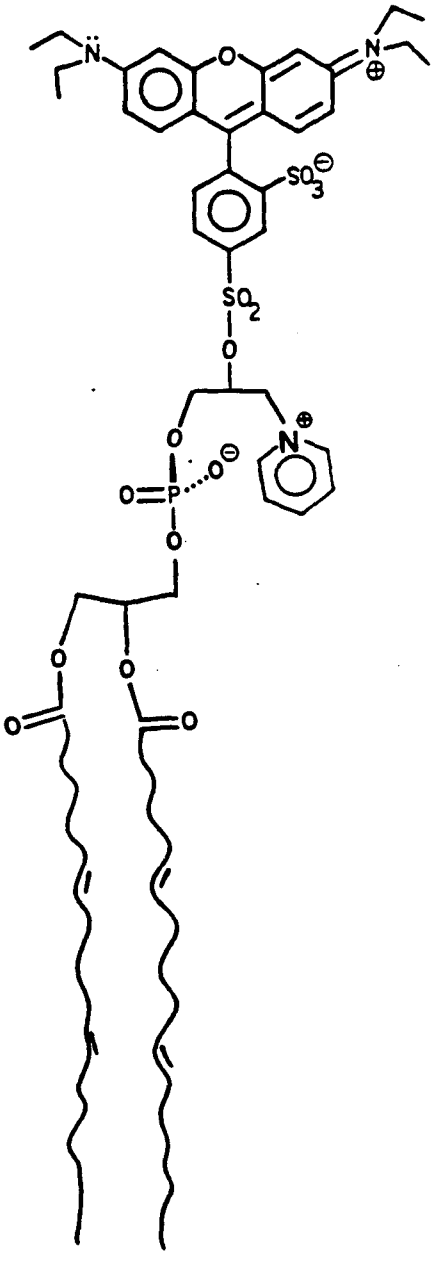

c

Figure IV-3

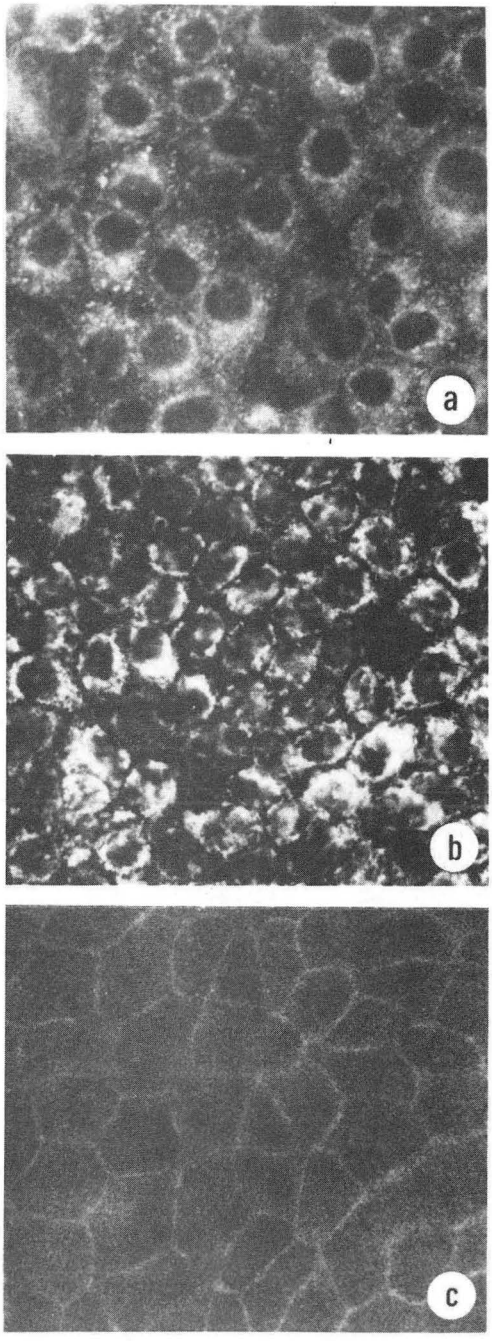

XBB 8210-8688B

Figure IV-4

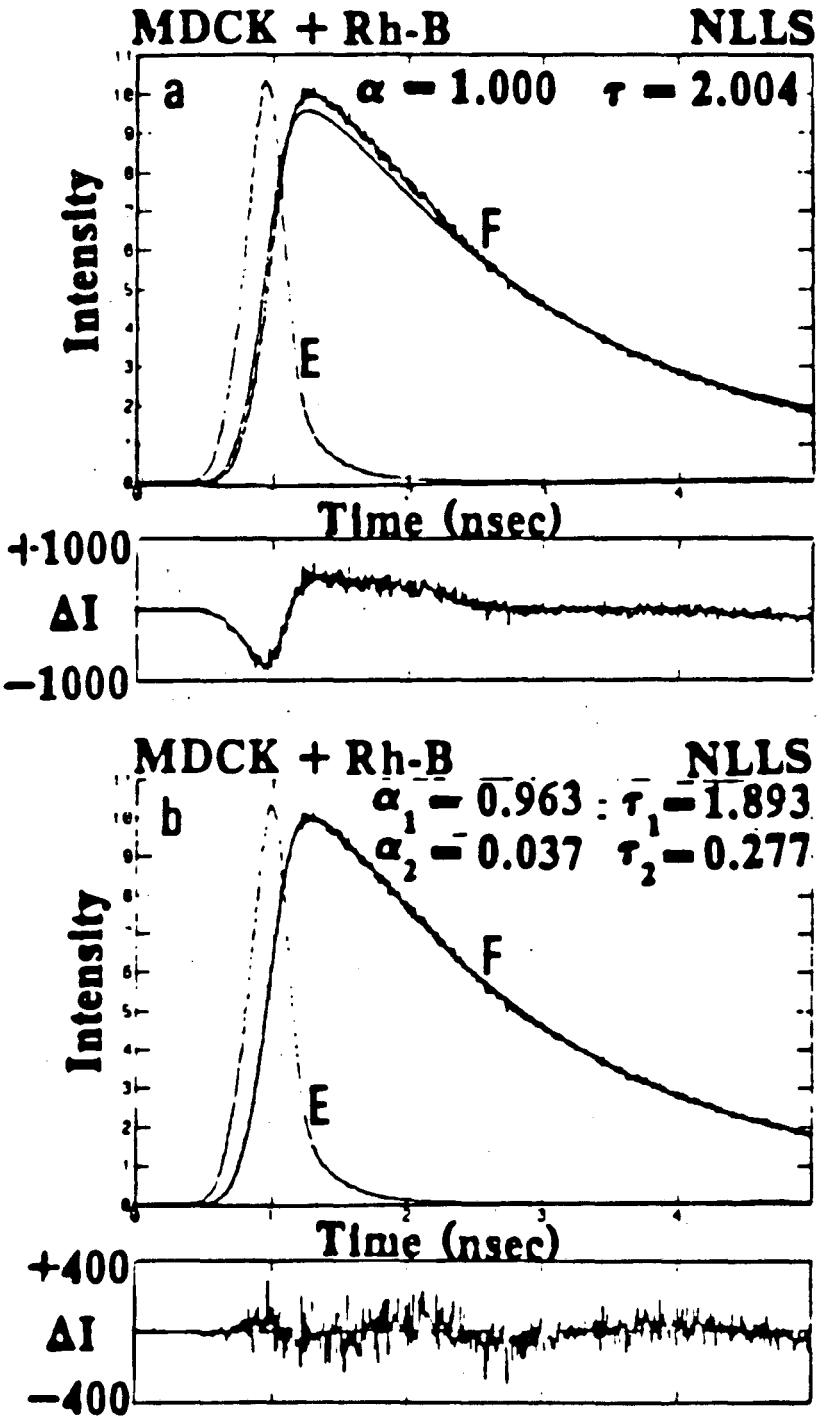

XBL 829-11814B

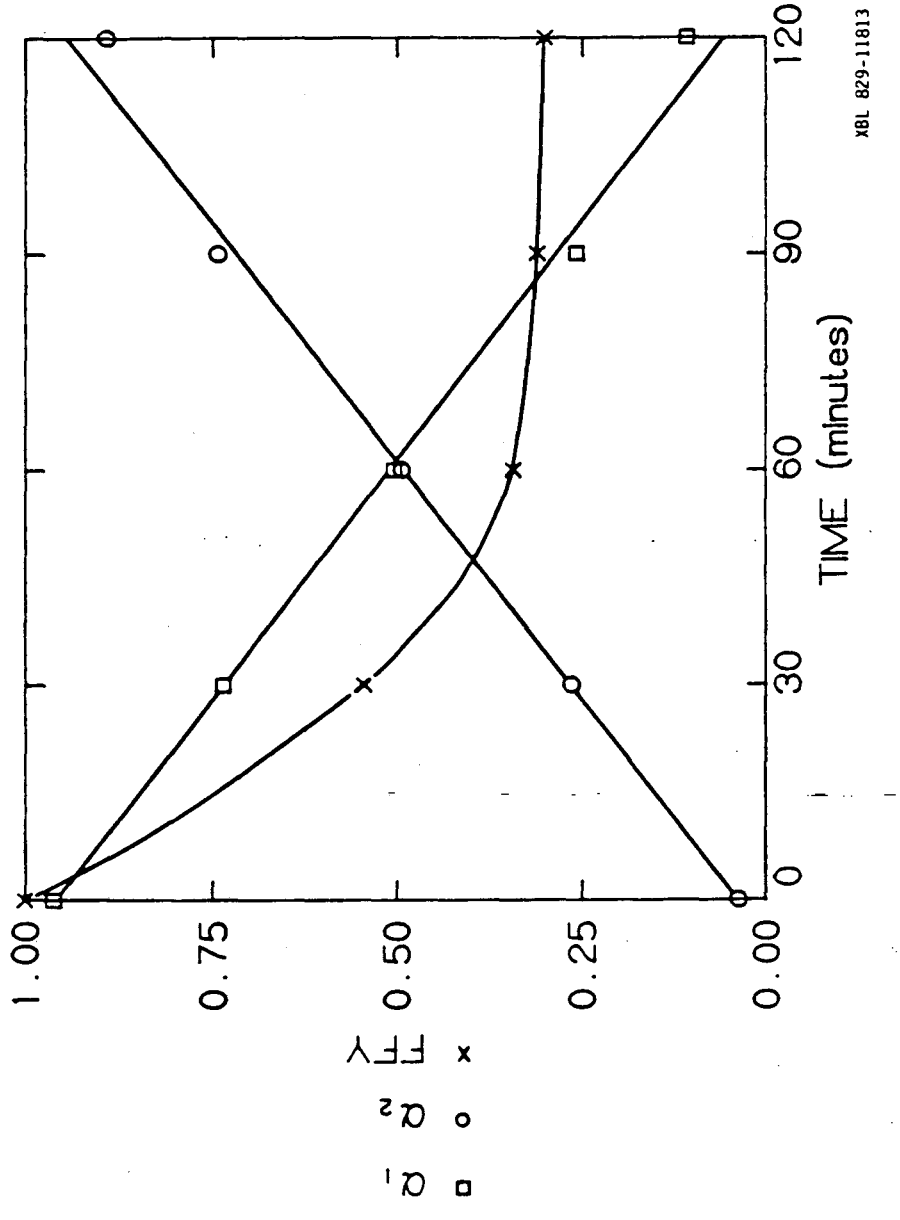
1.00
0.75
0.50
0.25
0.00
0
30
60
90
120
TIME (minutes)
x FFY
o α2
□ α1
XBL 829-11813

Figure IV-5

Figure IV-6

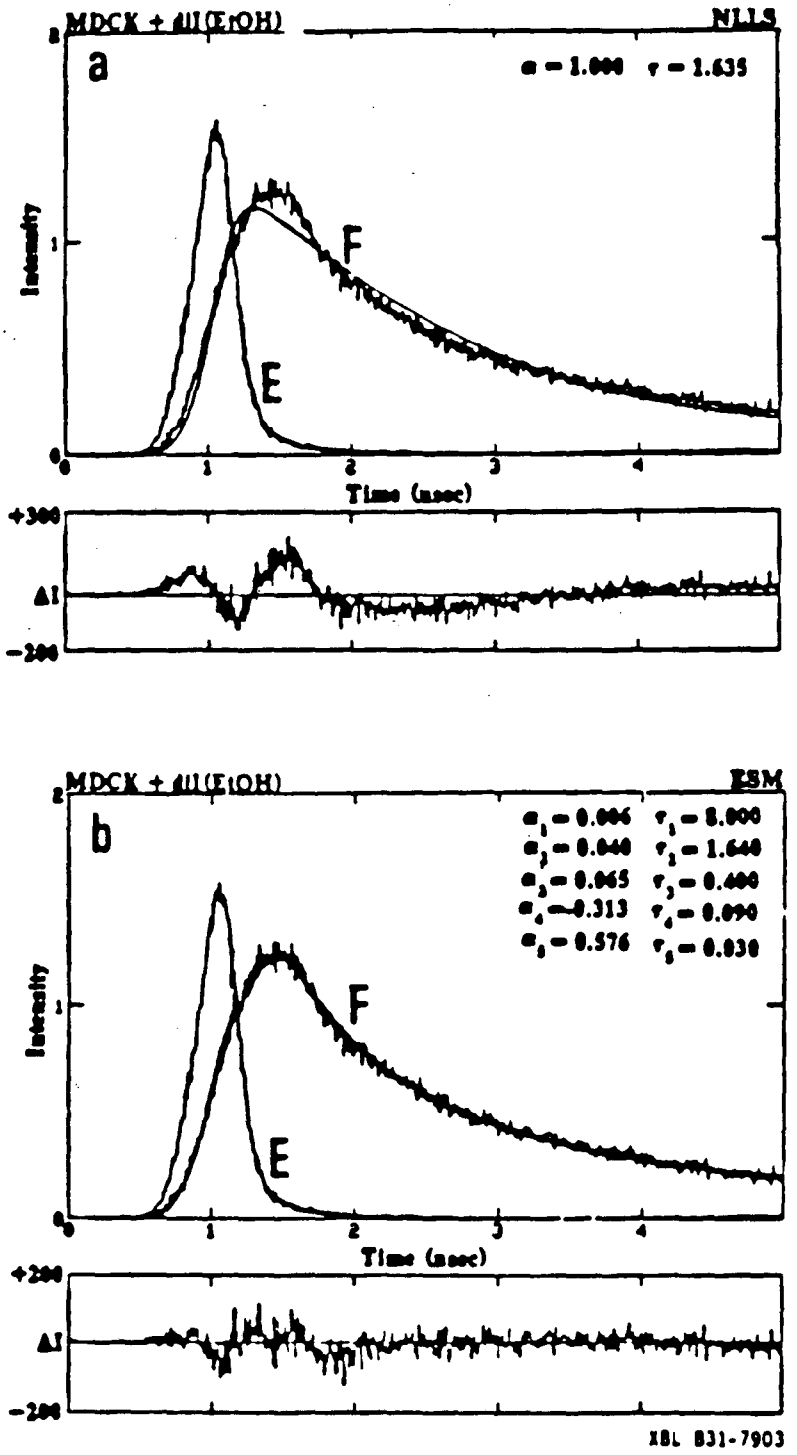
MDCK + 4II(EtOH)
NLLS
a
F
E
Intensity
Time (nsec)
ΔI
MDCK + 4II(EtOH)
ESM
b
F
E
Intensity
Time (nsec)
ΔI
XBL 831-7903

Figure IV-7

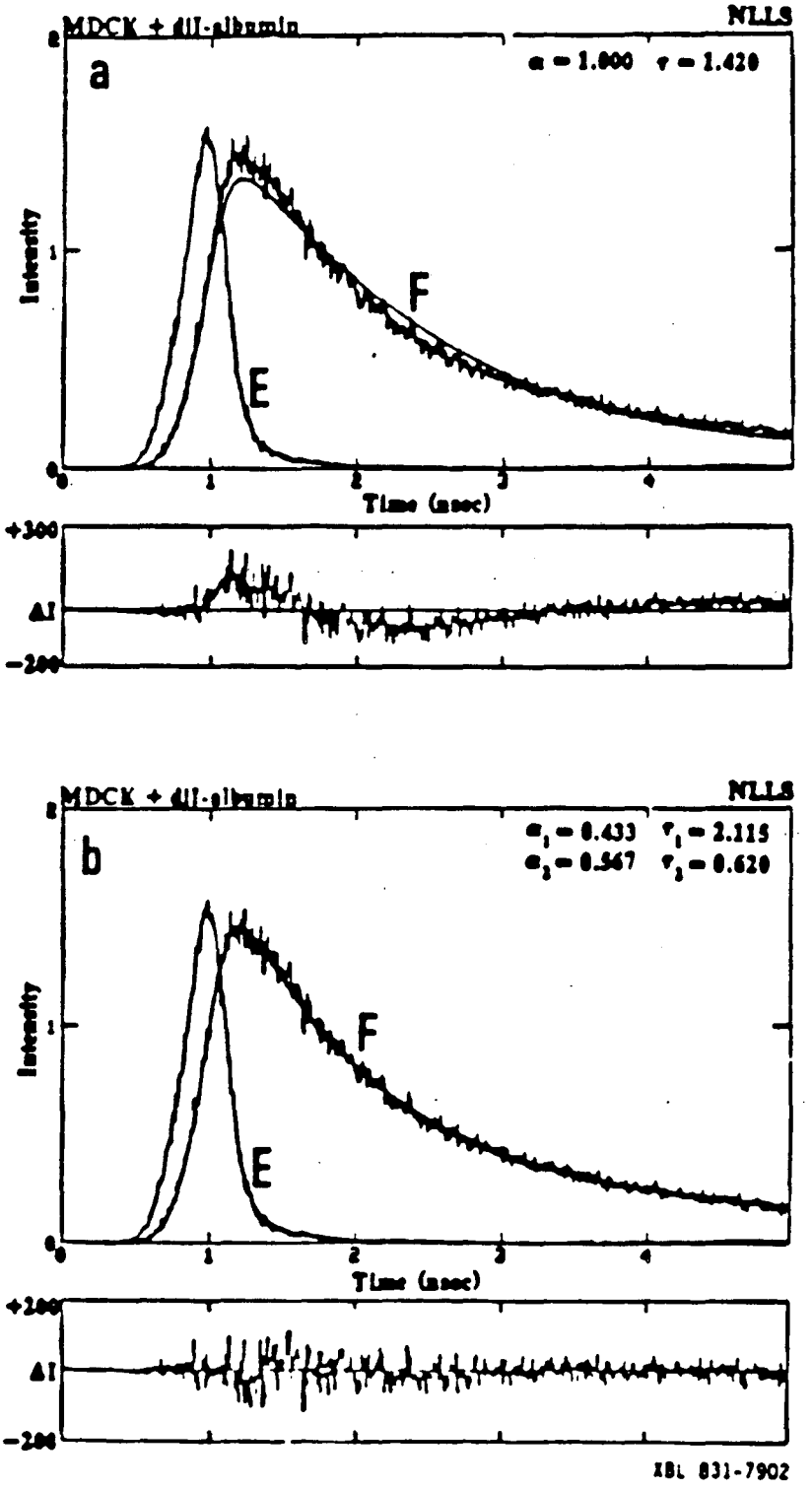
MDCK + dil-albumin
NLLS
a
F
E
Intensity
Time (nsec)
ΔI
MDCK + dil-albumin
NLLS
b
F
E
Intensity
Time (nsec)
ΔI
XBL 831-7902

Figure IV-8

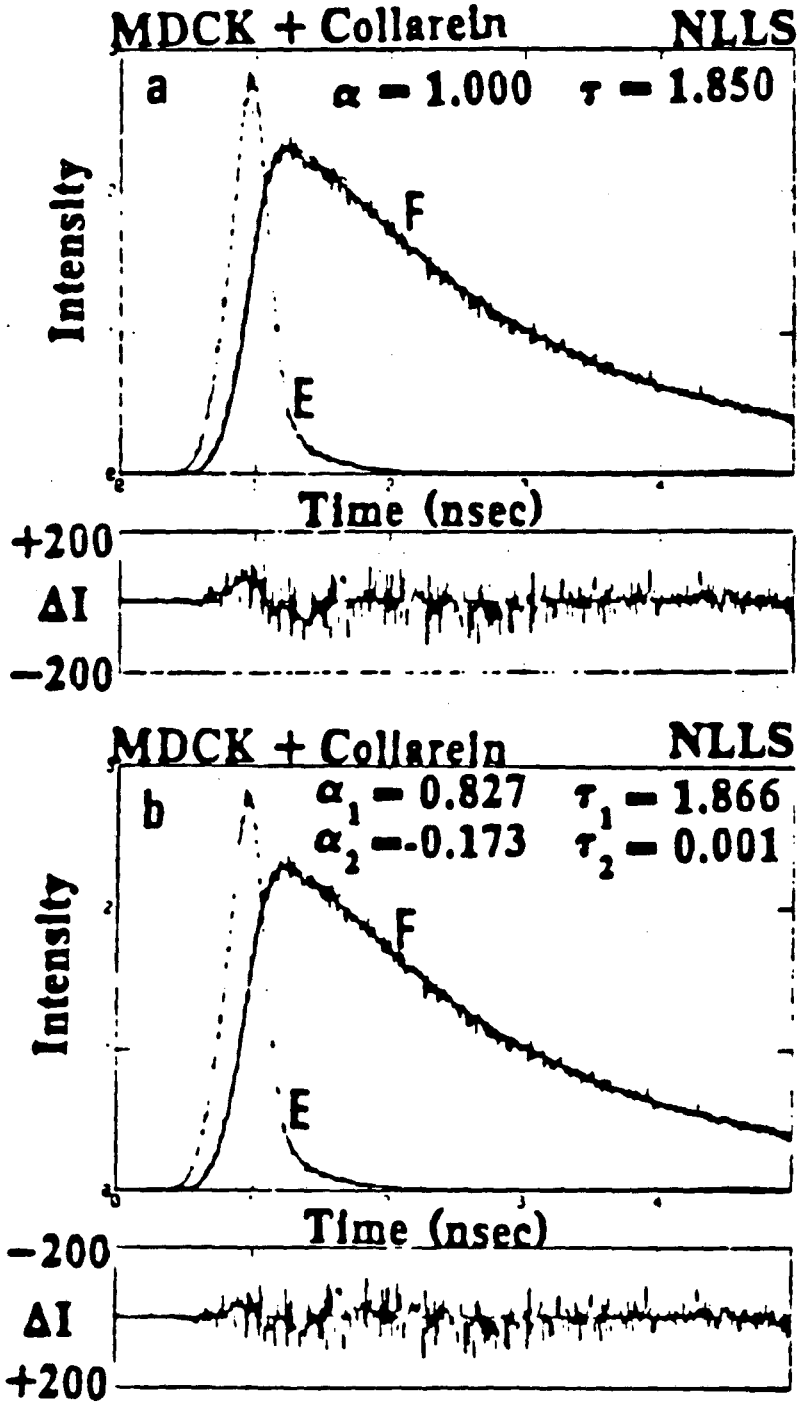

XBL 829-11814A

Figure IV-9

3 COMPARTMENT MODEL

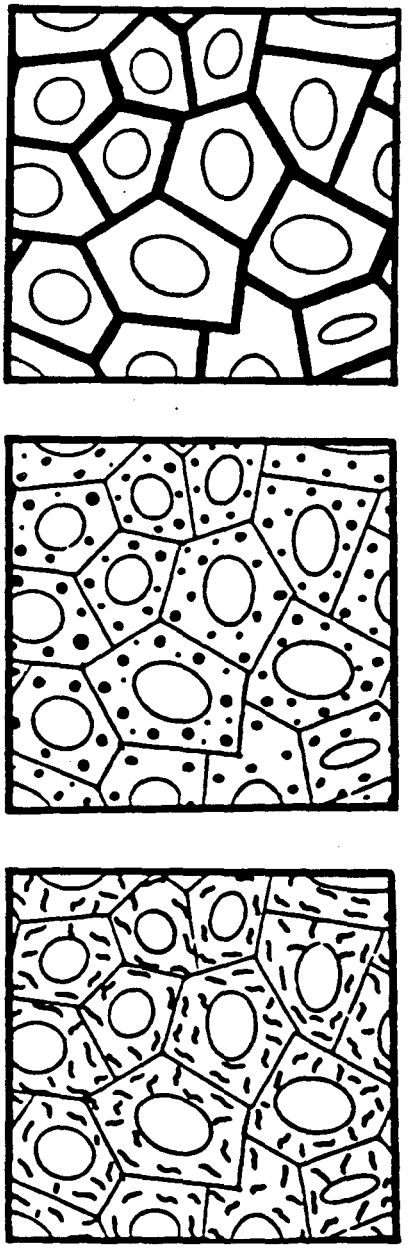

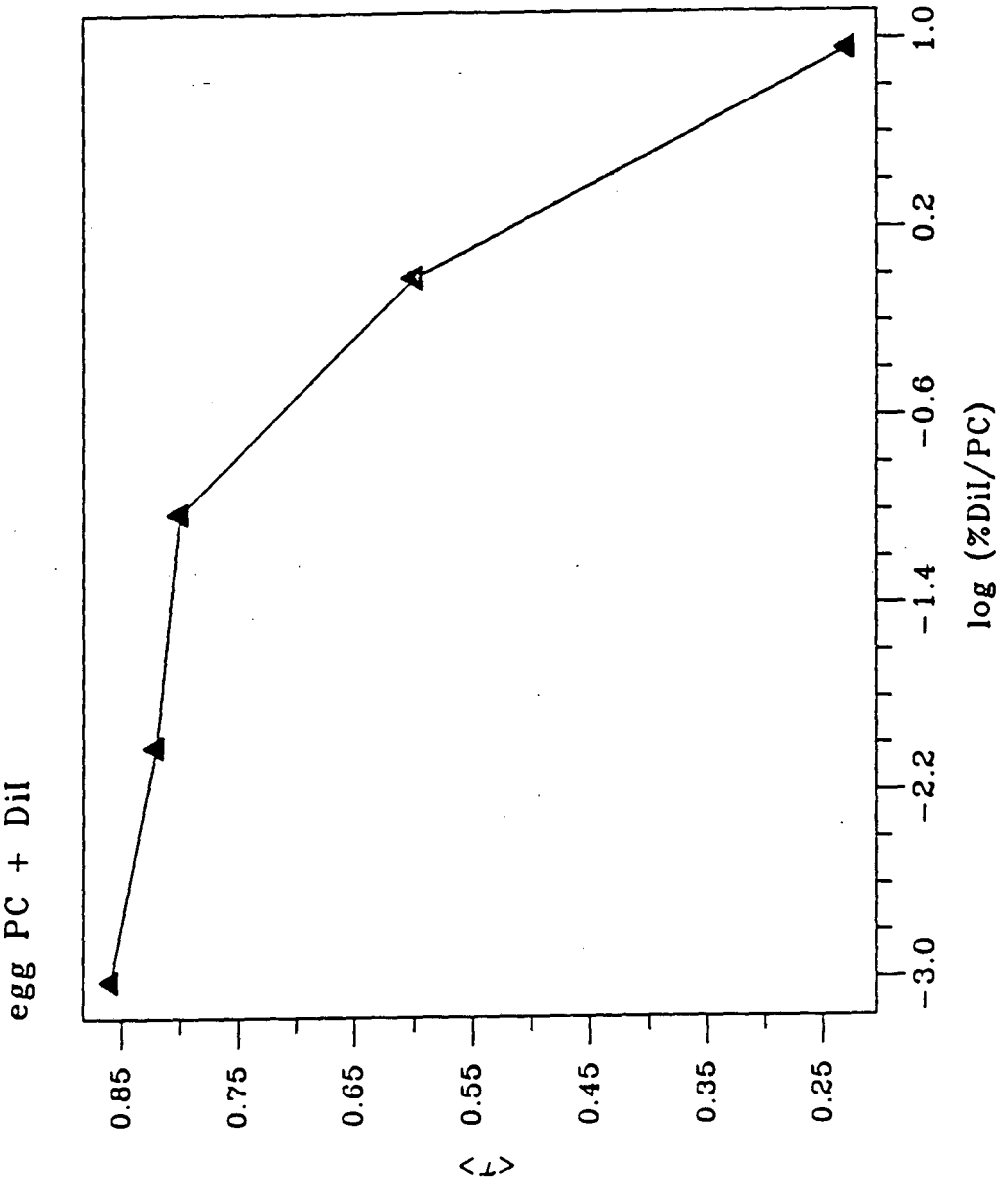
egg PC + DiI
<τ>
0.85
0.75
0.65
0.55
0.45
0.35
0.25
-3.0
-2.2
-1.4
-0.6
0.2
1.0
log (%DiI/PC)

Figure IV-10

Figure IV-11

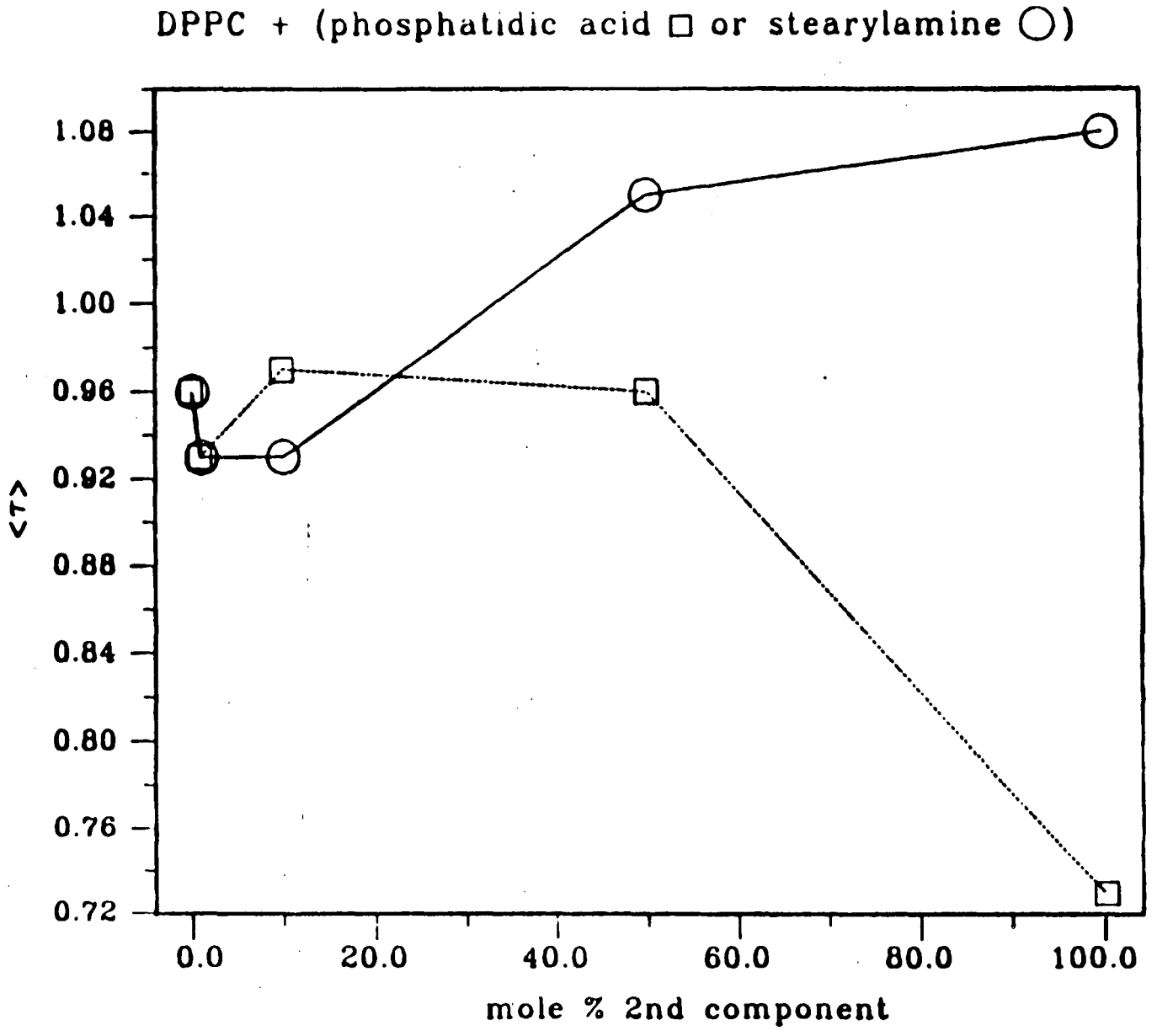
DPPC + (phosphatidic acid □ or stearylamine ○)
1.08
1.04
1.00
0.96
0.92
0.88
0.84
0.80
0.76
0.72
<T>
0.0
20.0
40.0
60.0
80.0
100.0
mole % 2nd component

Figure IV-12

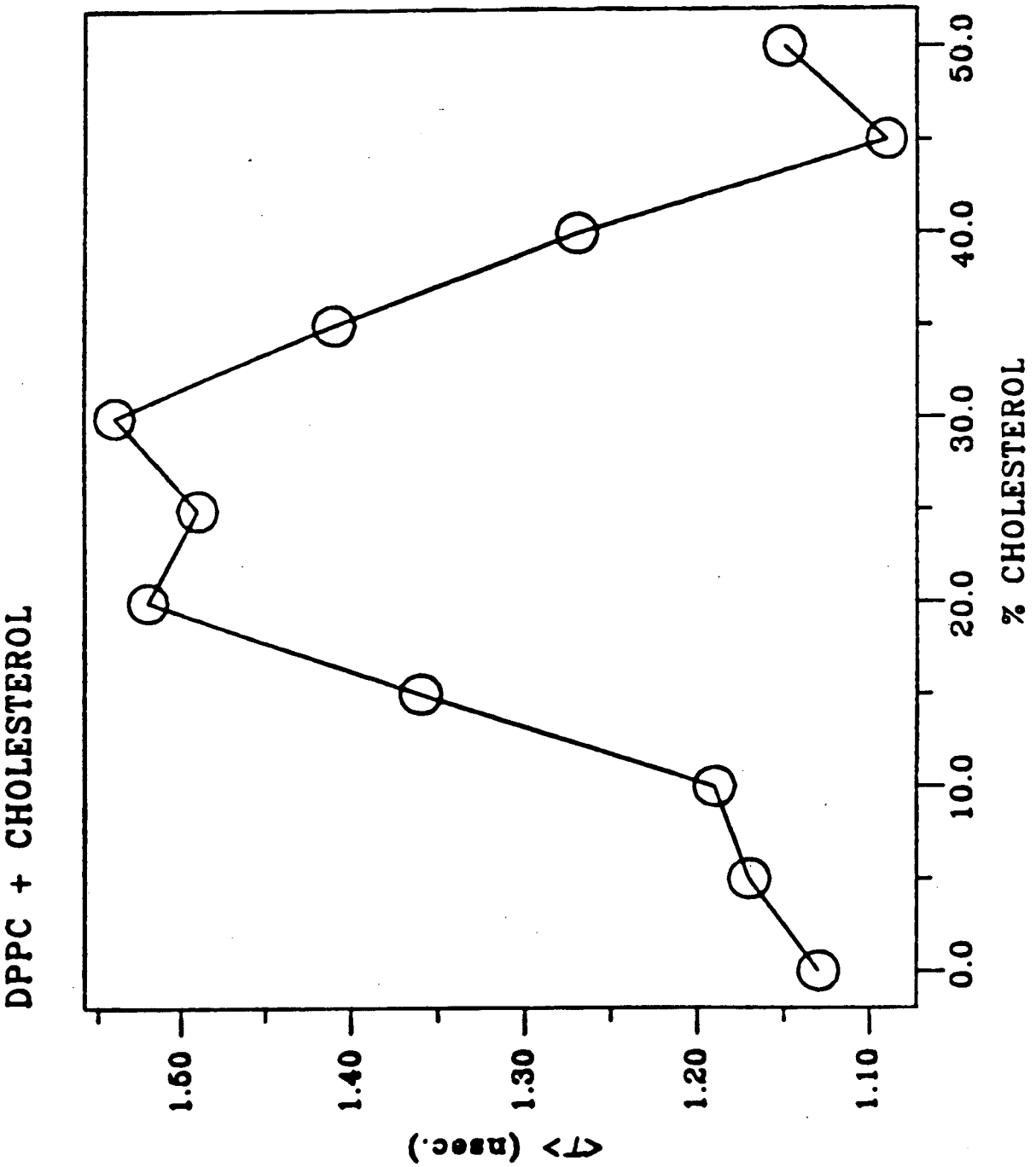
DPPC + CHOLESTEROL
<τ> (nsec.)
1.10
1.20
1.30
1.40
1.50
0.0
10.0
20.0
30.0
40.0
50.0
% CHOLESTEROL

Figure IV-13

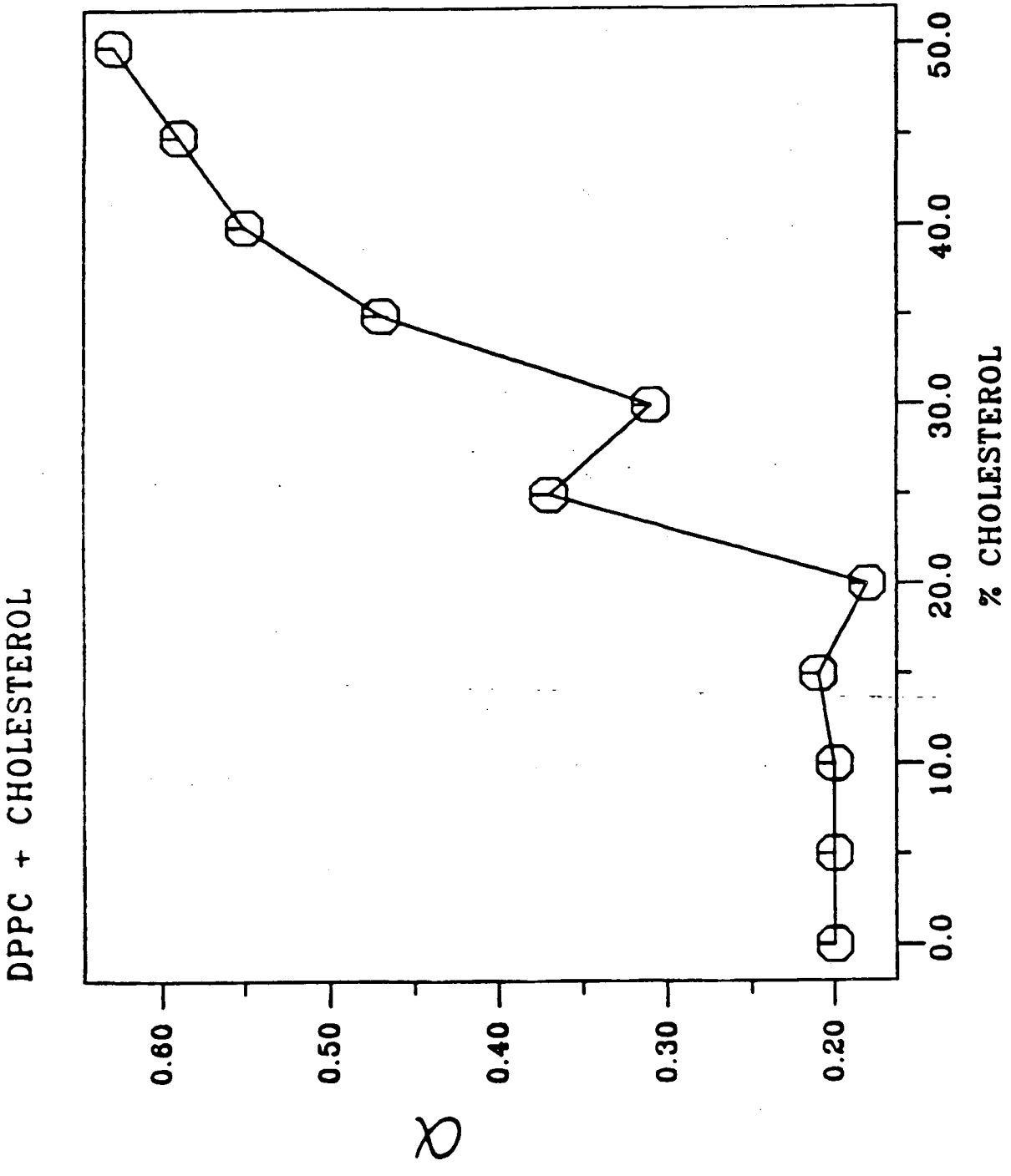
DPPC + CHOLESTEROL
0.80
0.50
0.40
0.30
0.20
α
0.0
10.0
20.0
30.0
40.0
50.0
% CHOLESTEROL

Table IV-1

Gel vs. Fluid

	1-comp	2-comp		<t>
	t	a1 a2	t1 t2	
DSPC + C12	0.84	.68 .32	0.98 0.35	0.89
DSPC + C18	1.34	.83 .17	1.37 0.31	1.32
DSPC + C22	1.05	.73 .27	1.16 0.42	1.07
DOPC + C12	0.72	.77 .23	0.84 0.31	0.78
DOPC + C18	0.74	.76 .24	0.86 0.33	0.80
DOPC + C22	0.76	.74 .26	0.88 0.36	0.81
1:1 + C12	0.82	.83 .17	0.84 0.30	0.80
1:1 + C18	1.19	.67 .33	1.42 0.40	1.30
1:1 + C22	0.83	.69 .31	0.96 0.38	0.87

Concentration Series
egg PC + DiI

[DiI]	1-comp	2-comp		
	t	a1 a2	t1 t	<t>
9.1%	0.22	.24 .76	0.32 0.17	0.23
.99%	0.61	.77 .23	0.64 0.19	0.60
9.9E-2	0.80	.75 .25	0.86 0.29	0.80
9.9E-3	0.82	.67 .33	0.91 0.34	0.82
9.9E-4	0.82	.49 .51	1.05 0.42	0.86

Headgroups

	1-comp	2-comp		
	t	a1 a2	t1 t2	<t>
100% EGG PC	0.90	0.60 0.40	1.10 0.47	0.96
99% EGG PC + 1% SA	0.87	0.57 0.43	1.08 0.45	0.93
90% EGG PC + 10% SA	0.82	0.36 0.64	1.29 0.47	0.97
50% EGG PC + 50% SA	0.85	0.42 0.58	1.22 0.49	0.96
100% SA	0.45	0.01 0.99	0.73 0.00	0.73
100% EGG PC	0.90	0.60 0.40	1.10 0.47	0.96
99% EGG PC + 1% PA	0.84	0.55 0.45	1.08 0.35	0.93
90% EGG PC + 10% PA	0.90	0.52 0.48	1.02 0.12	0.93
50% EGG PC + 50% PA	0.94	0.57 0.43	1.20 0.34	1.05
100% PA	0.96	0.55 0.45	1.26 0.42	1.08
100% DOPC	0.81	0.62 0.38	1.01 0.40	0.89
100% DPPC	1.11	0.70 0.30	1.30 0.33	1.20
DiI	0.18	0.00 1.00	0.55 0.00	

DPPC + cholesterol

	1-comp	2-comp		
	t	a1 a2	t1 t2	<t>
% cholesterol				
0	1.03	.80 .20	1.19 0.34	1.13
5	1.07	.80 .20	1.23 0.34	1.17
10	1.07	.80 .20	1.25 0.32	1.19
15	1.22	.80 .21	1.42 0.32	1.36
20	1.36	.82 .18	1.58 0.34	1.52
25	1.28	.63 .37	1.61 0.28	1.49
30	1.35	.69 .31	1.62 0.23	1.54
35	1.09	.53 .47	1.57 0.25	1.41
40	0.88	.45 .55	1.48 0.24	1.27
45	0.88	.41 .59	1.38 0.39	1.09
50	0.91	.37 .63	1.50 0.41	1.15

H-Bonding

				NFY
DPPC	1.03	.80 .20	1.19 0.34	1.13
DPPC:DPPE::1:1	1.29	.70 .30	1.54 0.34	1.44

Table IV-2

	C_{12}DiI	C_{18}DiI	C_{22}DiI
DSPC	$\alpha_1 = .68$ $\tau_1 = 0.98$ $\alpha_2 = .32$ $\tau_2' = 0.35$ **0.89**	$\alpha_1 = .83$ $\tau_1 = 1.37$ $\alpha_2 = .17$ $\tau_2' = 0.31$ **1.32**	$\alpha_1 = .73$ $\tau_1 = 1.16$ $\alpha_2 = .27$ $\tau_2' = 0.42$ **1.07**
DOPC	$\alpha_1 = .77$ $\tau_1 = 0.84$ $\alpha_2 = .23$ $\tau_2' = 0.31$ **0.78**	$\alpha_1 = .76$ $\tau_1 = 0.86$ $\alpha_2 = .24$ $\tau_2' = 0.33$ **0.80**	$\alpha_1 = .74$ $\tau_1 = 0.88$ $\alpha_2 = .26$ $\tau_2' = 0.36$ **0.81**
1:1	$\alpha_1 = .83$ $\tau_1 = 0.84$ $\alpha_2 = .17$ $\tau_2' = 0.30$ **0.80**	$\alpha_1 = .67$ $\tau_1 = 1.42$ $\alpha_2 = .33$ $\tau_2' = 0.40$ **1.30**	$\alpha_1 = .69$ $\tau_1 = 0.96$ $\alpha_2 = .31$ $\tau_2' = 0.38$ **0.87**

References

1. Taylor, D.L. and Y.-L. Wang. (1980) Nature 284: 405-410.
2. Johnson, L.V., M.L. Walsh, and L.B. Chen. (1980) Proc. Nat. Acad. Sci. 77: 990-994.
3. Pagano, R.E., K.J. Longmuir, O.C. Martin, and D.K Struck. (1981) J. Cell Biol. 91: 872-877.
4. Badea, M.G. and Brand, L. (1979) Meth. Enzym. 61: 378-415.
5. Lackowicz, J. (1983) Principles of Fluorescence Spectroscopy Plenum Press, New York.
6. Sims, P.J., A.S.Waggoner, C.-H. Wang, and J.F.Hoffman. (1974) Biochemistry 13: 3315-30
7. Shinitzky, M. (1978) FEBS Letts. 85: 317-20.
8. Leskovar, B., C. C. Lo, P. R. Hartig, and K. Sauer. (1976) Rev. Sci. Instrumen. 47: 1113-1121.
9. Turko, B.T., J.A.Nairn, K.Sauer. (1983) Rev. Sci. Instr. 54: 118-20.
10. Nairn, J.A. (1981) Ph.D. Thesis. University of California, Berkeley.
11. Reisberg, P., Nairn, J.A., and Sauer, K. (1982) Photochem. Photobiol. 36: 657-61.
12. Steinman, R.M., I.S. Mellman, W.A. Muller, and Z.A. Cohen. (1983) J. Cell Biol. 96: 1-27.
13. Duysens, L.N.M. (1952) Ph.D. Thesis. University of

Utrecht. 201-34.

14. Ethier, M.F., Wolf, D.E., and Melchior, D.L. (1983) Biochemistry 22: 1178-82.

15. Sims, P.J., Waggoner, A.S., Wang, C.-H., and Hoffman, J.F. (1974) Biochemistry 13: 1707-16.

16. Ross, J.B.A., Rousslang, K.W. and Brand, L. Biochemistry 20: 4361-9.

17. Szabo, A.G., and Rayner, D.M. (1980) J. Am. Chem. Soc. 102: 554-63.

17. Klausner, R.D. and Wolf, D.E. (1980) Biochemistry 19: 6199-203.

18. Sklar, L.A., Miljanich, G.P., and Dratz, E.A. (1979) Biochemistry 18: 1707-16.

19. Nakashima, N. and Kunitake, T. (1982) J. Amer. Chem. Soc. 104: 4261-2.

20. Klausner, R.D., Kleinfeld, A.M., Hoover, R.L., and Karnovsky, M.J. (1980) J. Biol. Chem. 255: 1286-95.

21. Pringle, M.J. and Miller, K.W. (1979) Biochemistry 18: 3314-20.

22. Chapman, D., Urbina, J., and Keogh, K.M. (1974) J. Biol. Chem. 249: 2512- .

23. Melchior, D.L., Scavitto, F.J., and Steim, J.M. (1980) Biochemistry 19: 4828-34.

24. Rubenstein,, J.L.R., Owicki, J.C., and McConnell, H.M. (1980) Biochemistry 19: 569.

25. Presti, F.T. and Chan, S.I. (1982) Biochemistry 21:3821-30.

26. Presti, F.T., Pace, R.J., and Chan, S.I. Biochemistry 21: 3831-5.

Appendix

Solvent series

In order to study the self-association of rhodamine-B the concentration dependence of four fluorescence related properties (fluorescence lifetime, fluorescence yield, and absorption and emission spectra) were measured in five solvents (water, methanol, acetonitrile, n-butanol, and tetrahydrofuran). The concentration of rhodamine-B ranged from 0.2 μg/ml to 2.0 mg/ml with increments in decadic units (except in cases where insolubility prevented and for methanol up to 20 mg/ml).

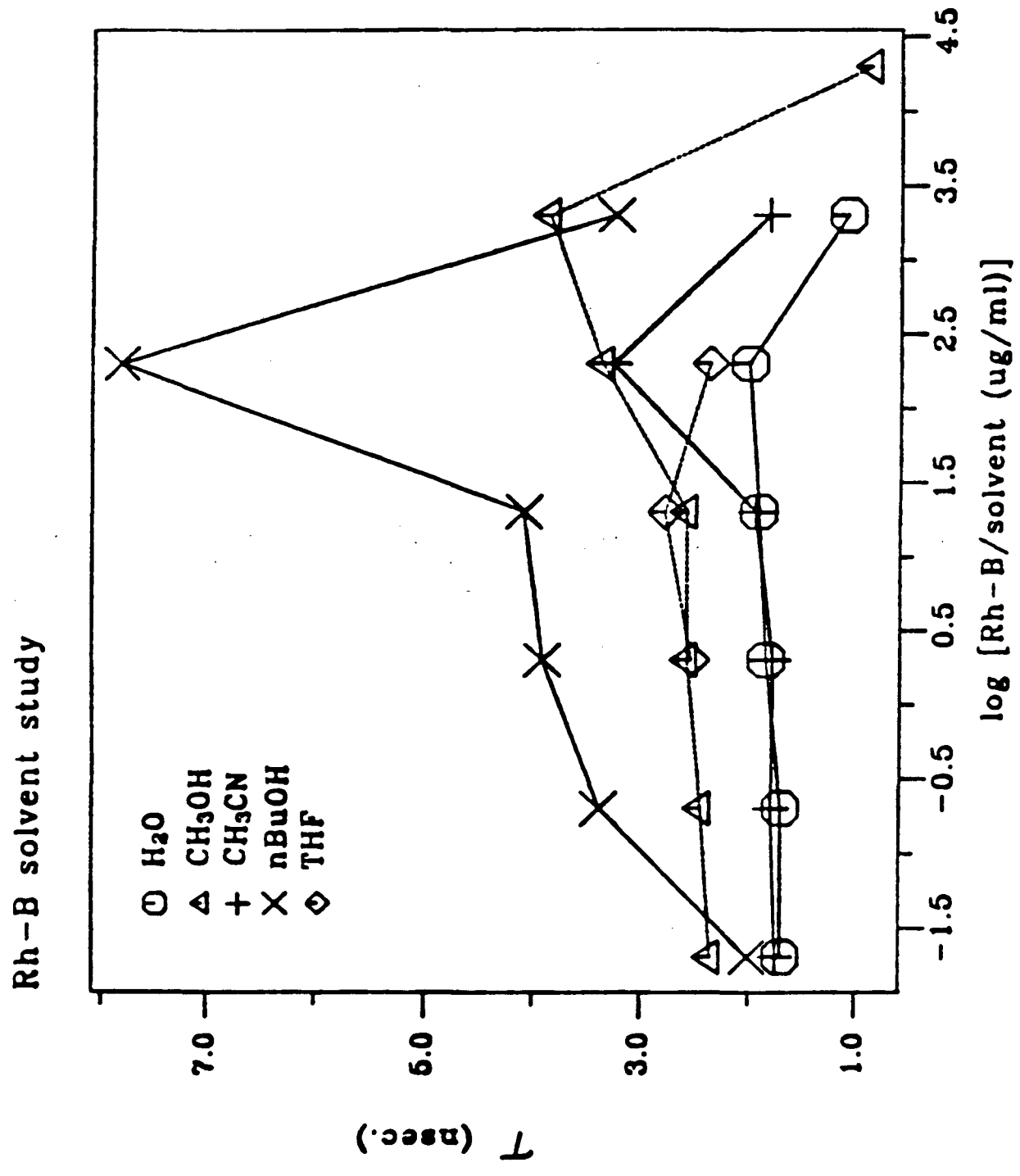
Rh-B solvent study
H2O
CH3OH
CH3CN
nBuOH
THF
7.0
6.0
3.0
1.0
T (sec.)
-1.5
-0.5
0.5
1.5
2.5
3.5
4.5
log [Rh-B/solvent (ug/ml)]

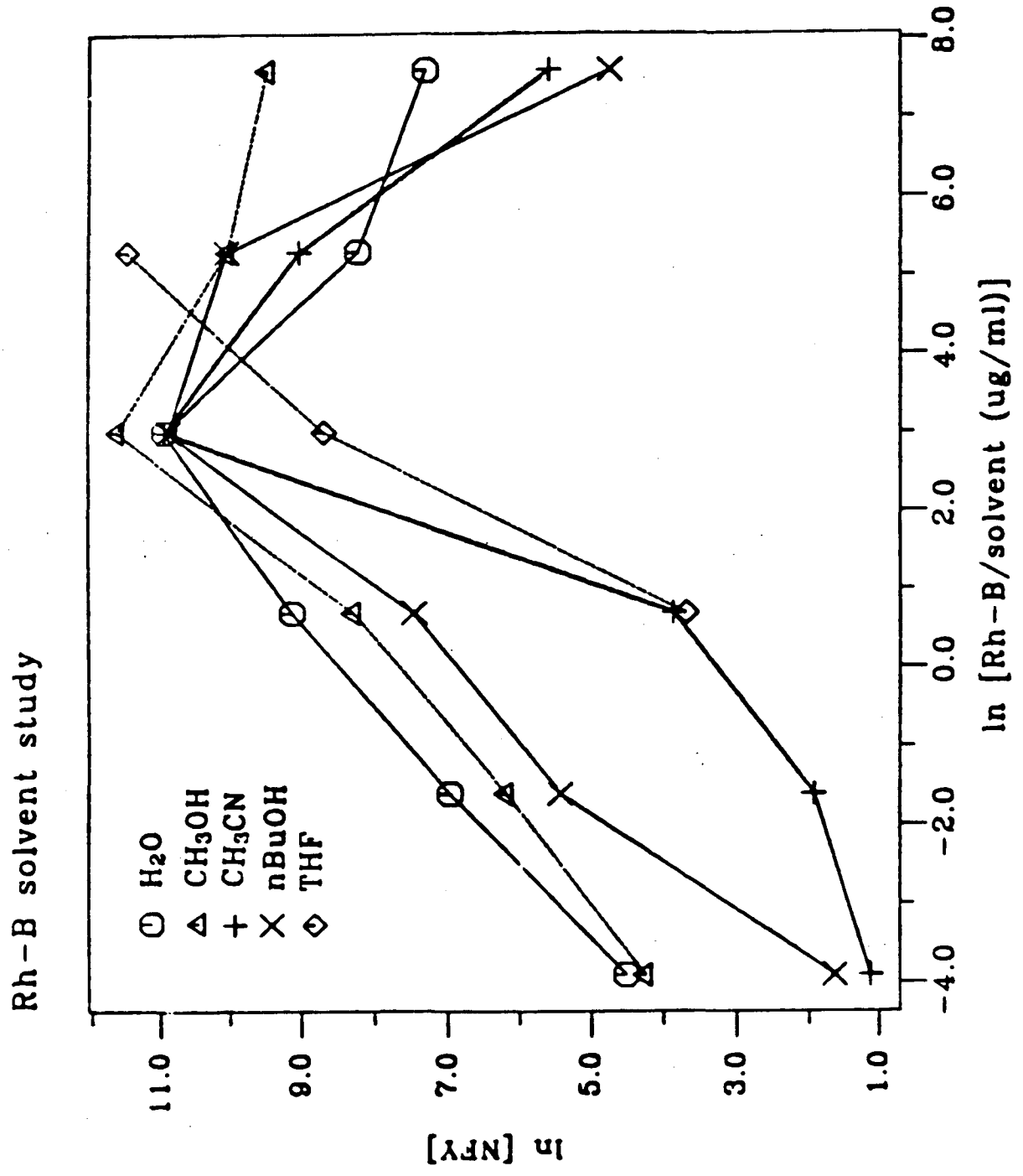
Rh-B solvent study
H2O
CH3OH
CH3CN
nBuOH
THF
ln [NFY]
11.0
9.0
7.0
5.0
3.0
1.0
-4.0
-2.0
0.0
2.0
4.0
6.0
8.0
ln [Rh-B/solvent (ug/ml)]

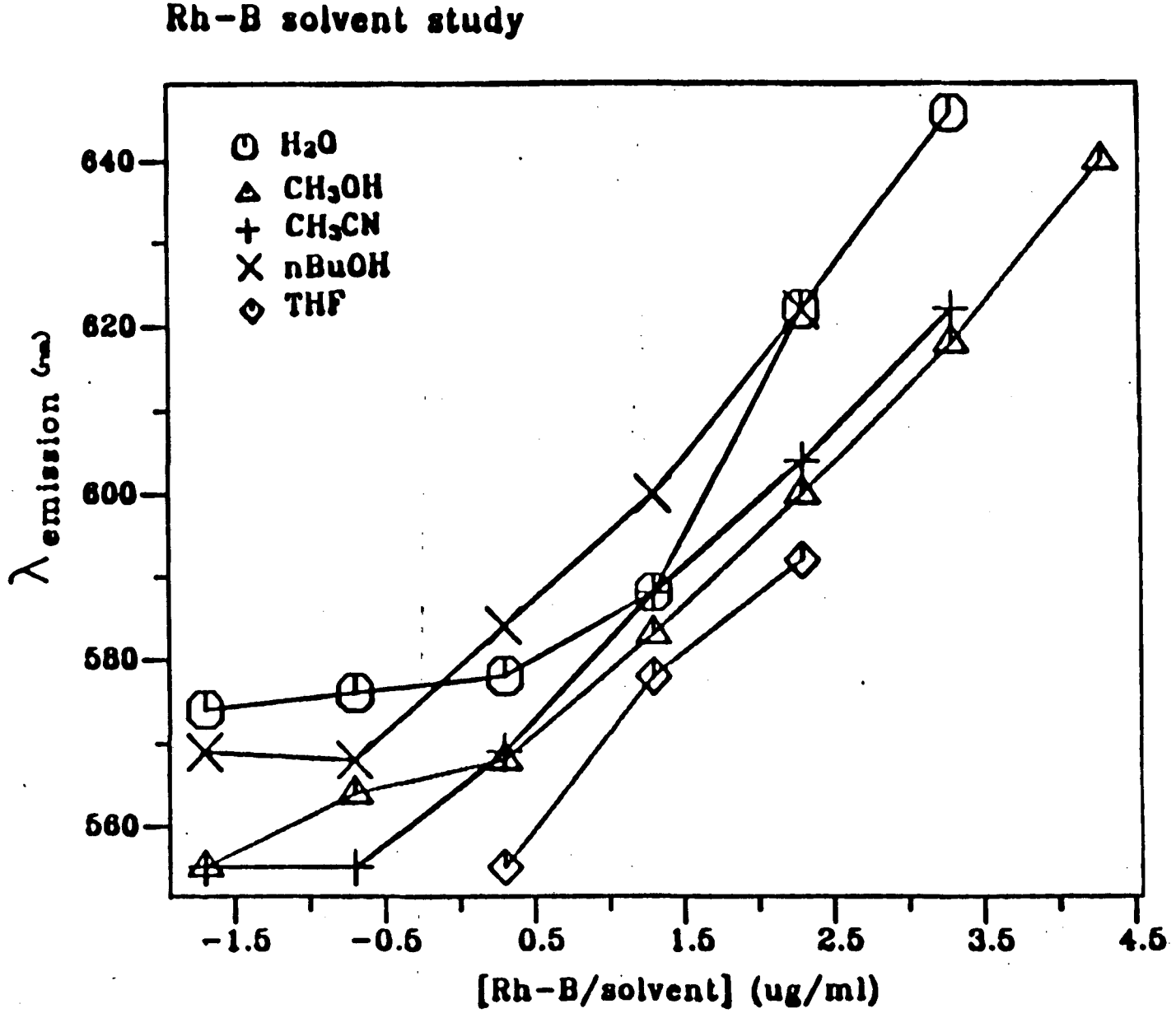
Rh-B solvent study
H2O
CH3OH
CH3CN
nBuOH
THF
640
620
600
580
560
λ emission (nm)
-1.5
-0.5
0.5
1.5
2.5
3.5
4.5
[Rh-B/solvent] (ug/ml)

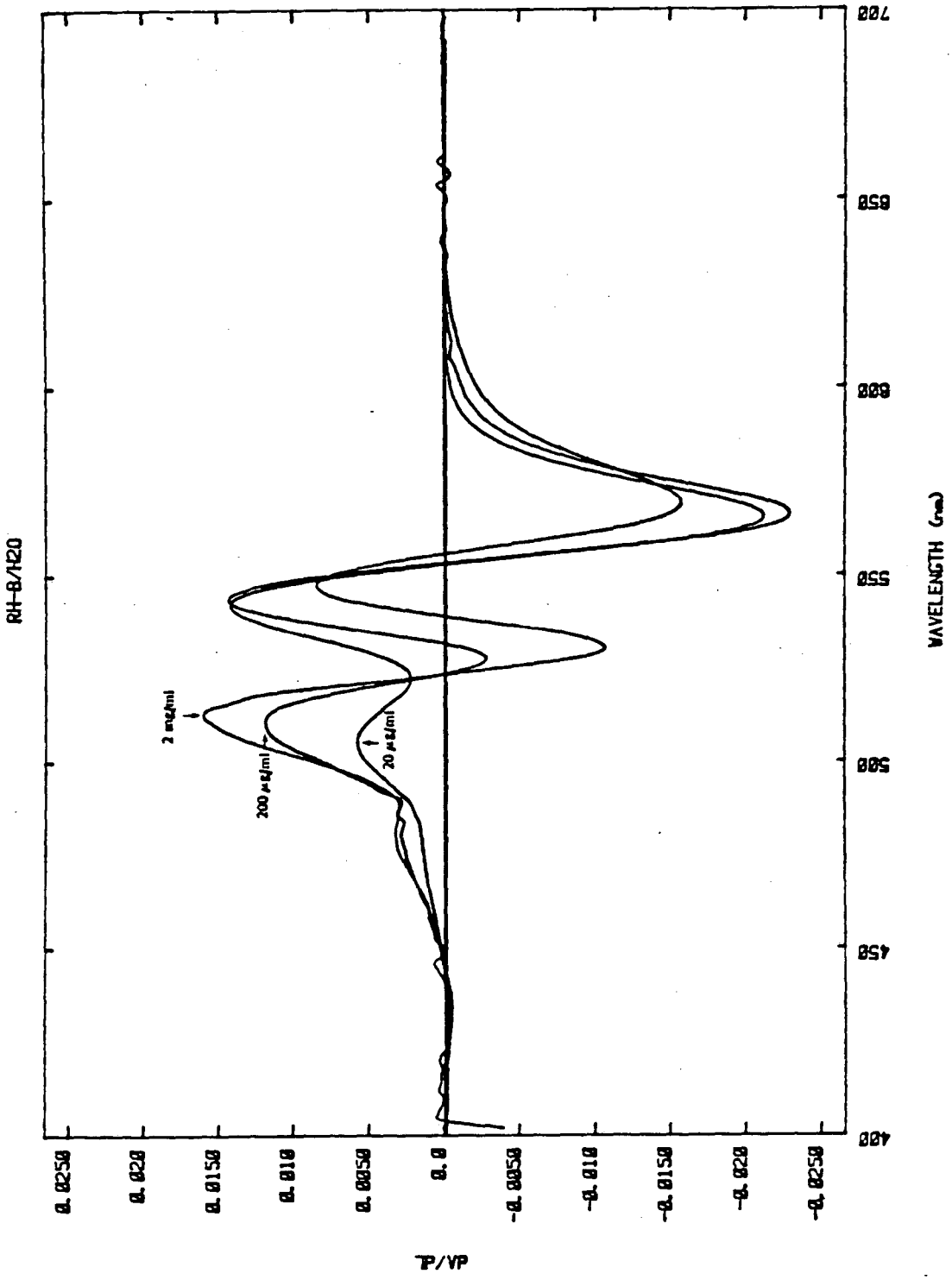
RH-B/H20
2 ug/ml
200 µg/ml
20 µg/ml
0.025B
0.02B
0.015B
0.01B
0.005B
0.B
-0.005B
-0.01B
-0.015B
-0.02B
-0.025B
ΔP/VP
400
450
500
550
600
650
700
WAVELENGTH (nm)

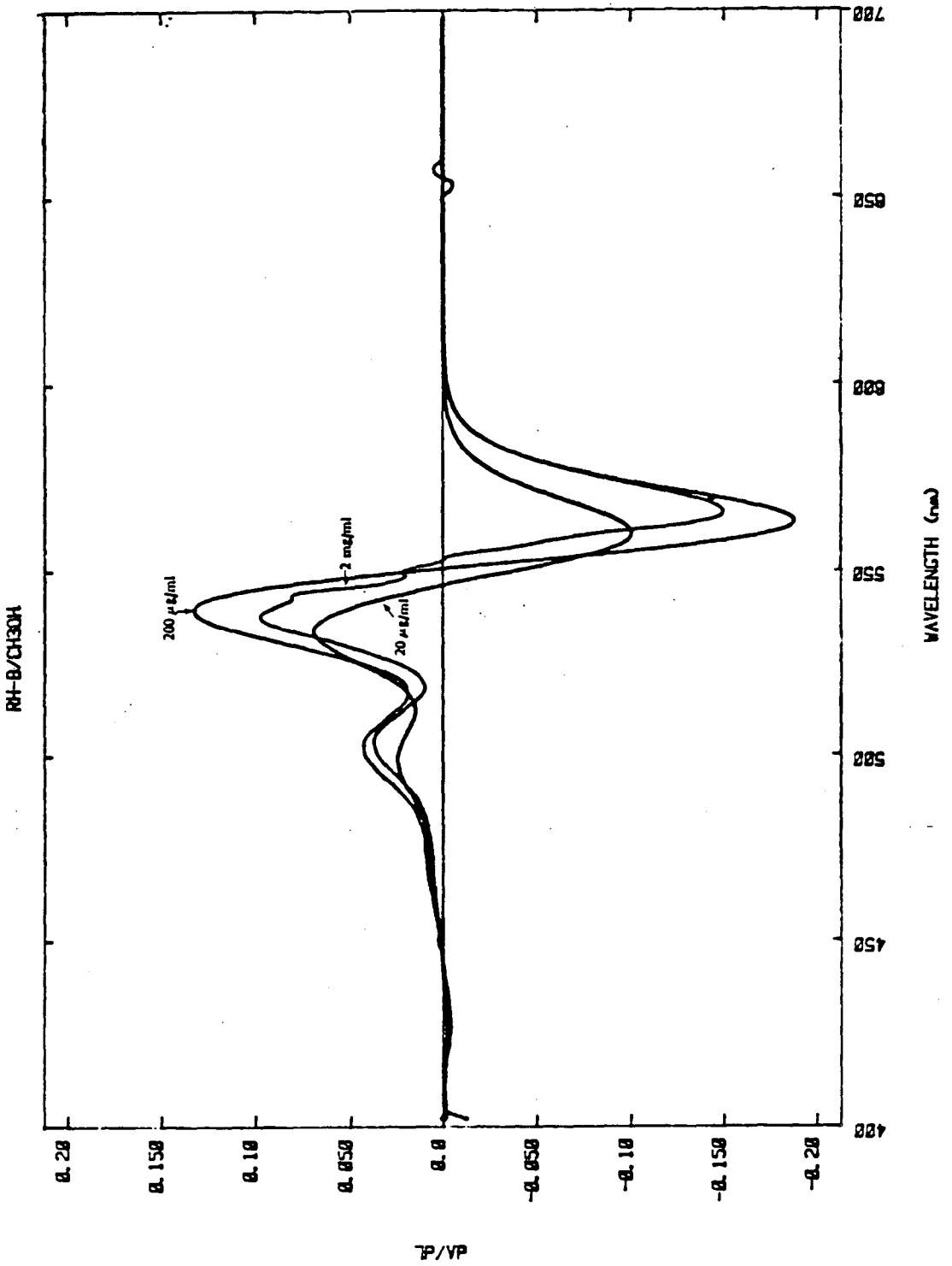
RH-B/CH3OH
200 µg/ml
2 mg/ml
20 µg/ml
0.20
0.150
0.10
0.050
0.0
-0.050
-0.10
-0.150
-0.20
400
450
500
550
600
650
700
WAVELENGTH (nm)
ΔA/Δλ

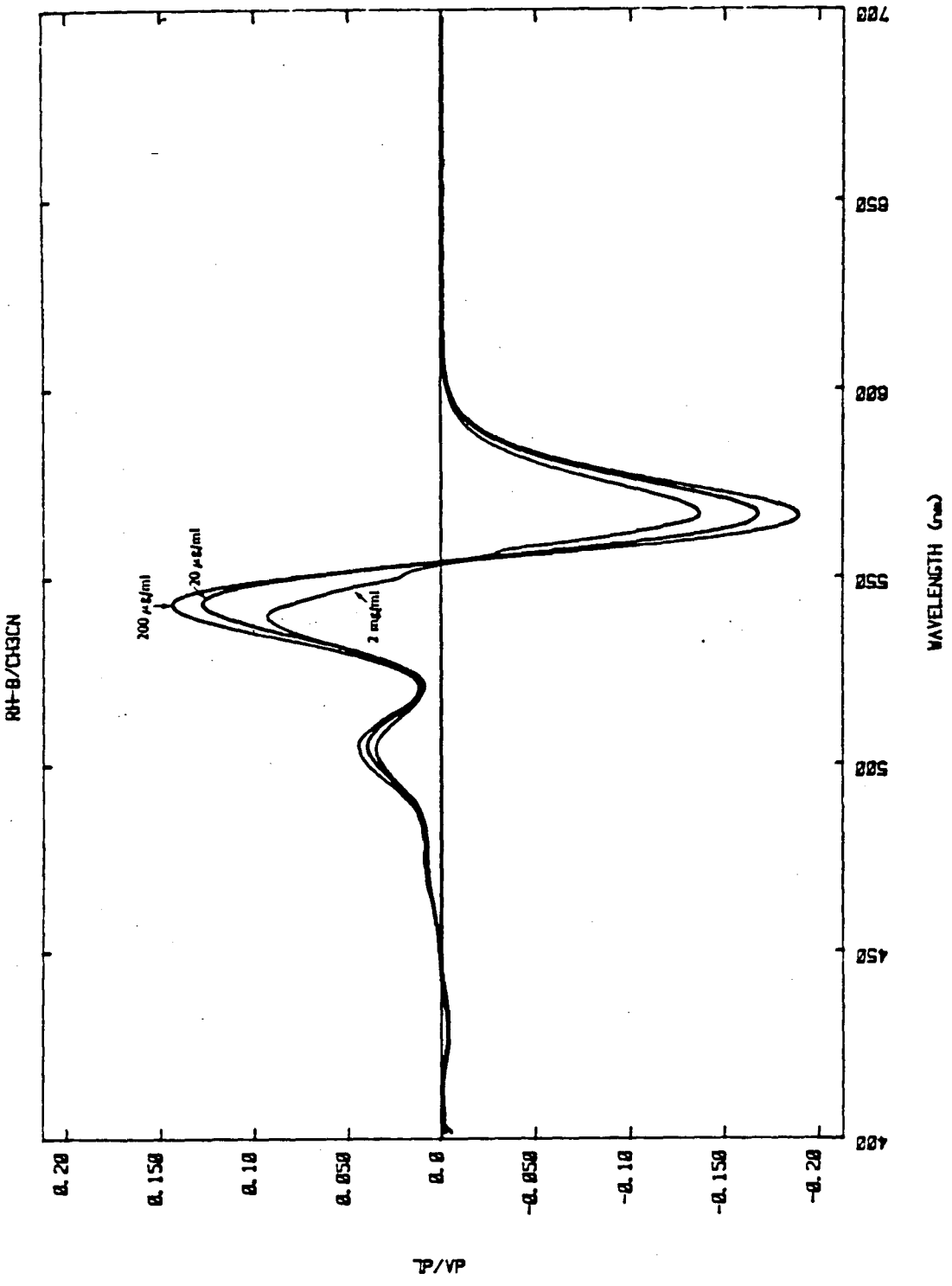
RH-B/CH3CN
200 µg/ml
20 µg/ml
2 mg/ml
0.20
0.150
0.10
0.050
0.0
-0.050
-0.10
-0.150
-0.20
ΔP/VP
400
450
500
550
600
650
700
WAVELENGTH (nm)

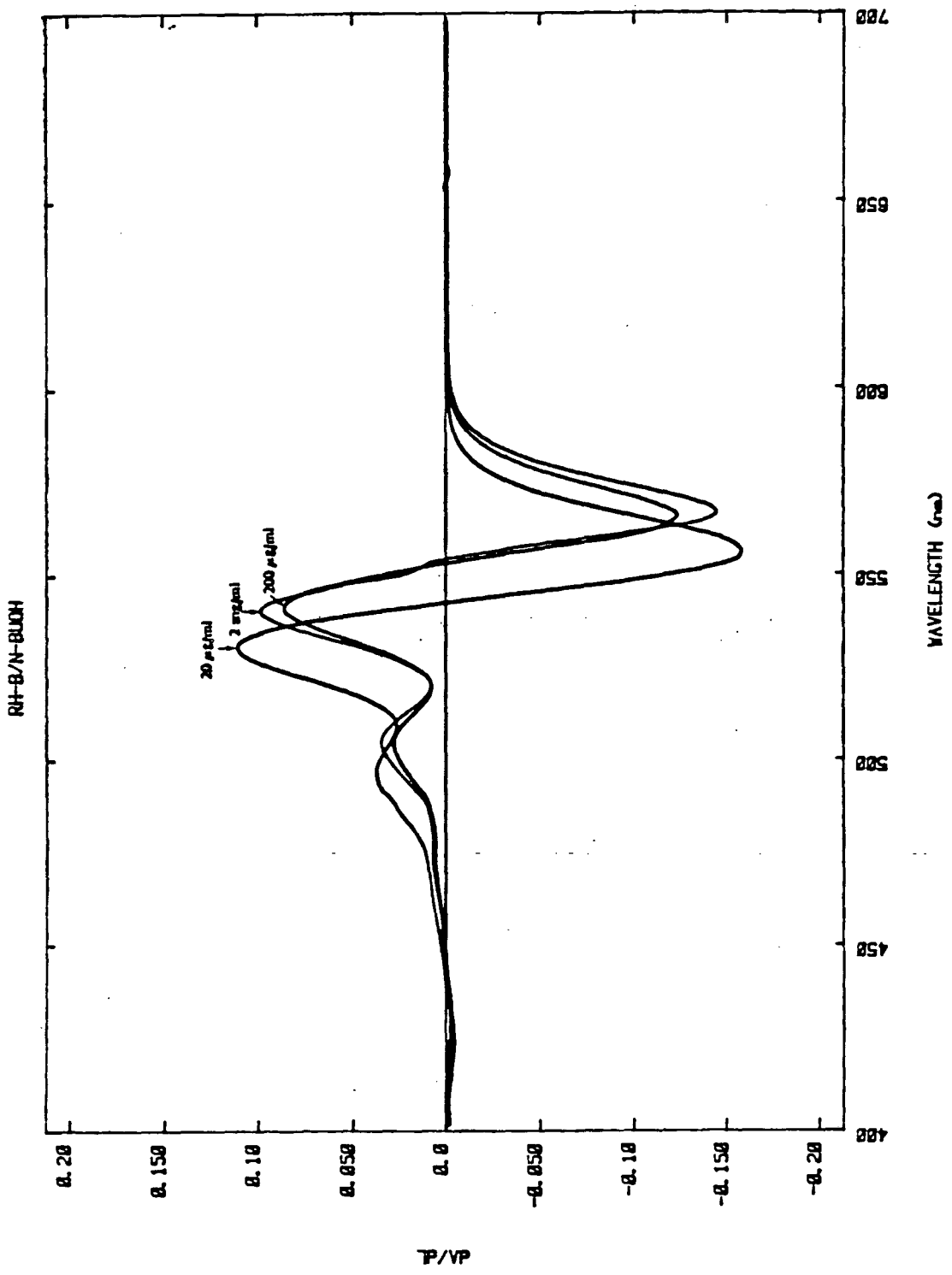
RH-B/N-BUOH
20 μg/ml
2 mg/ml
200 μg/ml
0.20
0.150
0.10
0.050
0.0
-0.050
-0.10
-0.150
-0.20
ΔA/A
400
450
500
550
600
650
700
WAVELENGTH (nm)

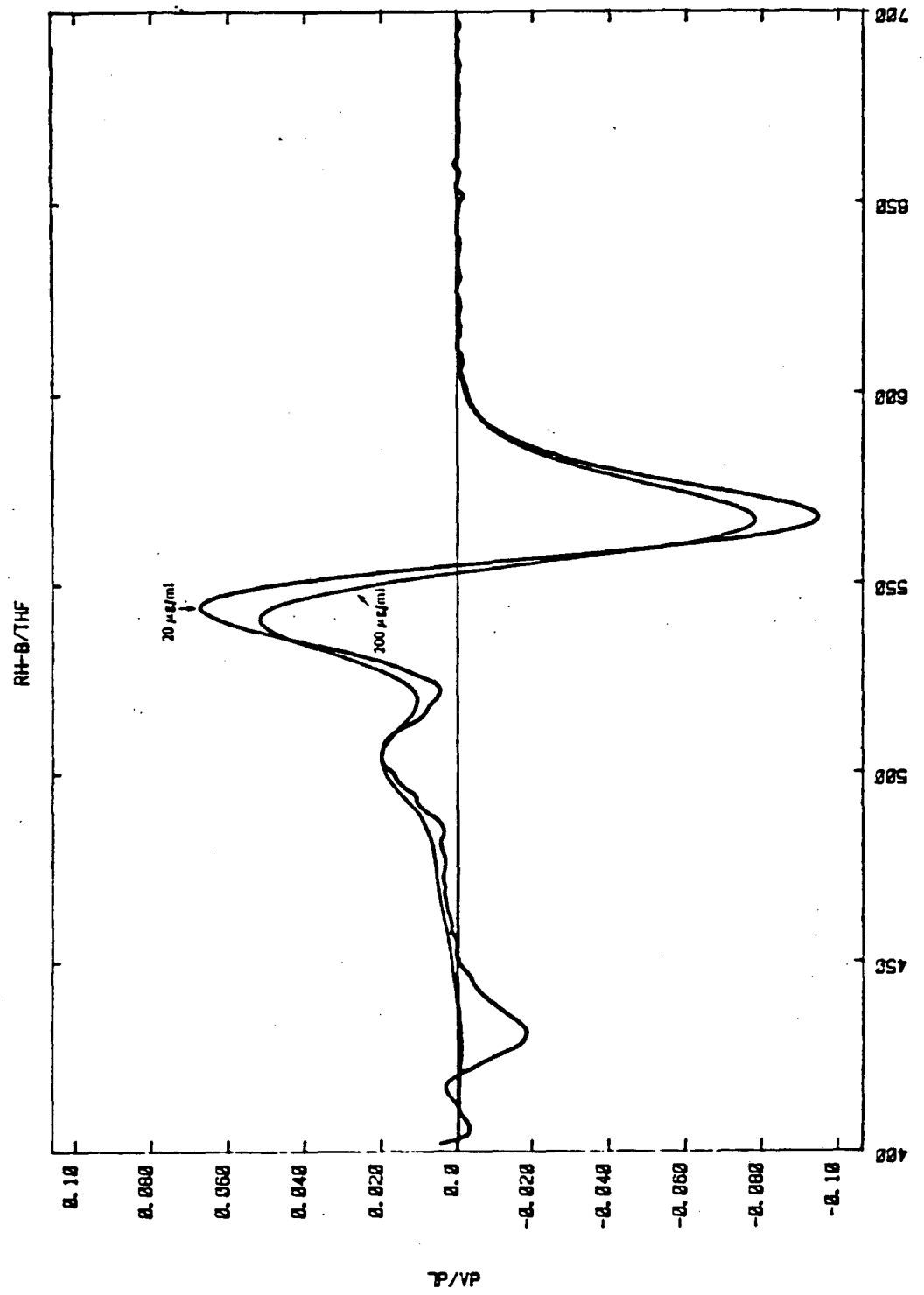
RH-B/THF
20 μg/ml
200 μg/ml
0.10
0.080
0.060
0.040
0.020
0.0
-0.020
-0.040
-0.060
-0.080
-0.10
ΔP/VP
400
450
500
550
600
650
700
WAVELENGTH (nm)

Chapter V

Perturbations of molecular motion in the plasma membrane of MDCK cells induced by phorbol esters

As discussed in chapter 1, all of the components of biologic membranes (phospholipids, cholesterol, proteins, glycoproteins, and glycolipids) are in motion relative to each other. The three basic types are shown below:

primitive: motion along interatomic axes

rotational: motion about a single molecular axis

translational: displacement from one locale to another

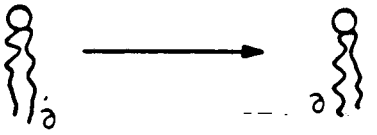

Measurements are dependent on the probes used; the types of information obtainable are determined by the locations accessible to the probe molecules, the timescales of their excited states, and the Boltzmann distributions of excited and ground states (1-3). Thus, the timescale of infrared spectroscopy best accommodates measurement of primitive (bending; stretching; rocking) motions; rotational motion can be quantitated by epr, nmr, differential scanning calorimetry, Raman spectroscopy, light scattering,

dielectric relaxation, electric dichroism, flow birefringence, phosphorescence, and steady state fluorescence measurements; translational motion has been observed using magnetic resonance and fluorescence techniques.

In comparison to the first two types of motion which are of a local nature, i.e., movement along interatomic or single molecular axes, resp., lateral motion is more global. Lateral diffusion coefficients for probes in pure phospholipid bilayers and biologic membranes have been measured as being between 10^{-8} and 10^{-12} cm^2/sec (4); these values correspond to mean distances traversed between a micron for phospholipids and a hundredth of a micron for proteins per second. Due to the relatively large signal:noise resulting from the zero or essentially null population of molecules in the excited (relative to the ground) state and the nanosecond lifetimes of fluorescent probes, instrumentation techniques to exploit these properties have been developed for measurements in biologic systems. Thus, studies of lateral diffusion in which fluorescence techniques have been employed include: antibody-heterokaryon fusion of rhodamine and fluorescein labeled human and mouse cells, respectively (5), agglutination of lectins using microscopy (6) and resonance energy transfer (7), excimer formation (8), fluorescence correlation spectroscopy (9) and fluorescence recovery after photobleaching (9). Precise quantitative information for

the distances and timeframes of interest in biologic membranes can be obtained most directly from the latter; therefore, this was the method of choice for the present work.

Materials and Methods

MDCK cells were grown under the conditions described in Chapter 4. For experiments involving components of the extracellular matrix, coverslips were coated with collagen by the method of Klebe (10) or with fibronectin or laminin by drying MEM solutions of either glycoprotein on coverslips.

For phorbol ester (Consolidated Midland, Brewster, N.Y.) experiments, serial dilutions were made from stock solutions of 1 mg. of phorbol ester per ml. of methanol into MEM; MEM containing 0.005% methanol served as the control. 12-O-tetradecanoylphorbol-13-acetate (TPA), phorbol 12,13-didecanoate (PDD), and 4-α-phorbol 12,13-didecanoate (4-α-PDD) were the phorbol esters used in this study. Final concentrations of phorbol esters ranged up to 0.812 μM, i.e., 50 ng/ml for TPA.

Cells were exposed to tumor promoters at 50 ng/ml for 2 hr. at 37°C, to cytoskeletal inhibitors (either cytochalasin B (Sigma) at 0.50 μg/ml. (1.04 μM) or colchicine (Sigma) at 39.9 ng/ml (0.1 μM) for 1 hr. at 37°C, or to these solutions sequentially.

Subsequent to final drug exposure(s), MDCK cells were

kept at room temperature for all succeeding procedures. They were washed twice with serum-free MEM; this was followed by a 17 minute incubation with collarein in MEM (O.D.=2.83, pathlength=1.0 cm.). The cells were then washed six times with MEM containing 10% FCS; coverslips were removed from petri dishes, placed on the microscope stage and examined for cellular integrity and fluorescence.

The fluorescence lifetime of collarein was determined by the method and instrumentation described in Chapter 4.

Photobleaching apparatus

The photobleaching apparatus and method of analysis are similar to those reported previously (11,12). Briefly, one watt or less of 514.5 nm. light from a 4 watt argon ion laser (Lexel) was threaded through a beam splitter-attenuator and thence a Zeiss microscope (60X, 0.85 N.A. oil immersion objective); the Gaussian beam of *ca.* 1.6 um radius was focussed on a plasma membrane by epi-illumination. Fluorescence from the focussed spot was excited by the laser beam which had been attenuated by at least two O.D. units to establish a baseline value. The attenuation was removed for 50 msec. resulting in the irreversible destruction of a fraction of the fluorescence in the focussed area. The recovery of fluorescence in this area was then monitored and the three parameters characteristic of this class of experiments were measured: the percent bleach, the percent recovery, and the half-time for recovery to a steady state

level. The same spot was bleached multiple times subsequent to this recovery and the three parameters were measured for each bleach pulse or hit.

Results

Initial photobleaching experiments indicated significant alterations in the lateral diffusion of collarein in cells treated with the phorbol esters TPA and PDD compared with untreated cells. Relative to the control cells decreases in the following parameters were measured (for the first hit per spot) with either agent: percent bleach, percent recovery, and half-time for recovery (Table 1). For the treated cells as the hit number per spot was increased (subsequent to recovery of fluorescence to a steady state level), the percent bleach decreased while the percent recovery increased (Fig 1b). The latter usually approached 100% by the fourth hit; thus, the mobile fraction, the percent of collarein with 100% mobility remaining after multiple bleaches, could be determined. Both parameters remained relatively constant for the control cells (Figure 1a). Lower concentrations of TPA resulted in intermediate values. Such behavior was in marked contrast to that exhibited by cells treated with the inactive congener 4α-PDD, by control cells, or by cells treated with colchicine (vide infra).

The fluorescence lifetime of collarein was fit by a single exponential component (within the current limits of resolution of the instrument) in both control (τ=1.85 nsec.) and TPA treated (τ=1.60 nsec.) cells. These data are consistent with the images observed under the fluorescence microscope of fluorescence confined exclusively to the

plasma membrane (Chapter 4).

Levels of cellular differentiation and growth have been shown to correlate with cell shape (13-15). The latter can be modulated by the exogenous extracellular matrix components collagen, fibronectin, and laminin which are able, in certain systems, to make cells flatten, to fold, or to cause, in general, some perturbation in cellular shape thereby implying a change in the intramembranous and perhaps submembranous molecular organization. The cytoplasmic cortical elements can also be perturbed directly by the cytoskeletal disrupting agents cytochalasin B and colchicine; treatment with either may alter the cellular morphology.

To determine if the results obtained with the active phorbol esters were due to a change in cell shape (Figures II-5,6), morphologic alterations of the MDCK cells were induced with both extracellular and intracellular perturbing agents, i.e., by growth on substrata composed of the extracellular matrix components collagen, fibronectin, or laminin and by incubation with the microfilament inhibitor cytochalasin B, respectively. Additionally, cells were exposed to the microtubule inhibitor colchicine; however, with this compound, no obvious cell shape change was detected.

Growth of cells on collagen or fibronectin reduced the percent recovery and half-time for recovery to values obtained with the active PEs while incubation with

cytochalasin B and growth on laminin reduced these parameters to values intermediate between those of the control and active PE treated cells. Growth on the three substrata resulted in an even greater decrease in the percent bleach.

Incubation with a combination of either cytoskeletal inhibitor and TPA treatment, irrespective of order, showed the behavioral characteristics induced by TPA or PDD at 50 ng/ml.

Discussion

The effects of the tumor promoting phorbol esters TPA and PDD on MDCK cells have been used as a means for understanding the mechanism of chemical transformation in culture. In the belief that the motions of lipophilic molecules in the plasma membrane bilayer might be transformation sensitive, collarein, a fluorescent probe molecule that localizes exclusively in the plasma membrane, was designed and synthesized.

In cells treated with active phorbol esters, the probe reports the induction of a second membrane environment that is characterized by a significantly lower mobility. Similar changes can be mimicked by altering the cell shape either intracellularly by perturbation of the microfilamentous organization with cytochalasin B or extracellularly by altering the substratum on which the cells adhere and grow. These data are consistent with the lateral diffusivity of some fraction of the lipophilic fluorophore collarein being strongly influenced by the organization of the larger and relatively immobile proteinaceous integral and peripheral structure of the plasma membrane. More specifically, in the untreated cell the membrane associated proteins may assume a fairly homogeneous distribution; upon treatment with an active tumor promoter, an intramembranous condensation of some of the molecular elements may occur rendering them relatively immobile. The lipids may then respond to this "reorganized" relatively immobile structure by forming

domains characterized by degrees of mobility. Some collarein molecules may get "caught" in condensed regions; this could lead to immobility on the photobleaching time scale. Others could be excluded from these regions and their diffusion coefficients would increase due to the increased lipid to protein ratio of the environment they are then probing. Thus, in the process of intramembranous "condensation" a more heterogeneous intramembranous scaffolding may appear resulting in a change from a relatively homogeneous distribution of lipid molecules to a heterogeneity of environments. This reorganization would be reflected in the mobility measurements reported here as a decreased fraction of recovery, an increased diffusion coefficient for molecules still free to diffuse due to the relatively increased local lipid:protein ratio, and perhaps a decreased fraction of molecules accessible to bleaching by the polarized laser light. The TPA-induced decrease in fluorescence lifetime by 250 psec. is not inconsistent with an increased mutual proximity of probe molecules.

This interpretation is consistent with previous work which has examined membrane changes associated with treatment of tumor promoting phorbol esters. Jacobson et al (16) observed no differential effects between the active and inactive phorbol esters in dipalmitoylphosphatidyl choline model membranes on the main transition temperature, fluorescence anisotropy, cationic permeability, electrophoretic mobility, or conductance of planar bilayers.

In contrast, when whole cells have been examined subsequent to TPA treatment, a picture of membrane susceptibility emerges. For example, Shoyab et al (17) have reported a decrease in the affinity of the epidermal growth factor (EGF) receptor for EGF subsequent to TPA treatment. The fluorescence anisotropy of the fluorophore diphenylhexatriene appears to correlate with TPA sensitivity of susceptible and resistant murine erythroleukemic cell clones (18). Thus, TPA appears to affect membrane lipid properties of cells but not lipids in bilayers devoid of protein.

Control of molecular diffusion in biologic membranes by the matrix of macromolecules associated with plasma membranes has been demonstrated by the measured increases in diffusion rates of both lipids and proteins in spectrin-deficient spherocytic mouse erythrocytes compared with normal cells (19), by changes in both macro- and microscopic state of intramembranous particles upon collapse of red cell ghost cytoskeletal elements (20), and by a reduction in protein mobility in the absence of any effect on the mobility of a lipid probe in L-6 myoblasts subsequent to treatment with cytochalasin B (21). Additional examples of altered mobilities upon release of constraints have also been reported (22,23).

Changes in dynamic interactions of molecules embedded in the plasma membrane may be an indication of or a means for major physiologic alterations at the molecular level

(24,25). Examples include changes in lateral diffusion rates of fluorescent lipid analogs in mouse egg plasma membranes upon fertilization and first cleavage (26) and in the mobile fraction of viral surface proteins upon activation of viral expression (27).

Thus, the primary biophysical membrane effect of TPA seems to be on the protein and protein-associated structure of plasma membranes. Furthermore, the increased diffusion coefficients of the mobile fraction observed upon chemical transformation or treatment with inducers of cell shape change appear to reflect changes in membrane organization, with collarein, a lipophile, probing an environment which is responding to a reorganization of the larger, more immobile membrane associated molecules.

Figures

Figure 1: Fluorescence recovery after photobleaching trace. (a) Eight successive hits and recoveries on the same spot of a control cell. (b) Eight successive hits and recoveries on the same spot of a TPA treated cell. Units of axes: abscissa = time; ordinate = fluorescence (volts).

Figure V-1

a

8 successive hits and recoveries

on the same spot of a control cell

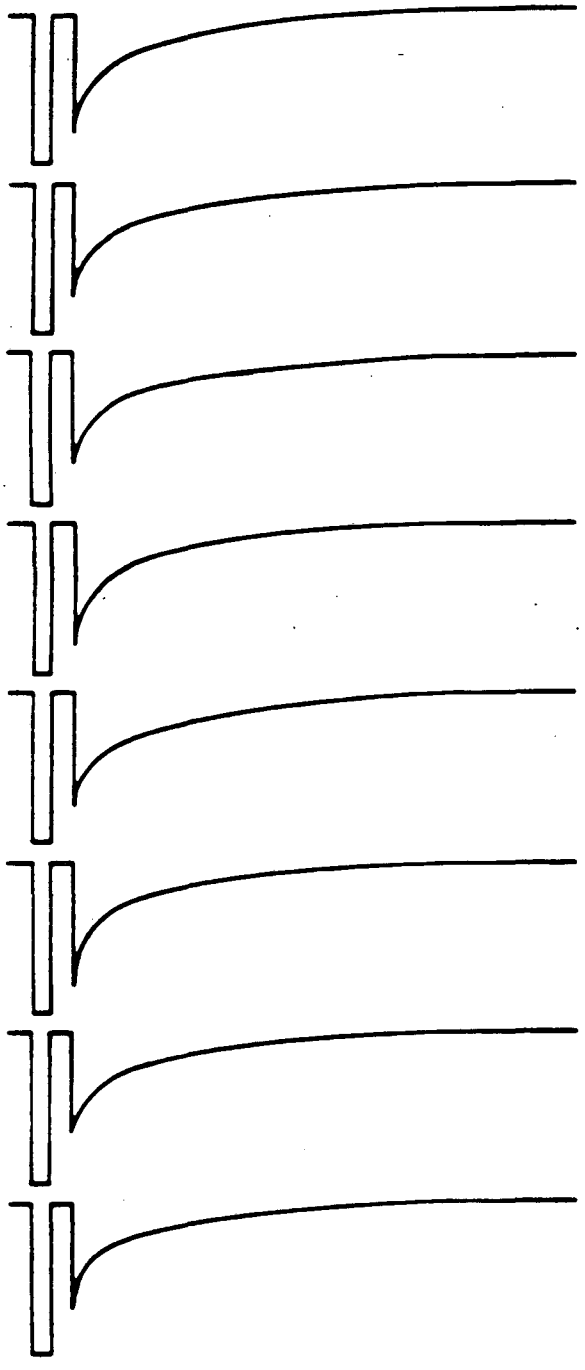

b

8 successive hits and recoveries

on the same spot of a TPA treated cell

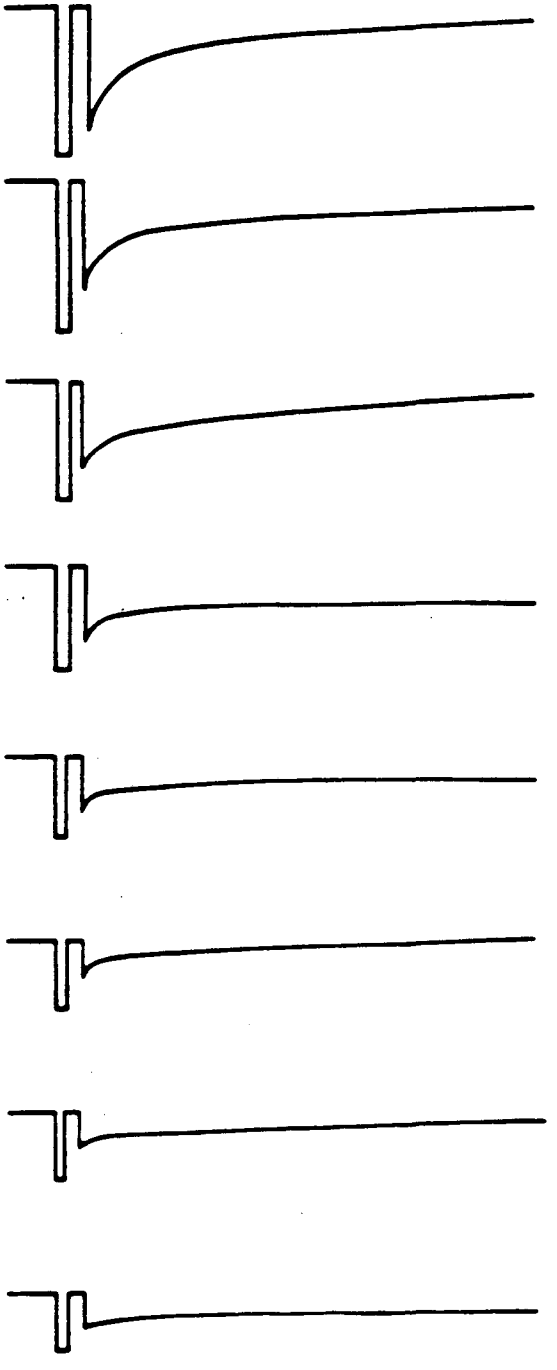

Table 1. Photobleaching data (first hit per spot)

Experiment*	% bleach	% recovery	$t_{1/2}$, sec	$D \times 10^{-9}$, cm-cm/sec
1. Control (43)	76.3 ± 3.40	98.5 ± 1.10	4.80 ± 1.20	2.88 ± 0.72
2. TPA (33)	53.2 ± 16.1	47.2 ± 4.40	2.30 ± 0.60	5.08 ± 0.33
3. PDD (18)	55.6 ± 8.40	53.2 ± 13.7	2.80 ± 1.00	4.24 ± 1.51
4. Colchicine (21)	82.3 ± 5.00	100.0 ± 0.00	5.40 ± 0.70	2.76 ± 0.36
5. Colchicine, TPA (13)	48.3 ± 10.2	28.2 ± 8.70	1.73 ± 0.33	6.60 ± 1.26
6. TPA, colchicine (20)	48.6 ± 13.7	40.9 ± 20.7†	1.90 ± 0.50	6.04 ± 2.63
7. Cytochalasin B (7)	65.3 ± 13.1	64.4 ± 23.7	4.21 ± 4.90‡	2.96 ± 3.45
8. Cytochalasin B, TPA (10)	49.9 ± 15.5	35.3 ± 14.7	1.70 ± 0.50	6.04 ± 1.78
9. TPA, cytochalasin B (10)	53.1 ± 10.6	29.0 ± 9.30	1.70 ± 0.60	6.88 ± 2.43
10. Collagen (13)	45.9 ± 6.60	52.8 ± 19.4	2.50 ± 1.20‡	4.76 ± 2.28
11. Fibronectin (15)	47.5 ± 1.50	40.9 ± 4.10	2.30 ± 1.00	4.96 ± 0.22
12. Laminin (22)	45.3 ± 11.2	56.5 ± 3.60	4.10 ± 1.10	2.76 ± 0.74

The data (means ± SD) reported in the respective columns give the cell treatment, the percentage of fluorescence bleached by the first of a series of bleach pulses, the percentage of fluorescence recovered, half-time ($t_{1/2}$) for recovery, and the self-diffusion coefficient derived therefrom. All values are within 95% confidence limit except those indicated † (90%) and ‡ (50%).

*Numbers in parentheses are the number of hits used for data in this table. (These numbers correspond to the number of individual cells examined, the number of distinctly different spots on a particular cell, or a combination of both.)

References

1. Thomas, D.D. (1978) Biophys. J. 24: 439-62.
2. Edidin, M. (1981) Membrane Structure, eds. Finean, J.B. and Michell, R.H. Elsevier/North-Holland Biomedical Press (New York).
3. Andersen, H.C. (1978) Ann. Rev. Biochem. 47: 359-83.
4. Jacobson, K. and Wojcieszyn, J. (1981) Comm. Mol. Cell. Biophys. 1: 189-199.
5. Frye, L.D. and Edidin, M. (1970) J. Cell Sci. 7: 319-355.
6. Rutishauser, U. and Sachs, L. (1974) Proc. Nat. Acad. Sci. 71: 2456-60.
7. Fernandez, S.M. and Berlin, R.D. (1976) Nature 264: 411-5.
8. Vanderkooi, J.M. and Callis, J.B. (1974) Biochemistry 13: 4000-6.
9. Schlessinger, J., Axelrod, D., Koppel, D.E., Webb, W.W., and Elson, E.L. (1977) Science 195: 307-9.
10. Klebe, R.J. (1974) Nature 250: 248-251.
11. Axelrod, D., Koppel, D.E., Schlessinger, J, Elson, E, and Webb, W.W. (1976) Biophys. J. 16: 1055-1069.
12. Wolf, D.E., and Edidin, M. (1981) Tech. Cell. Phys. P105: 1-14.
13. Folkman, J. and Moscona, A. (1978) Nature 273: 345-349.
14. Emerman, J.T. and Pitelka, D.R. (1977) In Vitro 13:

316-328.

15. Sugrue, S. P. and Hay, E.D. (1982) Dev. Biol. 92: 97-106.

16. Jacobson, K., Wenner, C.E., Kemp, G, and Papahadjopoulos, D. (1975) Cancer Res. 35: 2991-2995.

17. Shoyab, M., De Larco, J.E., and Todaro, G.J. (1979) Nature 279: 387-391.

18. Fisher, P.B., Cogan, U., Horowitz, A.D., Schacter, D., and Weinstein, B. (1981) Biochem. Biophys. Res. Comm. 100: 370-376.

19. Koppel, D.E., Sheetz, M.P., and Schindler, M. (1981) Proc. Nat. Acad. Sci. 78: 3576-3580.

20. Elgsaeter, A. Shotton, D.M., and Branton, D. (1976) Biochim. Biophys. Acta. 426: 101-122.

21. Schlessinger, J., Axelrod, D., Koppel, D., Webb, W.W., and Elson, E.L. (1977) Nature 195: 307-309.

22. Tank, D.W., Wu, E.-S., and Webb, W.W. (1982) J. Cell Biol. 92: 207-212.

23. Geiger, B., Avnur,Z, and Schlessinger, J. (1982) J. Cell Biol 93: 495-500.

24. Bissell, M.J., Hall, H.G., and Parry, G. (1982) J. Theoret. Biol. 99: 31-68.

25. Elson, E.L., and Reidler, J.A. (1979) J. Supramol. Struc. 12: 481-489.

26. Wolf, D.E., Edidin, M., and Handyside, A.H. (1981) Dev. Bio. 85: 195-198.

27. Reidler, J.A., Keller, P.M., Elson, E.L., and Lenard, J.

(1981) Biochemistry 20: 1345-1349.

Chapter VI

Epidermal Growth Factor Binding Perturbations Induced by Chemical Transformation

Introduction

The idea of a reorganization of the intra- and perimembranous macromolecular scaffolding of the plasma membrane consequent to the interaction of cells with tumor promoters was suggested by fluorescence recovery after photobleaching (FRAP) data (Chapter V). In said experiments Madin-Darby canine kidney (MDCK) cells, which had been exposed to the synthetic fluorescent phospholipid collarein, exhibited decreases in three parameters: (percent bleach (30%), percent recovery (52%), and half-time for recovery (52%)); these data connoted the appearance of an immobile (on the photobleaching timescale) fraction upon exposure to biologically active phorbol esters.

Several groups have reported the existence of two classes of receptor sites for epidermal growth factor (EGF) in the plasma membranes of cells in culture. Upon treatment with 12-tetradecanoylphorbol-13-acetate (TPA), the following changes in EGF binding have been observed: (a) decreases in binding capacities due to the disappearance of binding sites (1,2) or a reduction in the affinity of the EGF receptor-ligand interaction (3,4), (b) an increase in the amount of

EGF bound (5), and (c) an initial decrease (up to two hours) followed by an increase (6). Although the experimental systems and conditions varied greatly from one study to another, from all cases a reorganization of receptors in the plasma membrane can be inferred. To understand the nature of this reorganization it was first necessary to ascertain whether such an effect is induced by TPA under the conditions used in the photobleaching study. Therefore, the effect of TPA on the binding of EGF to MDCK cells was examined.

In agreement with previous work (1-6) it was found that MDCK cells contain two classes of EGF binding sites with K_d's of ca. 10^{-10}M and 10^{-8}M with ca. $5x10^4$ and $6x10^3$ receptors per cell, respectively. When binding is carried out in the presence of TPA the total number of EGF molecules that bind is increased, the percent of molecules that bind with high affinity is decreased, and the K_d's remain fairly constant. To determine the source of the increased number of total binding sites, studies were conducted in the presence of cycloheximide (a protein synthesis inhibitor), monensin (an ionophore that perturbs intracellular trafficking by altering ion transport), and dansylcadaverine (an inhibitor of endocytosis via coated pits); the time and temperature dependence of binding behavior were also examined. The results are consistent with an intramembranous rearrangement of EGF receptors and further support the idea of a global reorganization of the

macromolecular scaffolding of the plasma membrane upon treatment with TPA.

Materials and Methods

Cultures

Madin-Darby canine kidney (MDCK) cells were grown to confluence in 17 mm. diameter multi-well dishes at 37° C. The medium used for all experiments was Minimal Essential Medium (MEM) (GIBCO) containing 20 mM Hepes (Sigma) buffer and 10% fetal calf serum (FCS) at pH 7.4 and 310 mosm, i.e., the same conditions used for the photobleaching work.

For TPA experiments serial dilutions were made from stock solutions of 1 mg/ml TPA/methanol into MEM. MEM containing 0.005% methanol served as the control. The final concentration of TPA was 50 ng/ml (8.12×10^{-8} M). For experiments involving the cell biologic inhibitors cells were preincubated with cycloheximide (10 µg/ml), monensin (1 or 10 µM), and dansylcadaverine (100 µM) for 0.5, 1.0, and 0.5 hrs., respectively. Binding studies were then performed in the presence of these drugs at the same concentrations.

Binding studies

EGF was obtained from Collaborative Research in the ^{125}I-labeled form or as the unlabeled receptor grade. The latter was radioiodinated by the method of Fong and Hubbell (7) or was used for determining nonspecific binding.

Cultures were incubated with ^{125}I-EGF at twenty concentrations ranging from 0 to 200 ng/0.5 ml per culture for 2.0 or 0.5 hours at 37° or 4° C. All binding studies were done in the presence of 10% FCS. After incubation with the growth factor, media were removed and cells were washed

six times with phosphate buffered saline (PBS). Cells were solubilized with 2% sodium dodecylsulfate (SDS) and counted in a Tracor Analytic Gamma Counter. Nonspecific binding was determined by adding a 100-fold excess of cold EGF.

Cell number was determined by treatment of monolayers with a Ca^{++}-EGTA solution followed by counting in a hemacytometer.

Data were fit by the computer-assisted nonlinear least squares curve fitting program of Munson and Rodbard (8). Models involving single and multiple classes of binding sites were considered; the best model was based on objective statistical criteria.

Results

Two classes of binding sites for all cells except those treated with monensin at 10 μM were suggested by (1) the curvilinear shape of Scatchard plots which were fit by two straight lines and (2) the two component fits obtained from the Scatchard analysis using the Munson-Rodbard program. Nonspecific binding, which accounted for approximately 10% of total binding, was subtracted either before graphing or as part of the fitting routine.

Figure 1 is a Scatchard plot of data from cells exposed to EGF at various concentrations in the presence and absence of TPA. The total number of receptors per cell and the percent receptors in the high affinity state, i.e., $K_d < 10^{-10}$ M, are plotted in bar graph form in Figures 2 and 3, resp. The dissociation constants are listed in Table 1. In order to minimize the effects of fetal calf serum all experiments were carried out in the presence of at least two lots of serum; therefore, numbers reported in Table 1 and Figures 2 and 3 represent interpolated values.

The validity of Scatchard graphical analysis recently has been questioned (9); Klotz asserted that graphical methods of analysis of data are generally not correct; additionally, he has called into question the validity or suitability of applying equilibrium constants to describe states which are probably not at equilibrium, e.g., metabolizing cells. The computerized nonlinear least squares curve fitting routine used in this work avoided the

issue of graphical methods altogether. Figure 1 is merely a visualization of the data points; no statistical or other mathematical analysis was performed by the graphical fitting of this figure. Thus, Figure 1 is a Scatchard graph and the numbers plotted in Figures 2 and 3 were obtained by Scatchard analysis (10). Additionally, as alluded to by Munson and Rodbard (11), the K_ds reported here are not considered to be true values but relative indicators of changes induced by experimental conditions.

Consistent with the work of others, two classes of binding sites for EGF were found in control cells. Upon treatment with TPA, receptors of the high affinity class were observed at a finite level although at a decreased percentage of the total number. Thus, while a gain in the total number of receptor sites is observed, the high affinity site represents a reduced percentage of the total.

To determine whether the increased number of receptors observed in the presence of TPA required protein synthesis and/or was mediated by an ion dependent mechanism, binding experiments were carried out in the presence of cycloheximide or monensin, respectively.

In control cultures treatment with cycloheximide resulted in a significant increase in the affinity of the high affinity state, an increase (ca. 2.6-fold) in the total number of sites, and a decrease (ca. 0.07-fold) in the percent of high affinity sites (relative to control cells exposed to the growth factor in the absence of

cycloheximide). In TPA-treated cultures both the affinity of the high affinity state and the total number of sites increased 60%; however, the distribution between the two states in both the presence and absence of cycloheximide was virtually identical (ca. 1.1-fold difference).

Binding curves were generated in the presence of monensin at concentrations of 1 and 10 μM. At the lower concentration the control data were similar qualitatively to those for cycloheximide, i.e., the total number of receptors increased while the percent of high affinity sites decreased; the TPA-treated cells showed increases in both the total number (ca. 1.9-fold) and the per cent in the high affinity state (ca. 1.5-fold). As with cycloheximide the affinity of the high affinity state is increased; however, in this case the TPA-treated cells were affected to a greater extent. At the higher concentration the bound/free ratio was almost constant ($4.9 \times 10^{-2} \pm 1.4 \times 10^{-2}$ and $4.3 \times 10^{-2} \pm 0.9 \times 10^{-2}$ for control and TPA-treated cells, respectively). Morphologically, cells treated at the higher concentration showed a substantial amount of vacuolation throughout the cytoplasm -- suggestive of altered permeability.

To determine the dependence on residence time of receptors in the membrane binding curves were generated in the presence of dansylcadaverine. Control cells showed a slight (ca. 1.6-fold) increase in the number of binding sites and a substantial (3.5-fold) increase in the percentage of high affinity sites with a large increase in

affinity. In the TPA-treated case, dansylcadaverine caused a decrease in the total number and a large increase (ca. 4.2-fold) in the percent of high affinity sites also with increased affinity.

As receptors are not internalized at 4^{o} C , a series of experiments was carried out at this temperature to determine the effect of endocytosis on binding data. After incubation with TPA or methanol at 37^{o} C for 2 hours, cultures were placed in a 4^{o} C environment. Subsequent to temperature equilibration, EGF binding was carried out for 2 hours at this temperature in the presence of TPA or methanol, resp. In control cells binding at 4^{o} showed an increase in the total number of sites of almost three-fold with a decrease (0.44-fold) in the percent of high affinity sites. At the lower temperature the cells exhibited 0.45 the total number of binding sites with 0.60-fold the number in the high affinity state. The affinity of the high affinity state was increased in the control and TPA-treated cases with the latter affected to a greater extent.

Binding of virgin cells was also performed at 4^{o} C for both 2 and 4 hours in the presence and absence of TPA. Data from all four groups were virtually indistinguishable from each other.

To study the possible time dependence of the putative reorganization, binding experiments were performed for 0.5 hour as well as 2.0 hours. Relative to the numbers observed at 2.0 hours, these data showed less than 80% EGF molecules

bound for both the control and TPA-treated cases. Furthermore, the control cells at 0.5 hours had 35% the number of high affinity sites versus the 2.0 hour number, whereas the percent of high affinity sites in the TPA-treated cells decreased more than twenty-fold from 0.5 hour to 2.0 hours.

Discussion

Manifestations of the tumor promoting activities of phorbol esters have been observed in a broad range of morphologic, biochemical, and biophysical investigations. Most organelles, many enzymatic pathways, and the cellular surface have been implicated as targets of action (12-14). Although these data measure in culture phenomena, they may be representative of components of the process of malignant transformation *in vivo*. The timing of these events as well as the globality of effects may be key in understanding the transformation process.

The present work was undertaken in order to test the conclusions drawn from the fluorescence recovery after photobleaching (FRAP) work in which the lateral diffusion of the synthetic fluorescent phospholipid collarein in the plasma membrane of MDCK cells was measured. The effects of tumor promoters as well as agents that alter cell shape on the three parameters characteristic of this class of experiments (percent bleach, percent recovery, and half-time for recovery) were examined. The appearance of an immobile fraction upon the introduction of active phorbol esters or agents which induce cell shape change was consistent with lipid reorganization in response to a reorganization of the intra- and perimembranous macromolecular scaffolding. As several papers have appeared in the past few years indicating the number and classes of receptors for epidermal growth factor (EGF) are altered in the presence of TPA in

several cell lines (1-4), binding studies to determine if similar effects were generated in the MDCK cell line under the conditions used in the photobleaching work were performed.

Our initial binding experiments clearly indicated an increase in the cellular binding capacity due to an increase in the absolute number of low affinity sites per cell. A decrease in the percent of high affinity sites was also observed. Thus, the question of the source of the increased number of receptors arose.

One explanation may involve the configuration of the cells used in this study. MDCK cells grow as a monolayer of confluent polarized cells due to the presence of tight junctions; therefore, the ligand has direct access to only the apical side, which represents less than 40% of the total cell surface. Cells containing EGF receptors in vivo probably interact with EGF on their serosal surface which in culture is the basolateral and, thus, inaccessible aspect. As TPA has been reported to cause the disappearance of tight junctions in some cells (15), the increase in number of EGF receptors may be due at least in part to a freeing of those receptors that were previously functionally sequestered; however, striking quantitative or qualitative changes in junctional complexes due to TPA perturbations were not observed in this study (Chapter II).

Alternative explanations involve the age and residence time of the cellular receptors. To distinguish between

these possibilities, inhibitors that affect the receptor in various ways were employed: cycloheximide to determine the protein synthesis dependence, monensin to determine if an ion-dependent mechanism was operational (16), and dansylcadaverine to determine the effect of internalization and down regulation on the binding process (17). Additionally, the effects of a decrease in temperature ($4^{o}C$) and a shorter incubation time (0.5 hr.) were examined.

A decrease in binding due to the arrest of receptor synthesis would be expected if de novo receptor synthesis were responsible for the observed increased binding in the presence of TPA. The cycloheximide experiments with control cells evidenced a 2.6-fold increase in the total binding with the almost complete disappearance of high affinity binding while the TPA-treated cells, which also bound an increased total number of EGF molecules, showed virtually no change in the distribution between high and low affinity classes. These data suggested that some anabolic step, either as a modification of a receptor or as a step leading to the catabolism of the hormone-receptor complex, was obligatory for high affinity binding.

The influence of ion transport in the processing and accessibility of EGF receptors was approached by performing binding experiments in the presence of monensin, an ionophore which affects the intracellular trafficking of cellular organelles and which, due to its lipophilic nature, can alter membrane permeability (16). For control cells the

qualitatively similar effect of monensin at 1.0 uM to that of cycloheximide suggested that new receptor synthesis or processing is not responsible for the increase observed with TPA, per se. Because monensin is able to destroy a concentration gradient involving monovalent cations across a membrane (17) this ionophore could cause the release of vesicles that were located under the plasma membrane and contained receptors in a nonbinding state. The almost constant bound/free ratio in both control and TPA cases at 10 uM monensin tend to support the induction of a breakdown of the permeability barrier by this drug.

Dansylcadaverine, an inhibitor of transglutaminase, an enzymatic activity required for endocytosis via coated pits from the surface of cells, has been reported to cause the receptors to remain in the plasma membrane and, thus, escape down regulation and ultimate degradation (18). (The increase in binding in control cells at $4^{o}C$ vs. 37^{o} is indicative of down regulation being operative in these cells under normal conditions.) Increases in the percent of high affinity sites for both control and TPA-treated cultures indicate that the drug acts as reported, i.e., it prevents occupied receptors from being internalized. In control cells the conversion from low to high affinity sites is not blocked; however, if dansylcadaverine prevents the movement from receptors in the high affinity state into coated pits, then an increase in both the total number and percent in the high affinity state would be expected. Thus, the relatively

large increase in total number in the control cells induced by dansylcadaverine may be explained by the build up of receptors in the high affinity state with transition into the next state, i.e., localization in coated pits, being blocked. A dansylcadaverine-induced decrease in the total number of receptors for the TPA-treated cells may be due to the fact that in this case two steps (low to high conversion and coated pit formation) in the ligand-receptor complex pathway are inhibited.

Decreases in the high affinity state for both control and TPA-treated cases at $4^{o}C$ support the notion that the flow of receptors is from low to high affinity states with lateral diffusion as a contributing mechanistic element (vide infra and (19)). Additional support for conversion from low to high affinity binding comes from a comparison of the percent receptors in the high affinity site at 0.5 hr. relative to 2.0 hrs, i.e., an increase for controls and a decrease for the TPA-treated cells.

A hypothetical mechanism for the EGF binding and internalization process is sketched in Figure 4. The EGF receptor is synthesized in the rough endoplasmic reticulum, processed in the Golgi apparatus, and transported through a series of cytoplasmic vesicles to the plasma membrane. It is proposed that receptors can exist in a nonbinding state either in vesicles that are post Golgi and preplasma membrane or as latent sites in the plasma membrane. Receptors are converted from a nonbinding to a binding state

of low affinity (K_d *ca* 10^{-8}M) in the plasma membrane at rate k_0. The latter configuration is able to bind the ligand at rate k_1 whereupon it is further transmuted into a high affinity state (K_d *ca*. 10^{-10}M) at rate k_2; this is dependent on protein synthesis, receptor occupancy, and temperature. Upon treatment with TPA, k_2 is sharply decreased with k_0 and k_1 not being directly affected. Occupied receptors in the high affinity state are endocytized at rates k_3, k_4, and k_5 through the processes of intramembranous ligand-receptor agregation, coated pit formation and internalization, resp.

Therefore, any perturbation which can decrease processing of the receptor-ligand complex may cause a decreases in any of the forward rates k_{2-5} and a consequent increase in the concentration of low affinity receptors in the plasma membrane. Thus, if this processing requires protein synthesis or is affected by permeability changes, then treatment with either cycloheximide or monensin causes control cells to mimic those treated with TPA. A drop in temperature will also decrease this rate.

Inhibition of k_3 will result in an increase in the concentration of receptors in the high affinity state. Eventually, the whole system could be expected to shift back so that the forward rates k_0, k_1, and k_2 are decreased and pool sizes eventually level off.

In all cases where the normal flow along the proposed receptor pathway is perturbed the dissociation constant of the high affinity site is decreased in contrast to the

relative insensitivity of the low affinity constant. This may be reflected in a decrease in the k_n/k_{-n} ratios.

The data and model in this report are consistent with the work of others in that a decrease in the number of high affinity binding sites is effected by exposure of cells to TPA. However, with the conditions and cells used, an increase in the total number of EGF molecules binding was observed in these experiments. The differences may just be indigenous to this system and not central to the basic mechanism of plasma membrane tumor promoter induced perturbation. The cells used in this work are polarized, adherent, and epithelial. In contrast, previous studies of EGF interacting with TPA-treated cells employed cells which exist in vivo in suspension or normally grow as adherent monolayers and were suspended for the reported binding studies. An additional difference is the presence of serum at the 10% level in the presently reported studies, whereas others used lower concentrations or none at all.

Heterogeneity of receptor sites with respect to equilibrium and/or kinetic binding constants has been reported for the peptide hormones nerve growth factor (20-24), insulin (25), endogenous opiates (26), as well as EGF (6). Whether heterogeneity is induced by a ligand or exists prior to exposure such that receptors in various environments are in equilibium with each other still remains questionable. The idea of unmasking receptors has been discussed for NGF (22) and with respect to the phospholipid

metabolism of membranes. Phospholipid methylation (27) and digestion with phospholipases (28) have been implicated in this process.

The scheme proposed in figure 4 is consistent with the work of Zidovetzki et al (29) in which they studied both the rotational and lateral diffusion of EGF-receptor complexes in human epidermoid carcinoma (A-431) cells. The cells were exposed to erythrosin-EGF at $4^{o}C$; prolonged incubation or exposure to higher temperatures (23 or 37^{o}) resulted in decreased rotational (correlation time in the range 25-90 μs. at $4^{o}C$ and up to 350 μs. at $37^{o}C$) and increased lateral (D_t equal to 3×10^{-10} at 4^{o} and 8.5×10^{-10} cm^2/sec at 37^{o} with mobile fractions after 10 min. of 90 and 45%, resp.) diffusion coefficients. Thus, it was reasoned that k_2 and k_3 lead to decreased rotational and increased lateral diffusion coefficients as a consequence of aggregation of ligand-receptor complexes in the plasma membrane. Aggregation in sequence with internalization is believed to be part of the inactivation of the mitogenic activities of growth factors (18).

Using the synthetic phospholipid collarein as a probe molecule, our FRAP experiments indicated the appearance of an immobile fraction on the photobleaching timescale. We inferred this to be an indirect effect of the phorbol esters with a higher order effect being the reorganization of the proteinaceous scaffolding of the plasma membrane. The idea of a freezing of the macromolecular framework of the

membrane and consequent intramembranous immobility is consistent with Scheme 1. The immobilization could have a global influence on the entire plasma membrane and its associated structure.

Enzymatic activities such as kinases and those necessary to generate second messengers as well as the ability of receptors to aggregate and be cleared from the cell surface may be intimately associated with the transmission of biologic information across membranes (30); thus, a disturbance of these functions by a malignogenoid agent may be central to the transformation process. Cells which have been treated with tumor promoters in culture appear to respond to growth factors to a greater extent and at lower doses than their untreated counterparts. TPA has been reported to induce serine and/or threonine phosphorylation of the EGF receptor through an intracellular phosphorylation mechanism (31). Thus, binding of a biologically active phorbol ester could possibly lead to a conformational change in the receptor resulting in an altered binding behavior and/or activity of the tyrosine kinase activity of the EGF receptor. Additionally, it is possible that dispersion of receptors in the plasma membrane induced by a tumor promoter may cause an optimization of transmission function; by prolonging the display of receptors in a low affinity configuration, TPA may enhance the coupling between a growth factor and its later cellular messengers. It has been shown in 3T3 cells that blocking

EGF internalization with inhibitors of transglutaminase produced marked stimulation in the mitogenic response of cells to this hormone (19). The recent finding of sequence homologies between the EGF receptor and the v-erb-B transforming protein of avian erythroblastosis virus further implicates the association of regulation with plasma membrane organization (32).

This work supports the idea of a reorganization of the intra- and perimembranous macromolecular scaffolding upon treatment of this line of epithelial cells with the tumor promoter TPA. The organization of receptors in the plasma membrane and the perturbation that malignogenesis can effect may be of prime importance in understanding normal cellular growth regulation and how it is affected by transformation.

Figures

Figure VI-1. Scatchard graph of MDCK cells exposed to concentrations of EGF ranging from 0 to 200 ng/0.5 ml for two hours in the absence (circles and squares) and presence (triangles and diamonds) of TPA. abscissa: B=bound in units of counts per minute (cpm); ordinate: B/F=bound/free.

Figure VI-2. Bar graph of total number of EGF binding sites per cell as a function of treatment. Vertically shaded areas represent control (0.005% methanol) values and horizontally shaded areas represent TPA-treated cells.

Figure VI-3. Bar graph of % high affinity sites as a function of treatment. Vertical and horizontal shadings same as in Figure VI-2.

Figure VI-4. Scheme depicting the reorganization of EGF receptors induced by TPA and the sites affected by drug treatments. De novo protein synthesis occurs in the rough endoplasmic reticulum (RER) with processing, e.g., glycosylation taking place in the Golgi apparatus. Receptors are then inserted into the plasma membrane where they are initially in a nonbinding configuration. Conversions to

binding states and consequent sequelae are described in text.

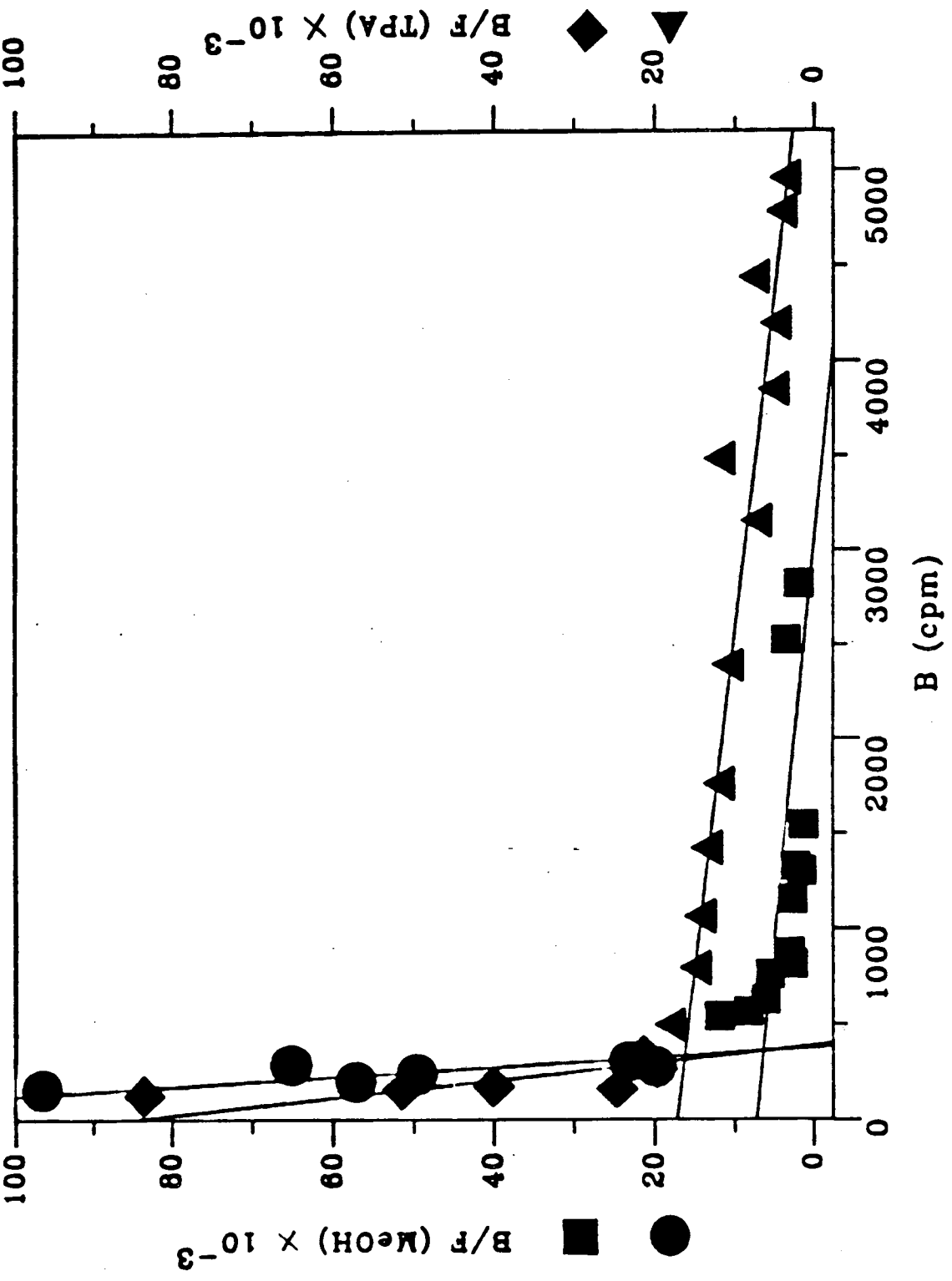
MDCK + EGF
B/F (MeOH) × 10⁻³
B/F (TPA) × 10⁻³
B (cpm)
0
20
40
60
80
100
1000
2000
3000
4000
5000

Figure VI-1

Figure VI-2

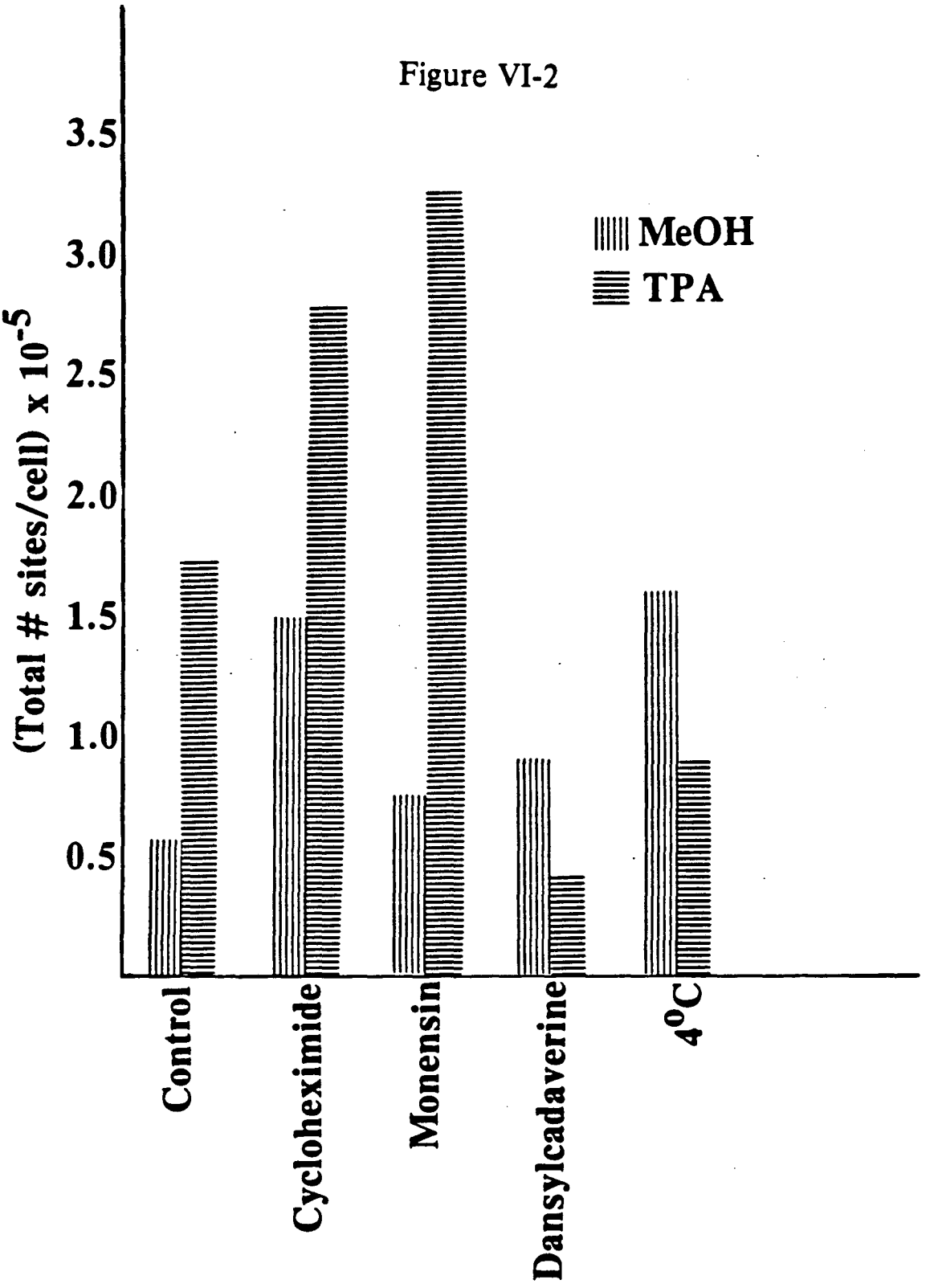

XBL 841-264

Figure VI-3

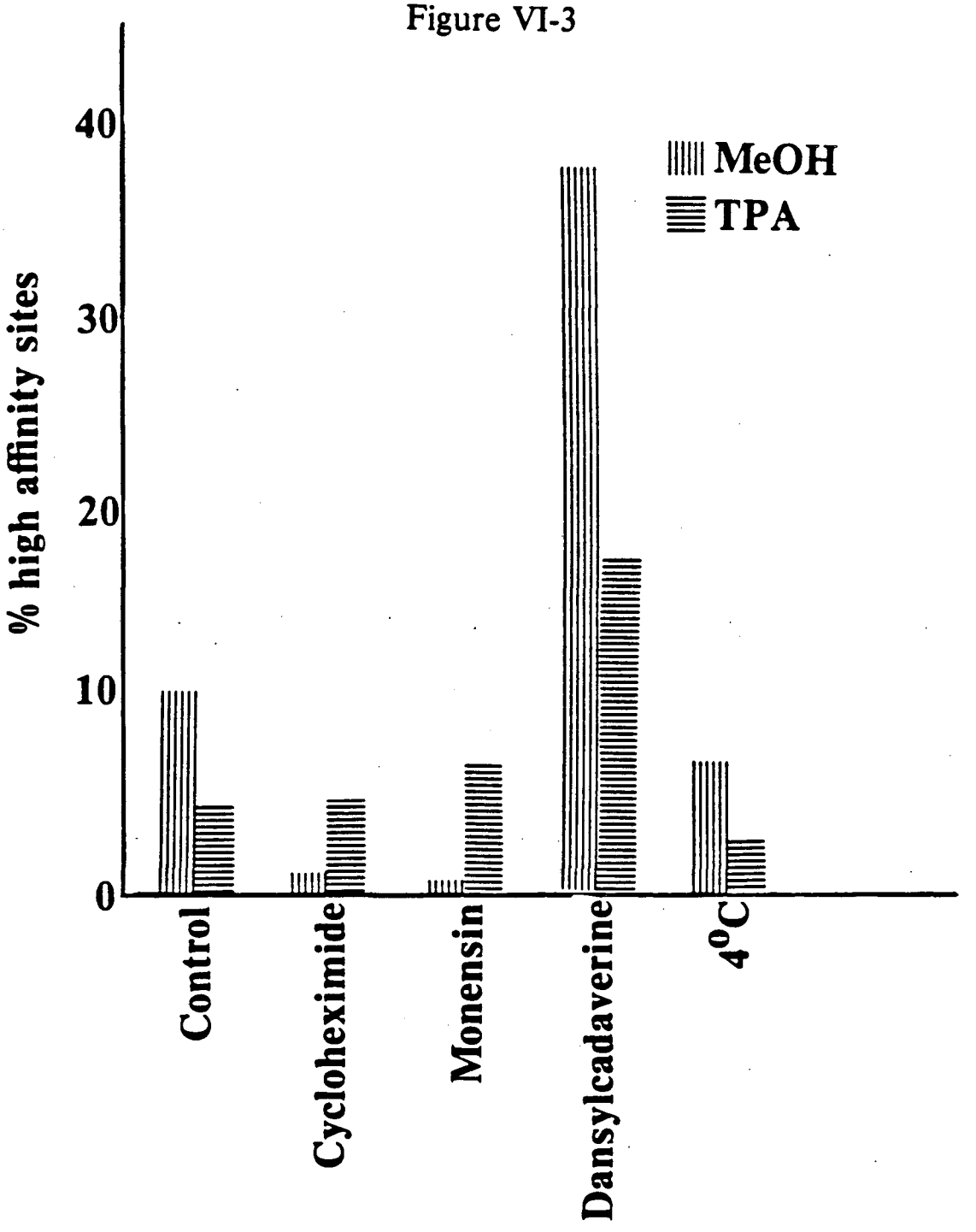

XBL 841-263

Figure VI-4

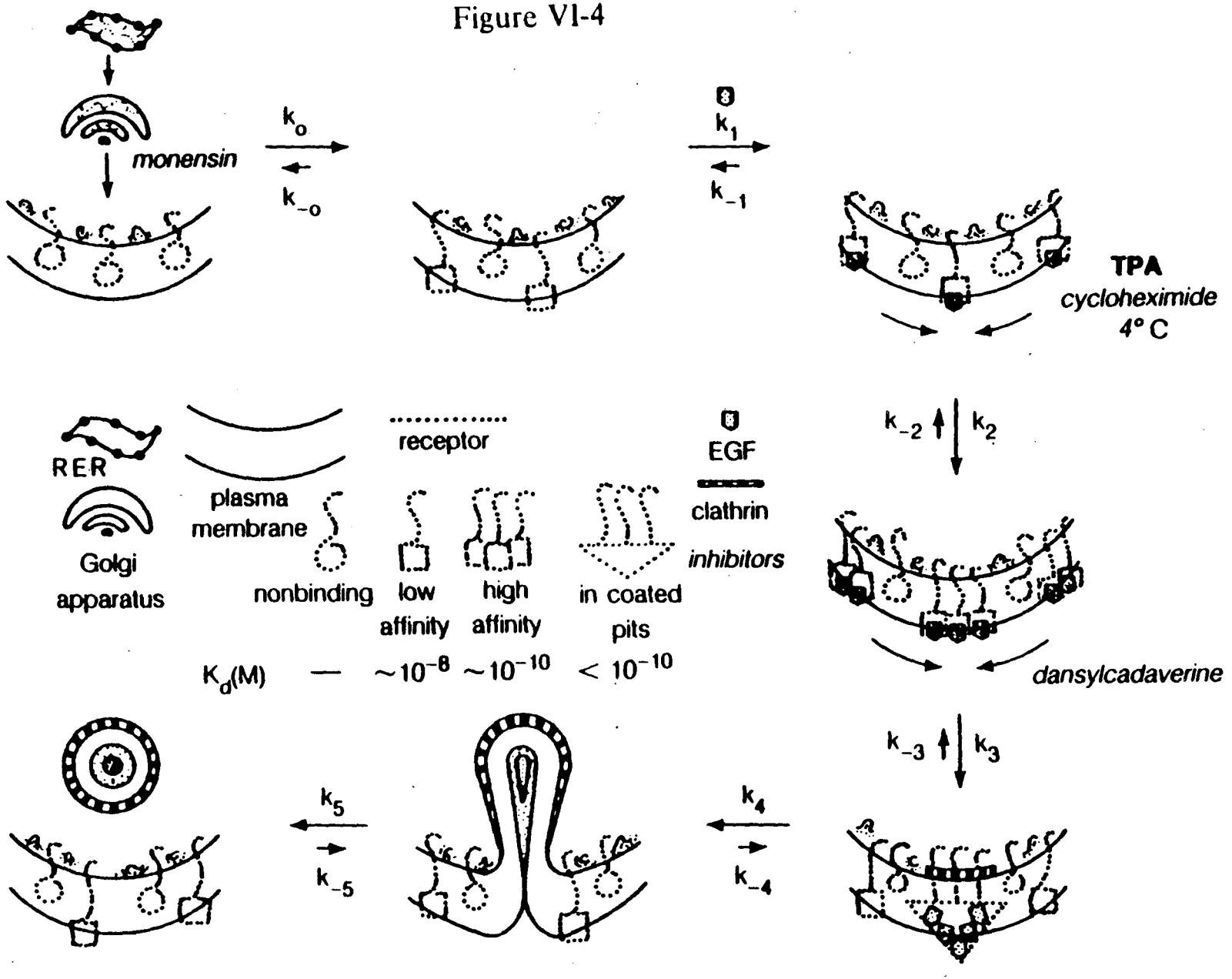
monensin
k_o
k_{-o}
k_1
k_{-1}
TPA
cycloheximide
4° C
RER
Golgi apparatus
plasma membrane
receptor
EGF
clathrin
inhibitors
nonbinding
low affinity
high affinity
in coated pits
K_d(M) — $\sim 10^{-8}$ $\sim 10^{-10}$ $< 10^{-10}$
k_{-2}
k_2
dansylcadaverine
k_{-3}
k_3
k_5
k_{-5}
k_4
k_{-4}

Table 1

Dissociation constants as a function of treatment

Treatment	K_d's (M)	
	MeOH	TPA
Control	7.25×10^{-8}	8.85×10^{-8}
	4.75×10^{-10}	4.75×10^{-10}
Cycloheximide (10 µg/ml)	2.03×10^{-7}	1.82×10^{-7}
	2.18×10^{-21}	1.50×10^{-14}
Monensin (1 µM)	8.49×10^{-7}	3.72×10^{-8}
	3.38×10^{-11}	2.17×10^{-17}
Dansylcadaverine (100 µM)	1.01×10^{-7}	2.81×10^{-8}
	3.35×10^{-19}	1.52×10^{-12}
4° C	2.18×10^{-7}	8.57×10^{-8}
	1.20×10^{-13}	6.74×10^{-16}

References

1. Saito, M., Ueno, I., and Egawa, K. (1982) Biochim. Biophys. Acta. 717: 301-4.
2. Lee, . and Weinstein, B. (1978) Science 202: 313-5.
3. Shoyab, M., De Larco, J.E., and Todaro, G.J. (1979) Nature 279: 387-91.
4. Brown, K.D., Dicker, P., and Rozengurt, E. (1979) Biochem. Biophys. Res. Comm. 86: 1037-43.
5. Yaketani, Y. and Oka, T. (1983) Proc. Nat. Acad. Sci. 80: 2647-50.
6. King, A.C. and Cuatrecases, P. (1982) J. Biol. Chem. 257: 3053-60.
7. Fong, B.K.-K. and Hubbell, W.L. (1982) Meth. Enzym. 81: 269-75.
8. Munson, P.J. and Rodbard, D. (1980) Anal. Biochem. 107: 220-39.
9. Klotz, I.M. (1982) Science 217: 1247.
10. Klotz, I.M. (1983) Science 220: 981.
11. Munson, P.J. and Rodbard, D. (1983) Science 220: 979-81.
12. Blumberg, P.M. (1980) CRC Crit. Rev. Tox. 8: 153-97.
13. Weinstein, I.B., Lee, L.S., Fisher, P.B., Mufson, A., and Yamasaki, H. (1972) J. Supramol. Struct. 12: 195-208.
14. Diamond, L, O'Brien, T.G., and Baird, W.M. (1980) Adv.

Cancer Res. 32: 1-74.

15. Ojakian, G. (1981) Cell 23: 95-103.

16. Tartakoff, A.M. (1983) Cell 32: 1026-8.

17. Geisow, M.J. and Burgoyne, R.D. (1982) Cell Biol. Internat. Rpts. 6: 933-9.

18. Davies, P.J.A., Davies, D.R., Levitzki, A., Maxfield, F.R., Milhaud, P., Willingham, M.C., and Pastan, I.H. (1980) Nature 283: 162-7.

19. Maxfield, F.R., Davies, P.J.A., Klempner, L. Willingham,M.C., and Pastan, I. (1979) Proc. Nat. Acad. Sci. 76: 5731-5.

20. Landreth, G.E. and Shooter, E.M. (1980) Proc. Nat. Acad. Sci. 77: 4751-5.

21. Grob, P.M. and Bothwell, M.A. (1983) J. Biol. Chem. 258: 14136-43.

22. Cattaneo, A., Biocca, S., Sergio, N. and Calissano, P. (1983) Eur. J. Biochem. 135: 285-90.

23. Costrini, N.V. and Kogan, M. (1981) J. Neurochemistry 36: 1175-80.

24. Calissano, P. and Shelanski, M.L. (1980) Neuroscience 5: 1033-8.

25. Donner, D.B. and Corin, R.E. (1980) J. Biol. Chem. 255: 9005-8.

26. Bowen, W.D., Gentleman, S., Herkenham, M., and Pert, C.B. (1981) Proc. Nat. Acad. Sci. 78: 4818-22.

27. Strittmatter, W.J., Hirata, F., and Axelrod, J. (1979) Science 204: 1205-7.

28. Cuatrecasas, P. (1971) J. Biol. Chem. 246: 6532-42.

29. Zidovetzki, R., Yarden, Y., Schlessinger, J., and Jovin, T.M. (1981) Proc. Nat. Acad. Sci. 78: 6981-5.

30. Nishizuka, Y. (1983) Trends Biochem. Sci. 8: 13-6.

31. Iwashita, S. and Fox, C.F. (1983) Fed. Proc. Fed. Am. Soc. Exp. Biol. 42: 849a.

32. Downward, J., Yarden, Y., Mayes, E., Scrace, G., Totty, N., Stockwell, P., Ullrich, A., Schlessinger, J., and Waterfield, M.D. (1984) Nature 307: 521-7.

Chapter VII

Conclusions

The major objective of this thesis was to gain a deeper understanding of the perturbations induced by a malignogenoid transformation on the organization of molecules constituting the plasma membrane. For experimental reasons as described in Chapter II the system chosen was an epithelial cell line which, when exposed to the tumor promoting phorbol esters, exhibits properties associated with a malignant-like state *in cultura*.

Induction of an increased rigidity in the plasma membrane in parallel with the manifestation of properties associated with a transformed state was suggested by two classes of experiments. The results from one technique, fluorescence recovery after photobleaching (FRAP), indicated the induction of a second environment in the plasma membrane in which the synthetic fluorescent phospholipid collarein was immobile on the FRAP timescale in comparison to the homogeneous, mobile environment of the control cells (Chapter V). Results from the other technique, the binding of epidermal growth factor (EGF) to cellular receptors, revealed a cryptic class of receptors which became accessible for binding upon chemical transformation (Chapter VI). These two lines of evidence are consistent with a reorganization of the plasma membrane induced by tumor

promoters.

Increased rigidity in the plasma membrane of a cell that has been induced to a transformed state may be associated with the autonomy to normal growth control mechanisms that transformed cells acquire (1-4). As signal transduction across a plasma membrane is generally believed to occur somewhere between the binding and internalization events, the mobility which the ligand-receptor complex is able to attain may be responsible for the quality of signal transduction (5). Thus, phosphorylation and higher order messenger generation may be strongly affected by the degree and type of movement accessible to the molecular components of sequential or cascading events.

Thus, by both a biophysical and a biochemical technique, this work indicates that a rigidity is induced in the plasma membrane of an epithelial cell that has been transformed to a malignogenoid state. This putative rigidity may effect or be associated with an autonomous state by preventing normal molecular movement in the plasma membrane and, thus, perturbing transduction of signals essential for normal control.

References

1. Poste, G. and Nicolson, G.L. Cell Surface Reviews vol. 1-N.
2. Sato, G.H. and Ross, R. (1979) Hormones and Cell Culture, Cold Spring Harbor conferences on cell proliferation, vol. 6.
3. Becker, F., ed. (1975-82) Cancer: a Comprehensive Treatise vol. 1-6. Plenum Press, New York.
4. Carcinogenesis-a Comprehensive Survey. vol. 1-6 (1976-82) Raven Press, New York.
5. Nishizuka, Y. (1983) Trends Biochem. Sci. 8: 13-6.

TECHNICAL INFORMATION DEPARTMENT
LAWRENCE BERKELEY LABORATORY
UNIVERSITY OF CALIFORNIA
BERKELEY, CALIFORNIA 94720